MOBILIZATION OF LEAD AND ZINC IN ACID SULFATE MINE TAILINGS

By

Angélica Vázquez-Ortega

A Thesis Submitted to the Faculty of the

SOIL, WATER AND ENVIRONMENTAL SCIENCE

In Partial Fulfillment of the Requirements
For the Degree of

MASTER OF SCIENCE

In the Graduate College

THE UNIVERSITY OF ARIZONA

2008

STATEMENT BY AUTHOR

This thesis has been submitted in partial fulfillment of requirements for an advance degree at The University of Arizona and is deposited in the University Library to be made available to borrowers under rules of the Library.

Brief quotations from this thesis are allowed without special permission, provided the accurate acknowledgement of source is made. Request for permission for extend quotation from or reproduction of this manuscript in whole or in part may be granted by the head of the major department or the Dean of the Graduate College when in his or her judgment the proposed use of the material is in the interest of scholarship. In all other instances, however, permission must be obtained from the author.

SIGNED: Angélica Vázquez Ortega

APPROVAL BY THE THESIS DIRECTOR

This thesis has been approved on the date shown below:

Dr. Jon Chorover	04/14/2008
Professor in Environmental Chemistry	Date

ACKNOWLEDGEMENTS

I would like to acknowledge my thesis advisor, Dr. Jon Chorover for his guidance and valuable suggestions and Mary Kay Amistadi for her technical support. Also, I would like to extend my thanks to my committee members Professors Raina Maier and Craig Rasmussen for their academic support and suggestions. Finally, I want to share this extraordinary achievement with my adorable husband, Carlos Soto López.

TABLE OF CONTENTS

LIST OF FIGURES

LIST OF TABLES

ABSTRACT

In this thesis, column experiments were conducted in order to determine the effect of irrigation with local groundwater on mobilization of lead and zinc in 50 years old sulfate-acid mine tailings. In addition, the influence of soluble oxalic acid, a common rhizosphere organic acid, was assessed by varying its concentration across an environmentally relevant range. In general, metal contaminant dissolution was not affected by the presence of oxalic acid. In both tailings, Zn mobilization was higher than Pb suggesting the presence of more kinetically labile Zn phases, regardless of the treatment used. Lead mobilization was also low because effluent solutions were near to equilibrium conditions with respect to gypsum, preventing Pb dissolution from Pb-sulfate minerals. Geochemical modeling also indicated that lead release was controlled by anglesite and plumbojarosite dissolution. Zinc release appears to be controlled by Zn-talc and goslarite.

CHAPTER 1: INTRODUCTION

Mining activities have adverse effects on the environment and human and animal health. Abandoned and improperly managed mine residues are subject to wind and water erosion in arid ecosystems. Water and wind erosion present a threat to surface and to ground water quality. Mineral weathering and further heavy metal mobilization in mine tailings are the key factors to understanding the possible fates of these contaminants.

1.1 Mineral Weathering in Mine Tailings

Mine tailings are subject to weathering processes when they are exposed to environmental conditions. Oxidation of sulfide-rich tailings is likely to happen when the minerals are exposed to atmospheric oxygen. In order to understand the consequences of a remediation technique it is essential to fully understand the geochemical processes that govern these contaminated sites.

1.1.1 Weathering of Sulfide Minerals

The oxidative dissolution of pyrite (FeS_2) and pyrrhotite ($Fe_{1-x}S$) produces sulfuric acid and, as a consequence, high concentrations of toxic metals can dissolve from the solid phase under the acidic conditions. Pyrite is a common sulfide mineral found in large amounts in the earth's crust; it is primarily associated with coal and metal ore deposits. The dominant process of proton production in mine tailings is controlled by pyrite oxidation through the oxygen path (Salmon & Malmstrom, 2004). When pyrite is

exposed to oxygen and water, it will oxidize to create acidic conditions by the following reaction:

$$FeS_{2(s)} + H_2O + 7/2\ O_{2\ (aq)} \rightarrow Fe^{2+}{}_{(aq)} + 2SO_4{}^{2-}{}_{(aq)} + 2H^{+}{}_{(aq)} \quad (1.1)$$

Ferrous iron (Fe^{2+}) also can be oxidized by O_2 to form ferric iron (Fe^{3+}). Ferric iron is a powerful oxidant that can promote further (autocatalytic) oxidation of pyrite. Under acidic conditions, the primary oxidant of pyrite is Fe^{3+} and under circumneutral conditions O_2 becomes the predominant oxidant (Singer and Stumm, 1970). The following reaction describes pyrite oxidation through this ferric iron path:

$$FeS_{2(s)} + 14Fe^{3+}{}_{(aq)} + 8H_2O \rightarrow 15Fe^{2+}{}_{(aq)} + 2\ SO_4{}^{2-}{}_{(aq)} + 16H^{+}{}_{(aq)}. \quad (1.2)$$

Pyrrhotite dissolution can also occur through oxic or anoxic pathways. Some important oxidants of pyrrhotite are O_2 and Fe^{3+}. Under anoxic conditions, the dissolution of pyrrhotite takes place in acidic environments when S^{2-} surfaces are exposed. The following reactions describe pyrrhotite oxidation by O_2 and Fe^{3+}:

$$Fe_{1-x}S_{2(s)} + (2\text{-}0.5x)O_{2\ (aq)} + xH_2O \rightarrow (1\text{-}x)Fe^{2+}{}_{(aq)} + SO_4{}^{2-}{}_{(aq)} + 2xH^{+}{}_{(aq)} \quad (1.3)$$

$$Fe_{1-x}S_{2(s)} + (8\text{-}2x)Fe^{3+}{}_{(aq)} + 4H_2O \rightarrow (9\text{-}3x)Fe^{2+}{}_{(aq)} + SO_4{}^{2-}{}_{(aq)} + 8H^{+}{}_{(aq)}. \quad (1.4)$$

Sulfide-rich mineral oxidation results in the release of H^+, SO_4^{2-}, Fe, Ni, Al, Cu, Co, Cr, and other metals into the pore water. The fate of these constituents depends on leaching intensity. High rain water precipitation promotes sulfate and metal translocation to depth and their release to surface waters as acid mine drainage (AMD). However, in more arid systems, pore water solutions can become supersaturated with respect to sulfate solids, such as jarosite [$KFe_3(SO_4)_2(OH)_{6(s)}$]. The precipitation of Fe(III) sulfate solids can store significant amounts of acidity that is released when they dissolve.

Mines abandoned for long periods of time often exhibit a vertical oxidation profile. The degree of alteration can be simplified into three main categories: strongly oxidized zone, transition zone, and unaltered zone. The oxidation zone is mainly characterized by high concentrations of gaseous oxygen, high alteration and/or depletion of sulfide minerals, and high concentrations of sulfate secondary minerals (Gunsinger et al., 2006). Gunsinger et al. (2006) demonstrated that sulfide minerals found in the transitional zone show signs of rim chemical alteration, suggesting gradual primary mineral oxidation. Mineral oxidation depends on the oxygen diffusion rate through the tailings pore space, which is controlled by the water content in the tailings.

Figure 1-1 Possible slow geochemical processes occurring in the unsaturated zone of sulfidic mine tailings after deposition.

- Pyrite oxidation (oxygen path):
  $FeS_{2(s)} + H_2O + 7/2\ O_{2\ (aq)} \rightarrow Fe^{2+} + 2SO_4^{2-} + 2H^+$
- Pyrite oxidation (ferric iron path):
  $FeS_{2(s)} + 14Fe^{3+} + 8H_2O \rightarrow 15Fe^{2+} + 2\ SO_4^{2-} + 16H^+$
- Chalcopyrite oxidation (oxygen path):
  $CuFeS_{2(s)} + 4O_2 \rightarrow Fe^{2+} + Cu^{2+} + 2\ SO_4^{2-}{}_{(aq)}$
- Chalcopyrite oxidation (ferric iron path):
  $CuFeS_{2(s)} + 16Fe^{3+} + 8H_2O \rightarrow 17Fe^{2+} + Cu^{2+} + 2SO_4^{2-} + 16H^+$
- Sphalerite oxidation (oxygen path):
  $ZnS_{(s)} + 2O_2 \rightarrow Zn^{2+} + SO_4^{2-}$
- Sphalerite oxidation (ferric iron path):
  $ZnS_{(s)} + 8Fe^{3+} + 4H_2O \rightarrow Zn^{2+} + SO_4^{2-} + 8Fe^{2+} + 8H^+$
- Ferrous iron oxidation:
  $Fe^{2+} + ¼\ O_{2(aq)} + H^+ \rightarrow Fe^{3+} + ½\ H_2O$
- Ferrous iron precipitation:
  $Fe^{3+} + 3H_2O \rightarrow Fe(OH)_{3(s)} + 3H^+$

  $K^+ + 3\ Fe^{3+} + 2\ SO_4^{2-} + 6\ H_2O \rightarrow KFe_3(SO_4)_2(OH)_{6(s)} + 6\ H^+$
- Calcite acid-dissolution:
  $CaCO_{3(s)} + H^+ \leftrightarrow Ca^{2+} + HCO^-_3$

Salmon and Malmstrom (2006) studied mineral dissolution rates for sulfide-rich tailings and freshly crushed pyrite samples in an acid medium, using long-term batch experiments. Salmon and Malmstrom (2006) found that pyrite was primarily responsible for sulfate production in sulfide-rich tailings. They found that high amounts of SO_4^{2-} and Fe were released during the initial stage of batch experiments. Zinc and Cu release

showed similar behavior to SO_4^{2-} and Fe during the initial stage but showed a decreasing release rate with time. They also found that mineral composition and surface area have a strong influence on mineral weathering rates. Tailings samples with similar chemical and mineral compositions but with different specific surface areas, e.g. fine and coarse texture, exhibit different dissolution rates. In general, coarse textures showed slow release rates of sulfate (e.g. 7.73 x 10^{-7} mol g^{-1} d^{-1}) when compared with fine tailings (e.g. 9.81 x 10^{-6} mol g^{-1} d^{-1}).

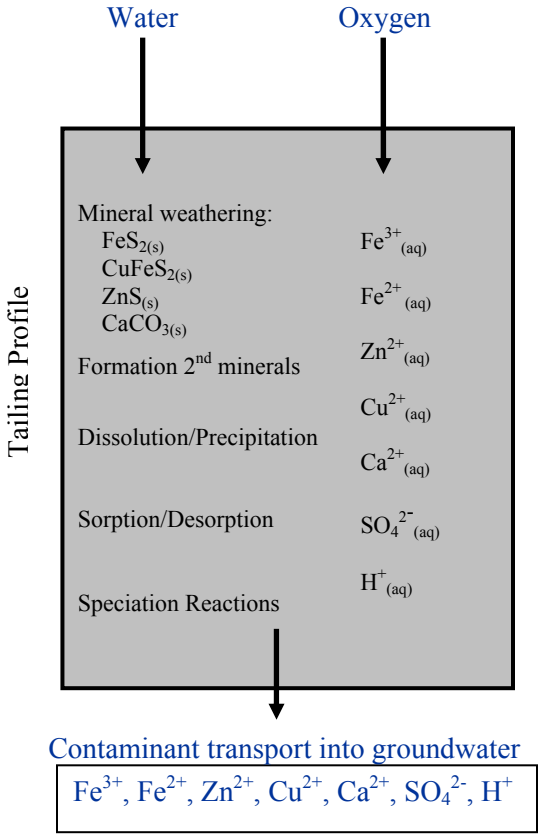

Figure 1-2 Conceptual model for possible geochemical processes in Klondyke site after tailing deposition.

1.1.2 Weathering of Sulfate Minerals

Sulfide-rich mine tailing deposits under oxic conditions tend to weather into sulfate containing minerals. In semi-arid and arid systems, a high precipitation of secondary sulfate minerals will be observed in the soil profile due to low rainfall and minimal solute leaching. Common examples of secondary sulfate minerals formed after the oxidation of sulfide-rich minerals are gypsum ($CaSO_4 \bullet 2H_2O$), jarosite ($KFe_3(SO_4)_2(OH)_6$), plumbojarosite ($PbFe_6(SO_4)_4(OH)_{12}$), schwertmannite ($Fe_8O_8(OH)_6(SO_4)$), melanterite ($FeSO_4 \bullet 7H_2O$), rozenite ($FeSO_4 \bullet 4H_2O$) and goslarite ($ZnSO_4 \bullet 7H_2O$). Figure 1-3 describes the oxidation processes of primary Fe-sulfide minerals and the formation of secondary sulfate minerals.

The earliest secondary crystallized mineral formed in sulfide mine tailings is usually gypsum, followed by hydronium jarosite (Giere et al., 2003). Ludwig et al. (1999) concluded that as pyrite oxidation increases, large amounts of gypsum are formed, and highly oxidized pyrite-containing sediments showed evidence of hydronium-jarosite formation.

Dissolution of secondary sulfate minerals can result in a tremendous release of metals and sulfate ions into the soil solution. Smith et al. (2006) studied the breakdown and release of K^+, Fe^{3+}, and SO_4^{2-} in synthetic jarosite, using batch experiments at two different pH values. At pH 2, which tried to mimic environments affected by acid mine drainage (AMD), only aqueous products (K^+, Fe^{3+}, SO_4^{2-}) were observed. In contrast, at pH 8 (which tried to mimic environments affected by AMD remediated with calcium hydroxide), poorly crystalline goethite precipitates were observed; iron ions were re-

precipitated into secondary phases, preventing Fe incorporation into the soil solution. Similar experiments were conducted by Smith et al., 2006 in order to describe plumbojarosite dissolution.

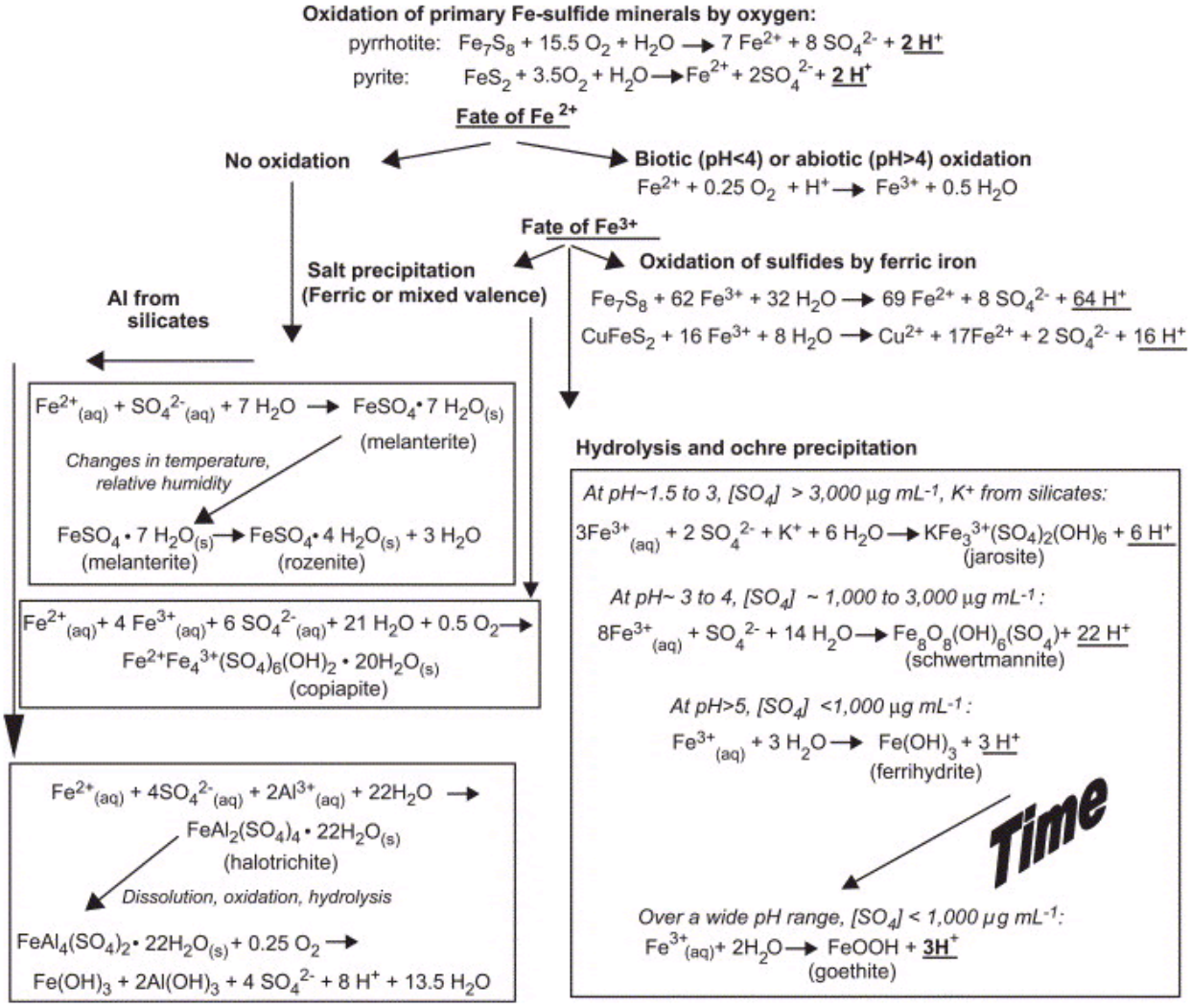

Figure 1-3 Processes describing the oxidation of primary Fe-sulfide minerals and secondary sulfate minerals formation. Figure obtained from (Hammarstrom et al., 2005).

Baron & Palmer (1996) also studied the solubility of jarosite ($KFe_3(SO_4(OH)_6$) in a series of dissolution experiments. They reported a log K_{sp} of -11.0 ± 0.3 for jarosite dissolution,

$$KFe_3(SO_4)_2(OH)_{6(S)} + 6H^+_{(aq)} \leftrightarrow K^+_{(aq)} + 3Fe^{3+}_{(aq)} + 2SO_4^{2-}{}_{(aq)} + 6H_2O. \quad (1.5)$$

Giere et al. (2003) studied the mobility and sequestration of Cu, Zn, Pb, and As in high sulfide waste piles. They found that the mobility and sequestration of Cu, Zn, Pb, and As is controlled by secondary minerals such as Fe-sulfoarsenates, melanterite, rozenite, and jarosite. They also established that the principal mechanism of metal transportation is through surface drainage during and after rainfalls.

Shum and Lavkulich (1999) studied solutions extracted from leached mine waste rock and the chemical data obtained was modeled in MINTEQA2 (US EPA 1991), a chemical equilibrium program. Saturation indices calculated in MINTEQA2 indicated that for pH less than 5 the Al activity can be controlled by jurbinite, alunite, and gibbsite. Goethite, hematite, and lepidocrocite, at pH values higher than 4, appear to control Fe activity. Cu solubility appears to be controlled by cupric ferrite and chalcanthite for pH values above 4.

The dissolution of jarosite can also be affected by the presence of organic matter. Chu et al., (2006) demonstrated that the addition of organic matter produces an increase in jarosite dissolution. In addition, high concentrations of sulfate and Fe^{3+} ion in soil solution were observed when organic matter was present.

Metal speciation is essential in order to understand the transport and fate of metals. Ostergren et al. (1999) characterized Pb speciation in tailings materials by using X-ray absorption fine structure (XAFS) spectroscopy. Empirical fittings for extended XAFS spectroscopy suggested that in tailings materials with low pH, the majority of Pb is in the form of Pb-bearing jarosite.

1.2 Phytostabilization as a Remediation Approach

In order to separate ore minerals from gangue minerals, miners often accelerate the process by milling up ores and dumping the leftover materials onto mine tailings piles. Gangue minerals are defined as worthless minerals mixed in with valuable ore minerals. These milled materials have a high surface area; therefore, the environmental conditions affect them more easily. Mine tailings occupy extended areas of our landscape and they are exposed to constant wind and water erosion. A possible strategy to minimize mine tailings erosion can be the use of phytostabilization techniques which try to immobilize contaminants in soil through the use of plants.

Phytostabilization is the use of plants to diminish contaminant migration by wind or water erosion. In the context of metal or metalloid contamination resulting from mine tailings, mechanisms of phytostabilization include contaminant absorption and accumulation by roots, adsorption onto root tissue surfaces, and/or precipitation within the root zone of plants. These processes result from a complex interplay relationship between plant roots, rhizosphere microorganisms, and inorganic soil media.

Phytostabilization techniques are intended to prevent human and ecosystem exposure and to avoid contamination of ground and surface waters.

In arid environments, such as the desert southwestern U.S. and northern Mexico, mine tailings are usually bare of vegetation and the introduction of plants can alter the speciation of toxic metals. The effect of plant exudates, such as organic acids, on heavy metals is likely to have important implications for phytostabilization strategies. The predominant characteristic of organic acids is the presence of metal complexing organic functional groups. These include most predominantly carboxyl (-COOH) and phenolic hydroxyl (phen-OH) functional groups, and smaller amounts of sulfhydryl (-SH) and amide (-NH-) groups. Some examples of organic acids commonly excreted by plants are citric, malic, and oxalic acid. Organic acids are implicated in numerous soil processes such as metal complexation, root nutrient uptake, mineral dissolution and microbial metabolism (Jones, 1998).

1.3 Organic Acids

Organic acids are found in different plant organelles including vacuoles, cytoplasm and mitochondria. The total organic acid concentration found in plant cells is about 5-50 mM (Ryan et al., 2001). Under neutral conditions, organic acids such as malic and citric are dissociated (pH > pKa) and are excreted from plant roots into soil media as organic anions. The maximum oxalate concentration in soil solution rarely exceeds 50 μM, since this is the concentration at which Ca^{2+}-oxalate precipitates are formed in soil solution (Jones et al., 2003). The organic anion concentration found

experimentally in the soil solution is 1-100 μM (Jones, 1998). The release of organic anions into the rhizosphere soil depends on the root system and the associated microorganisms.

Environmental conditions associated with increased organic anion excretion from plants include nutrient deficiency, high concentrations of toxic metals, and others. Organic anions have been related to the solubilization and mobilization of Mn, Cu, Zn, Fe, and P. Organic anions that contain tricarboxylate functional groups (e.g., citrate^{3-}) have a high affinity for cations such as Al^{3+}, Fe^{3+}, and Ca^{2+} and form stable complexes (Ryan et al., 2001). Other associated functions of organic acids are energy production and balancing the cation charge (Jones, 1998).

1.3.1 Fate of Organic Acids

Excretion of organic anions from the root system can be followed by sorption to the soil solid phase, biodegradation by microorganisms, metal complexation, and/or leaching to groundwater (Jones et al., 2003). The behavior of monovalent (acetate), divalent (malate or oxalate), and trivalent (citrate) organic anions in soil differs depending on the number of carboxyl groups. Trivalent anions have a high tendency to be absorbed into the soil solid phase (Jones et al., 2003).

Organic acids are utilized as carbon and energy sources by microorganisms; therefore, a lower concentration of organic anions is available for mineral dissolution, nutrient uptake, and metal detoxification (Ryan et al., 2001). The biodegradation rate of

organic anions by soil microorganisms is fast and the half-lives can range from 1 to 5 h in organic rich surface soils and 5 to 12 h in mineral subsurface soils (Jones et al., 2003).

1.3.2 Organic Acid Influence on Solubilization and Mobilization of Different Metals

1.3.2.1 Lead and Zinc

Wu et al. (2003) studied the effect of organic acids on the adsorption of Pb to montmorillonite, goethite, and humic acids. In general, the amount of Pb adsorbed to the soil mineral components (montmorillonite and goethite) decreased with increasing concentrations of citric acid, whereas this was not observed for humic acid. Ousmanova and Parker (2007) studied the removal of Pb from contaminated soils, using organic acids generated in batch experiments with different fungal species. Solutions containing high concentrations of citric acid produced the greatest Pb extraction. Yang et al. (2006) found that lead exhibits high solubilization at lower pH values. High concentrations of citric or acetic acid ($>10^{-3}$ mol L^{-1}) enhance lead mobilization from clayey soils. Oxalic acid showed little effect on lead mobilization.

Fomina et al. (2004) studied the influence of mycorrhizal fungi on zinc phosphate (hopeite) and lead chlorophosphate (pyromorphite) solubilization. Mycorrhizal fungi cultures exposed to Zn-Pb-phosphate minerals (toxic metal minerals) were capable of producing a wide variety of organic acids in response to phosphate deficiency. *Beauveria caledonica 4* was the only strain capable of producing citric and oxalic acid when exposed to phosphate minerals. In addition, a substantial amount of pyromorphite was

solubilized when exposed to *B. caledonica 4*, suggesting that oxalic acid plays an important role in pyromorphite transformation.

Miretzky et al. (2006) determined the effect of weak organic acid salts on Zn(II) desorption from a sandy loam soil, using small column experiments. The most efficient organic acids for removing Zn were citrate and oxalate anions.

1.3.2.2 Aluminum

Micromolar concentrations of Al^{3+} in the soil solution can slow the growth of several plant species (Ryan et al., 2001). Hence, complexation by organic acids is a strategy that is used by some plants to diminish the size of the inorganic monomeric pool of this toxic cation, thereby reducing its bioavailability. However, organic acid production can also increase the rate and extent of Al dissolution from mineral solids. Some hydroxide and aluminosilicate minerals controlling Al^{3+} concentrations in soil solution are gibbsite, illite, vermiculite, smectite, and kaolinite. Prior research has shown that Al-tolerant plants release significant amounts of malate and citrate organic anions into the rhizosphere zone (Nian et al., 2002; Jones, 1998). After organic anion excretion, Al-organic complexes are formed making the roots more resistant to aluminum.

1.4 Research Objectives

The specific objective of this study was to examine the effect of irrigation with local groundwater and the impacts of low molecular weight organic acids produced by plants and root-associated microbes on the fate and transport of heavy metals in 50 years

old sulfate-acid mine tailings. I hypothesized that tailing irrigation with local groundwater will promote incongruent weathering of metal-sulfate minerals and further formation of thermodynamically stable (oxyhydr)oxide solids phases. The nature of this incongruent weathering process will control the release of heavy metals into the soil solution, and possibly their re-sorption to newly formed solid phase precipitates. The formation of (oxyhydr)oxide products is also hypothesized to sequester some of the Pb, Zn, Al, and Fe that might be otherwise released from the columns. Another expected result is the incremental increase in metal mobilization with increasing concentration of oxalic acid.

CHAPTER 2: MATERIALS AND METHODS

2.1 Study Site Description

2.1.1 Klondyke Tailings

The Klondyke State Superfund Site is located in Graham County, Arizona (N32 50.990 W110 20.552) within the Aravaipa Creek watershed. The Klondyke area was mined from the 1870s to the mid 1900s and the primary extracted metals were lead and zinc. The mineral composition of the deposited material, after ore extraction, was pyrite (FeS_2), sphalerite (ZnS), galena (PbS), chalcopyrite ($CuFeS_2$), and calcite ($CaCO_3$) (Arizona Department of Environmental Quality, 2000). The Arizona Department of Health Services reported that approximately 54,000 m^3 of tailings remain on the property on an area of 100.6 by 73.2 meters and constitute a significant source of contamination. Klondyke tailings are the byproducts of a flotation mill that was abandoned in 1950. The tailings piles contain a gradient in pH and metal concentrations (Scott White and Tom Thompson, pers. commun.). For the purposes of this study, tailings were sampled from two representative locations to assess the effects of pH and metal concentration differences.

Klondyke tailings are barren of vegetation (Figure 2-1) and have poor aggregate structure. As a consequence, they are susceptible to wind and water erosion. The tailings were deposited about 9 m from the east bank of Aravaipa Creek. The proximity of the tailings to the creek increases the risk of surface and ground water contamination. It has been estimated that 49% of the original deposition has been eroded from the tailings by

the action of wind and water. Figure 2-2 shows a significant loss of tailings in the study area.

Figure 2-1 Klondyke mine, located at Graham County.

Figure 2-2 A significant loss of tailings can be observed in this picture as a consequence of wind and water erosion at the Klondyke site. Pictures were taken by the author.

2.2 Tailings Collection

Contaminated tailings were collected from the abandoned Klondyke Site in 2006. The upper layer of Tailing One (T1), about 20 cm, was tilled using a roto-tiller. The tilled tailing was mixed, in order to ensure homogeneity, and transferred into five-gallon buckets that were then sealed. The same procedure was followed for collection of Tailing Two (T2). Upon arrival at the Environmental Biogeochemistry Laboratory at the University of Arizona, the tailings were sieved to obtain the fine earth (< 2 mm) size fraction, which was air dried for a period of two weeks, and stored in five-gallon buckets at room temperature.

2.3 Tailings Characterization

2.3.1 Solid Phase

A series of analytical methods were employed in order to assess the physical, chemical and mineralogical characteristics of the mine tailings. Total carbon, total nitrogen, and inorganic carbon in the solid samples were determined in triplicate using high temperature oxidation followed by infrared detection of CO_2 and NO using a Shimadzu TOC-VCSH system equipped with a solid sample module SSM-5000A (Columbia, MD). Five grams of each tailings material were sent to Activation Laboratories (Ancaster, Ontario) for determination of total elemental concentrations by lithium metaborate/tetraborate fusion followed by inductively coupled plasma optical emission spectrometry (ICP-OES) and mass spectrometry (ICP-MS). [Actlabs Procedure:

ICP whole rock, Major Elements Fusion ICP (WRA), Trace Elements Fusion ICP/MS (WRA4B2), and Total Digestion ICP (TOTAL)].

Particle size analysis was completed using the pipette method (Gee and Bauder, 1986). Particle density (ρ_s) was determined using the pycnometer method (Blake and Hartge, 1986.). The pycnometer is a small glass container that can be filled repeatedly on an exact constant volume. The bulk density (ρ_b) was assessed by mass difference, and porosity was determined by the following equation:

$$\text{Porosity} = 1 - (\rho_b / \rho_s) \qquad (2.1)$$

2.3.2 Saturation Aqueous Extraction

To provide a measure of pore water chemistry and the influence of tailings-water equilibration time, a saturation aqueous extraction was performed and the extracted solution was characterized after 1 h and 24 h equilibration times. Ten grams of air-dried tailings were measured into polypropylene-copolymer (PPCO) vessels and ultrapure (Barnstead) water was added at a mass ratio of 1:1. The samples were agitated for either 1 h or 24 h at 10 rpm. The suspensions were then centrifuged for 30 min with average relative centrifugal force (RCF) of 12,000 (g force). The supernatant solution was collected, filtered through an acid washed and water rinsed filter (GHP: Hydrophilic polypropylene membrane, 0.2μm), and stored at 4°C until it was analyzed.

The pH and electrical conductivity (EC) were measured using a pH/ISE/Conductivity meter (VWR symoHony Model SR60IC). Total organic carbon

(TOC), inorganic carbon (IC) and total nitrogen (TN) were measured using a Shimadzu TOC-VCSH analyzer. Inorganic anions (Cl^-, F^-, NO_2^-, NO_3^-, SO_4^{2-}, PO_4^{3-}) were measured by ion chromatography (Dionex Ion Chromatograph DX-500, Sunnyvale, CA) using the Ion Pac AS11 column with a guard column (AG11) and sodium hydroxide (50mM) as the mobile phase. The metals and metalloids were determined by inductively coupled plasma mass spectrometry (ICP-MS) (ELAN DRC-II, Perkin Elmer, Shelton CT). Ammonium was measured colorimetrically (Mulvaney, 1996) using a Shimadzu UV-2501PC Spectrophotometer.

2.4 Ground Water Characterization

In Klondyke site, phytostabilization may make use of local groundwater wells for irrigation. Since the chemistry of groundwater differs from that of pure water, its composition was determined so that a model surrogate could be used in the column experiments. A ground water well located approximately 90 m from the north bank of the tailings was sampled with water being transferred into an amber bottle, and filled to avoid head space. Upon arrival at the University of Arizona, the water sample was stored at 4°C and analyzed within a week. The pH, inorganic anions, major cations and metals were determined. All measurements were run in triplicate. The data gathered from these analyses were used to prepare a synthetic ground water (SGW) solution that was then used to irrigate columns containing mine tailings.

2.5 Column Experiments

2.5.1 Column Packing and Setup

Polypropylene columns, 3.2 cm high by 0.9 cm diameter (total volume 2.0 cm^3), were packed with sieved and air-dried tailings and stored in the dark until experiments were performed. A polyethylene frit with a pore size of 20 μm was placed at the bottom and top of the column. An extra nylon filter with a pore size of 0.45 μm was placed in the outlet of the column in order to avoid fine silt and clay loss. In order to calculate the bulk density, the empty column plus frits and the filter were weighted. The column was filled with tailing material and re-weighed. The mass of tailings was divided by their volume for each column to assess the bulk density.

The experimental setup for the column studies is shown in Figure 2-3. A peristaltic pump (Sarah Standard Cassette Pump) was set up to drive a constant flow of 0.04 ml min^{-1}, which translates to a Darcy flux of 0.06 cm min^{-1}. The slowest flow rate available was chosen in order to maximize fluid-tailings interaction time. The influent solution was added from the bottom to provide upward solution flux in order to diminish preferential flow. The effluent solution was collected every 25 min using a fraction collector (Foxy 200, Isco Inc., Lincoln, Nebraska); a total of ca. 26 pore volumes (PV) were collected for each replicate. Each column experiment comprised three phases. During the first phases of the experiment, ca. 13 PV were collected. The second phase is characterized by the cessation of the constant flow. During this phase, the water saturated columns were immediately capped and placed in an end-over-end shaker for a period of two weeks at 7 rpm. The aim of this "equilibration period" was to make it possible to assess the extent to

which metal dissolution exhibits kinetic limitations. After the equilibration period, the column was reinstalled at the pump and influent solution was re-applied at 0.04 ml min^{-1} for collection of ca. 13 additional pore volumes (3^{rd} phase). The effluent was collected in 8 ml-glass tubes. All column experiments were run in triplicate.

Figure 2-3 Column experimental setup.

2.5.2 Treatments

Based on analysis of local groundwater (section 2.4), a synthetic ground water (SGW) solution was prepared by adding the following reagents to Barnstead water: $KHCO_3$, $NaHCO_3$, $MgSO_4$, $CaCl_2$, $Ca(NO_3)_2$, and $CaSO_4$ (See Table 2.1). The SGW solution was bubbled with "breathing quality" air for 24 h in order to equilibrate it with ambient CO_2. The solution pH was then adjusted to 7.75 by dropwise addition of 0.1 M HCl.

Table 2-1 Groundwater recipe

Reagent	μmoles L^{-1}
$KHCO_3$	472
$NaHCO_3$	1550
$MgSO_4$	111
$CaCl_2$	733
$Ca(NO_3)_2$	119
$CaSO_4$	50

Both native groundwater and SGW represent solutions close to equilibrium with calcite, the principal aquifer lithology. A NaCl solution with the same ionic strength as the SGW was used to assess tailings dissolution under conditions of lower calcite and gypsum saturation state, to see if influent solution chemistry strongly affects element release patterns. The ionic strength of the NaCl solution was 0.0142 moles L^{-1} in order to match that of the SGW solution.

A stock solution of 1 mM oxalic acid was used to prepare solutions of 10 and 100 μmol L^{-1} oxalic acid in a background of SGW solution. Sodium chloride, and 10 and 100 μmol L^{-1} oxalic acid solutions were all equilibrated with breathing quality air for 24 h and the solution pH was adjusted to 7.75. The resulting solutions were applied to mine tailings in column experiments in order to simulate field conditions. The high prevalence of oxalic acid in the soil solution makes this low molecular weight organic acid a good candidate to be used in this experiment. In addition, oxalic acid exhibits a high affinity toward heavy metals, suggesting the formation of strong metal-oxalate complexes.

2.5.3 *Effluent Analysis*

The pH, anions, metal(loids), total nitrogen, and total organic carbon concentration were measured in each pore volume. Dilutions used for ICP-MS analyses were made with 1% HNO_3.

2.5.4 Speciation and Dissolution Model

MinteqA2 for Windows, (Version 1.50, Allison Geoscience Consultants, Inc.), an equilibrium speciation model, was used to predict chemical processes taking placed in the column systems. The MinteqA2 for Windows database was supplemented with data from the literature for plumbojarosite and Zn talc (Kashkay et al., 1975 and Allada et al., 2006, respectively); mineral formation reactions and stability constants were obtained from NIST Standard Reference Database 46 Version 7.0 (Martell and Smith, 2003). Saturation indices were employed to determine the possible minerals that were undergoing precipitation or dissolution and to predict which minerals were controlling the species dissolution.

The value of the saturation index (Ω) describes quantitatively the relative saturation of an aqueous solution with respect to equilibrium with a solid phase. Saturation index is defined with the following equation:

$$\Omega = IAP/K_{so} \tag{2.2}$$

The ion activity product (IAP) is the reaction quotient that includes all species activities involved in a chemical reaction with the exception of solvent water and solids (which are assigned unit activity). Hence, IAP is the reaction quotient under any specified condition. The solubility product constant (K_{so}) is also the reaction quotient including all species with the exception of water and solids, but specified for equilibrium conditions.

MinteqA2 for Windows reports the logarithm value of the saturation index (Ω) for all pertinent minerals for which thermodynamic data are located in the database. For log Ω higher than zero, the system is supersaturated with respect to that specific mineral. For log Ω equal to zero, the system is in equilibrium with respect to that specific mineral, and for log Ω lower than zero, the system is undersaturated with respect to that specific mineral.

CHAPTER 3: RESULTS

3.1 Physico-Chemical Characterization of Tailings

3.1.1 Solid Phase Characterizations

The particle size distribution for Klondyke tailings is shown in Table 3-1. This particle size distribution places both tailings (T1 and T2) into the texture class of sandy loam.

Mineralogical characterization of the tailings has been conducted by Ph.D. candidate Sarah Hayes, and a summary of her data is provided here. The detected mineral constituents of T1 and T2 are: orthoclase ($KAlSi_3O_8$), quartz (SiO_2), gypsum ($CaSO_4 \bullet 2H_2O$), jarosite ($KFe_3(SO_4)_2(OH)_6$), plumbojarosite ($PbFe_6(SO_4)_4(OH)_{12}$), goslarite ($ZnSO_4 \bullet 7H_2O$), Zn-talc ($Zn_xMg_{3-x}Si4O10(OH)_2$), and anglesite ($PbSO_4$). Likely solid phase products from dissolution reactions of these minerals are: goethite (FeOOH), hematite (Fe_2O_3), ferrihydrite ($Fe(OH)_3$), kaolinite ($Al_2Si_2O_5(OH)_4$), melanterite ($FeSO_4 \bullet 7H_2O$), rozenite ($FeSO_4 \bullet 4H_2O$), illite, smectite, and vermiculite.

Table 3-1 Particle Size Distribution

Tailing	% sand	% silt	% clay	% Recovery	Texture Class
T 1	57.05	23.17	9.03	89.25	Sandy Loam
T 2	64.06	19.46	6.66	90.18	Sandy Loam

Table 3-2 Elemental content of untreated mine tailings at Klondyke and the tailing enrichment factor with respect to the crustal rock content. All data are given in mg kg^{-1}. Enrichment factor values calculated from concentration ratio of tailings to average crustal rock (Sposito, 1989). n.a represents no available data.

Element	Crust	T1	EF	T2	EF
Si	277,000	339,000	1.22	321,600	1.16
Al	82,000	22,600	0.28	14,500	0.18
K	21,000	19,800	0.94	11,800	0.56
Ca	41,000	19,000	0.46	47,200	1.15
Fe	41,000	17,300	0.42	23,900	0.58
S	260	17,000	65.38	26,900	103.46
Pb	14	4,600	328.57	13,800	985.71
Mn	950	2,800	2.95	12600	13.26
Zn	75	1,400	18.67	5,600	74.67
Mg	23,000	1,200	0.05	2,900	0.13
Ba	500	910	1.82	600	1.20
Ti	5,600	840	0.15	850	0.15
Na	23,000	740	0.03	890	0.04
Cu	50	650	13.00	1,600	32.00
Sr	370	110	0.30	60	0.16
As	1.5	91	60.67	230	153.33
P	1000	65	0.07	110	0.11
Bi	n.a.	48	n.a.	96	n.a.
Cr	100	40	0.40	20	0.20
Mo	1.5	30	20.00	73	48.67
Cs	3	26	8.67	15	5.00
V	160	19	0.12	18	0.11
Se	0.05	14	280.00	<3	n.a.
Sb	0.2	10	50.00	50	250.00
Ag	0.07	5.2	74.29	10.4	148.57
U	2.4	3.6	1.50	3.5	1.46
Sc	16	3	0.19	3	0.19
Ni	80	3	0.04	4	0.05
Be	2.6	3	1.15	3	1.15
Sc	16	3	0.19	3	0.19
Cd	0.11	2.4	21.82	18.3	166.36
Co	20	2	0.10	8	0.40
Sn	2.2	2	0.91	24	10.91
Br	0.37	1.2	3.24	<0.5	n.a.

Lithium metaborate fusion followed by ICP-MS provided a total elemental analysis of T1 and T2 (Table 3-2). These solid phase element concentrations can be normalized to average crustal rock abundances to provide a measure of the tailings enrichment factor (EF) in the measured elements. Enrichment factor values calculated from concentration ratio of tailings to average crustal rock. Sposito (1989) indicates that values of EF between 2 and 10 indicate significant enrichment and values higher than 10 indicate strong enrichment. Considering these criteria, Zn, Pb, As, Sb, Cu, Cd, S, Ag, and Mo are strongly enriched in the tailings material relative to uncontaminated crustal rock. In general, T2 contains a higher concentration of toxic metals than T1.

The organic and inorganic carbon, and total nitrogen values for the Klondyke tailings are shown in Table 3-3. The inorganic carbon of T1 was below detection limits, whereas T2 yielded an inorganic carbon content of 14.16 ± 0.53 mg C kg^{-1}.

Table 3-3 Organic carbon, total nitrogen, and inorganic carbon for untreated Klondyke tailings. All values are given in mg kg^{-1}. S.D. represents the standard deviation of three replicates.

Tailing	Organic Carbon	S.D.	Total Nitrogen	S.D.	Inorganic Carbon	S.D.
T1	358.6	67.9	66.6	12.1	n.a.	n.a.
T2	411.44	84.97	68.5	10.7	14.16	0.53

n.a. Under detection limit.

3.1.2 Aqueous Phase Characterization

To assess the chemical composition of the aqueous phase following reaction of pure water with the tailings, T1 and T2 were equilibrated with ultrapure (Barnstead)

water for 1 and 24 h in saturated pastes. The pH and electrical conductivity (EC) values for the aqueous extractions at 1 h and 24 h are summarized in Table 3-4. The results show that T1 is significantly more acidic than T2, which is also consistent with the lack of detectable carbonate in the solid phase of the former tailing. Total dissolved solids are slightly higher in T2 relative to T1, but the difference in EC is small relative to the pH difference. Sposito (1989) reported the traditional and proposed classification categories for salt affected soils. Traditional classification defines saline-sodic soils as soils with high soluble salt and high exchangeable sodium with an EC higher than 4 dS m^{-1}. On the other hand, the Terminology Committee of the Soil Science Society of America has proposed EC > 2 dS m^{-1} for saline-sodic soils. Under the traditional classification, Klondyke tailings (T1 and T2) are not classified as saline-sodic soils, but under the proposed classification both tailings can be classified as saline-sodic soils. Saline soils affect plant growth because large amounts of energy have to be expended for water absorption from the soil solution.

Table 3-4 pH and electrical conductivity for two different equilibration times (1h and 24h) after a saturated aqueous extraction. All units but pH are dS m^{-1}. S.D. represents the standard deviation of three replicates.

Tailing	pH (1hr)	S.D.	EC (1hr)	S.D.	pH (24hrs)	S.D.	EC (24hrs)	S.D.
T1	3.87	0.06	3	0.1	3.82	0.05	3.1	0.01
T2	5.44	0.03	3.49	0.05	5.54	0.10	3.63	0.07

Dissolved anions in the aqueous extracts as measured by ion chromatography (IC) are shown in Table 3-5. In addition to those anions measured by IC, aqueous HCO_3^-

concentrations were calculated from the total inorganic carbon (TIC) and pH values. Most notable is the high concentration of sulfate released to solution. Sulfate values for T1 after 1 h and 24 h are 21,400 ± 100 μmoles L^{-1} and 21,500 ± 50 μmoles L^{-1}, respectively. Slightly higher sulfate values were consistently observed for T2.

Table 3-5 Anions in solution for two different equilibration times (1h and 24 h) after a saturated aqueous extraction. All values are given in μmol L^{-1}. S.D. represents the standard deviation of three replicates.

Anion	T1 (1h)	S.D.	T2 (1h)	S.D.	T1 (24h)	S.D.	T2 (24h)	S.D.
SO_4^{2-}	21,400	100	25,200	600	21,500	500	25,900	400
F^-	900	20	710	30	1200	15	860	13
NO_3^-	260	13	600	90	210	4	590	80
Cl^-	140	30	150	30	110	16	140	10
NO_2^-	85	30	90	10	110	40	100	30
HCO_3^-	0.292	0.076	10.237	1.149	0.276	0.017	13.631	1.627

Elements accessible to ICP-MS analysis include all major cations and trace elements and their concentrations in solution following 1 or 24 h equilibration times are given in Table 3-6. In T1 (1h), Ca, Zn, Mn, K, Cu, and Al were the most abundant cations and trace elements in the aqueous extraction. For T2 (1h), the most abundant cations and trace metals in the aqueous solution were: Ca, Zn, Mn, Mg, K, and Si.

The aqueous extraction contains higher concentrations of Ca, Zn, and Pb in T1 (1h) than T2 (1h), even though the elemental concentration of Ca, Zn, and Pb in the solid phase is higher in T2 than T1, suggesting the presence of labile minerals in T1.

Table 3-6 Element aqueous concentrations measured by ICP-MS following 1 h and 24 h equilibration times. All values are given in μmol L^{-1}. S.D. represents the standard deviation of three replicates.

Element	T1 (1hr)	S.D	T2 (1hr)	S.D	T1 (24hrs)	S.D	T2 (24hrs)	S.D
Ca	17,800	4,800	13,900	1,050	14,700	430	13,900	500
Zn	5,900	1,400	4,700	150	4,500	200	5,300	200
Mn	1700	13	4,400	200	1,830	40	5,100	300
K	880	5	770	20	800	9	720	40
Cu	430	5	18.3	2.6	500	10	18.9	0.23
Al	390	5	13	3	660	30	16.66	0.16
Mg	360	3	4,200	300	460	5	4,500	300
Si	230	20	590	30	690	5	1,000	10
Na	130	4	290	6	130	2	230	7
Pb	11.21	0.62	9.12	2.83	13.24	0.08	9.32	0.18
Cd	5.8	0.11	19.61	0.02	7.27	0.06	29.45	0.82
Ni	5.7	0.14	2.53	0.07	5.82	0.04	2.85	0.04
Co	3.72	0.09	1.54	0.05	3.32	0.03	1.32	0.02
Se	2.01	0.02	1.1	0.03	1.77	0.003	0.94	0.02
As	0.43	0.01	0.36	0.03	0.34	0.02	0.3	0.01
P	0.42	0.73	1.94	0.24	2.8	2.6	2.8	2.6
Ti	0.17	0.02	0.25	0.03	0.05	0.03	0.06	0.02
U	0.153	0.008	0.003	0.0001	0.156	0.017	0.004	0.001
Fe	0.1	0.02	0.45	0.74	0.34	0.14	0.42	0.58
Ba	0.08	0.02	0.132	0.001	0.05	0.01	0.15	0.003
Ag	0.004	0.0001	0.001	0.0002	0.004	2E-04	0.01	0.001
Mo	0.002	0.0002	0.009	0.004	0.02	0.004	0.01	0.002
Sn	0.002	0.00002	0.002	0.001	0.02	0.01	0.02	0.01
Bi	0.002	0.0002	0.002	1E-04	0.002	0.001	0.001	0.0004
Cr	<1.81E-12		<1.81E-12		0.013	0.014	<1.81E-12	
Sb	<2.71E-13		<2.71E-13		0.005	0.001	0.003	0.001

Table 3-7 shows the organic and inorganic carbon and the total nitrogen of Klondyke tailings after 1 h and 24 h of equilibration. Colorimetric methods were employed in order to determine the ammonium concentration in aqueous extracts of the Klondyke tailings after 1 and 24 hr equilibration times (Table 3-8).

Table 3-7 Total organic carbon, total nitrogen, and inorganic carbon in solution after 1 h of equilibration time for a saturated aqueous extraction. All values are given in mg L^{-1}. S.D. represents the standard deviation of three replicates.

	T1 (1h)	S.D.	T2 (1h)	S.D.	T1 (24h)	S.D.	T2 (24h)	S.D.
Total Organic Carbon	38.3	6.9	30.2	2.1	20.4	3.7	18.2	5.2
Total Nitrogen	19.8	1.2	13.6	1.8	15.3	1.6	12.1	1.5
Inorganic Carbon	5.4	1.4	5.7	1.4	5.73	0.36	6.2	0.74

Table 3-8 NH_4^+-N values after 1hr and 24 hrs of equilibration time for a saturated aqueous extraction. All values are given in μmol L^{-1}. (Mean ± standard deviation of three replicates)

Tailing	NH_4^+-N (1hr)	NH_4^+-N (24hr)
T1	0.94±0.04	0.95±0.05
T2	0.61±0.01	0.61±0.03

3.2 Ground Water Characterization

A ground water well near the Klondyke tailings was sampled and analyzed in order to create a synthetic background solution that models irrigation water and could be used in the column experiments. Tables 3-9 and 3-10 summarize the groundwater (GW) chemistry data. The pH of the groundwater sample was 7.74 ± 0.01 (from three replicates) and the ionic strength was 14.22 mM. Only the major anions and cations were included in the ground water recipe.

The most abundant anion in the groundwater sample was Cl^- followed by NO_3^- and SO_4^{2-}. In contrast with the aqueous extraction solution in T1 (1h), the most abundant anion was SO_4^{2-} followed by F^- and NO_3^-. High concentrations of sulfate were observed in the aqueous extractions because Klondyke tailings are rich in labile sulfate minerals. See section 2.5.2 (Table 2.1) for the actual groundwater recipe.

Higher concentration of Na was observed in the groundwater sample than in the aqueous extraction solution for T1 (1h). Both the groundwater sample and the aqueous extraction solution for T1 (1h) contain high concentrations of calcium; Ca concentration in GW solution was 900 μmol L^{-1} and in the aqueous extraction solution (T1/1h) was 17,800 μmol L^{-1}.

Table 3-9 Inorganic anions in groundwater well near the Klondyke Site. S.D. represents the standard deviation of three replicates.

Anion	μmoles L^{-1}	S.D.
Cl^-	441.73	0.01
NO_3^-	237.5	0.3
SO_4^{2-}	161.1	0.2
NO_2^-	0.57	0.3
PO_4^{3-}	<0.2721	
F^-	<0.0286	

Table 3-10 Metal(loids) in groundwater well near Klondyke Site.

Element	Groundwater (μmoles L^{-1})	Element	Groundwater (μmoles L^{-1})
Na	1500	U	0.0818
Ca	900	Ag	0.0593
Si	480	Al	0.0237
K	470	Cr	0.0223
Mg	110	Mn	0.0206
Ba	0.3371	Ni	0.0203
As	0.2736	Ti	0.0102
Zn	0.2156	Mo	0.0055
Fe	0.1898	Pb	0.0006
Se	0.1199	Sb	0.0006
Cu	0.1007	Cd	0.0001

3.3 Column Experiments

Saturated flow column experiments were run to compare the effects of different influent solutions on element release from T1 and T2. The influent solutions included (i) a simple 1:1 electrolyte solution (14.22 mM NaCl solution), (ii) a synthetic ground water (SGW) solution of the same ionic strength that models the groundwater well chemistry, and (iii) SGW solution plus oxalic acid at two concentrations (10 and 100 μM). The latter two solutions, referred to hereafter as SGW+10 and SGW+100 respectively, were intended to model the influence of a common rhizosphere low molecular weight organic acid. Effluent solutions were analyzed for pH, TOC, anions and metal(loids). The experiments comprise three "phases": (i) initial constant flow for *ca*. 13 pore volumes, (ii) a stopped flow equilibration period of two weeks, and (iii) final constant flow for *ca*. 13 pore volumes. The intent of the stopped flow was to assess kinetic limitations to geochemical release.

Each treatment was run in triplicate. The data points shown in the following figures represent the mean of three replicate samples extracted at a given pore volume, and the error bars represent the 95% confidence interval. Therefore, differences significant at the $\alpha = 0.05$ level are indicated by those cases where the error bars do not overlap.

3.3.1 pH

The eluted pH from T1 increased with increasing pore volume in phases 1 and 3 (Figures 3-1a). The effluent pH values for the SGW treatment showed an increase during

phase 3. In T1, the pH values did not show statistically significant differences, regardless of the treatment used.

In T2, the eluted pH increased with increasing pore volume during phase 1, it dropped at the beginning of phase 3, right after the stopped flow equilibration period, and then increased again with re-introduction of flow (Figure 3-1b). Also in T2, the NaCl treatment had the lowest mean values when compared to the other treatments, suggesting this treatment had less impact on proton consumption. In T2, during phase 1 of NaCl treatment, the data suggest a statistically significant difference between this treatment and SGW, SGW+10 and SGW+100 treatments, with the exception of the first collected pore volume. The effluent pH values in T2 were closer to influent solution pH (7.74) than was the case for T1. T1 is more acidic and apparently better buffered than T2.

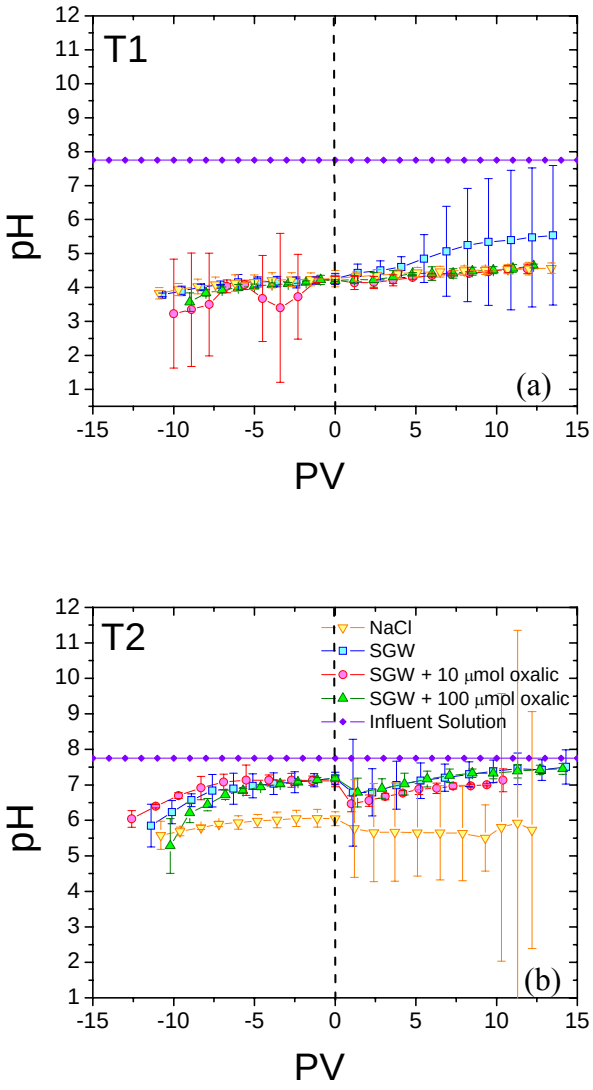

Figure 3-1. Effects of NaCl, SGW, SGW+10 and SGW+100 treatments on effluent pH during and after the stopped-flow experiment. Negative PV values represent the constant flow pore volumes preceding the stopped flow period (phase 1), dashed line indicates the stopped flow period (phase 2), and positive PV values represent re-application of the constant flow (phase 3). Error bars represent 95% confidence limit.

3.3.2 Total Organic Carbon Elution

Total organic carbon (TOC) was measured for SGW, SGW+10 and SGW+100 treatments (Figure 3-2). In T1 and T2, the higher concentration of TOC was observed during the first eluted pore volume. In T1, high mobilization of TOC was reported during the application of SGW treatment (Figure 3-2a). Similar TOC mobilization was observed during SGW+10 and SGW+100 treatments in T1. In T2, TOC mobilization was similar during SGW, SGW+10 and SGW+100 treatments (Figure 3-2b). The total organic carbon reported for T1 and T2 (after 1hr of equilibration time) in µmoles L^{-1} was 3,190 and 2510, respectively (section 3.1.2, Table 3-7). The total organic carbon eluted during the column experiments did not exceed the TOC reported after the aqueous extraction for 1 hr of equilibration time.

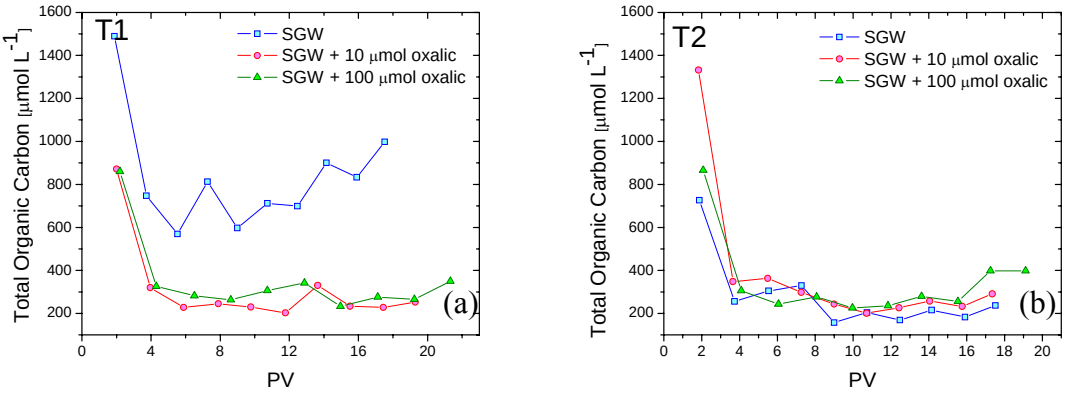

Figure 3-2. Total organic carbon in effluent solution after the application of SGW, SGW+10 and SGW+100 solution treatments to T1 and T2. The data presented in these figures correspond to only one replicate. All data was collected from the application of a constant flow with out stopping the flow.

3.3.3 Column Anion Elution

A large amount of SO_4^{2-} was mobilized from T1 and T2 (Figures 3-3a and 3-3b). In T1 and T2, high amounts of SO_4^{2-} mobilization were observed during the first pore volumes and decreased with increasing pore volume during phase 1. The increase in sulfate concentration after the equilibration period (phase 2) suggests that sulfate mineral dissolution exhibits kinetic limitations on the time scale of the column experiment. Sulfate mobilization did not appear to be affected by the different treatments used in this experiment with the exception of the first pore volume in SGW+10 and SGW+100 treatments during phase 1 (T1).

Fluoride mobilization in T1 decreased over phase 1, and then increased just after phase 2, suggesting that F-containing minerals exhibited dissolution kinetic limitations (Figure 3-3c). A higher amount of F^- mobilization was observed during the early part of phase 1 (first pore volume for all treatments), with the exception of SGW+10. In T1 (phase 1), the data suggest that there was no significant difference in F mobilization associated with treatment with the exception of SGW+10 and SGW+100 during the first PV. During phase 3 of NaCl treatment, the data suggest a statistically significant difference in pore volume 4 between this treatment and SGW, SGW+10 and SGW+100 treatments. In addition, the last PV (phase 3) exhibited statistically significant differences between all treatments with the exception of SGW+10 treatment.

Fluoride mobilization in T2 did not show a clear trend, but in general, higher amounts of F^- were mobilized during the first pore volumes (Figure 3-3d). During pore volume 4 (phase 1) of SGW+10, F^- mobilization exhibited statistically significant

differences between this treatment and NaCl, SGW, and SGW+100 treatments. Also, in pore volume 6 (phase 1), the data suggest a statistically significant difference between SGW+10 and SGW+100 treatments.

In general, NO_3^- mobilization in T1 and T2 decreased when NaCl treatment was applied to the columns (Figure 3-3e, f). The influent solution contained about 340 μM of NO_3^- with the exception of NaCl treatment. In T1, the NO_3^- concentration in the effluent solution was below this value in all treatments with the exception of SGW+100. The same effect was observed in T2, especially with the NaCl treatment. In both tailings, the mean values for NO_3^- mobilization exhibited a large variability.

Similar Cl^- mobilization was observed in T1 and T2 with the exception of NaCl treatment. Obviously, the NaCl treatment introduced a high concentration of Cl^-, which affected the Cl concentration in effluent solution (Figures 3-3g, h). In T1, during pore volume 2 (phase 1), Cl^- mobilization exhibited a statistically significant difference between SGW and SGW+100.

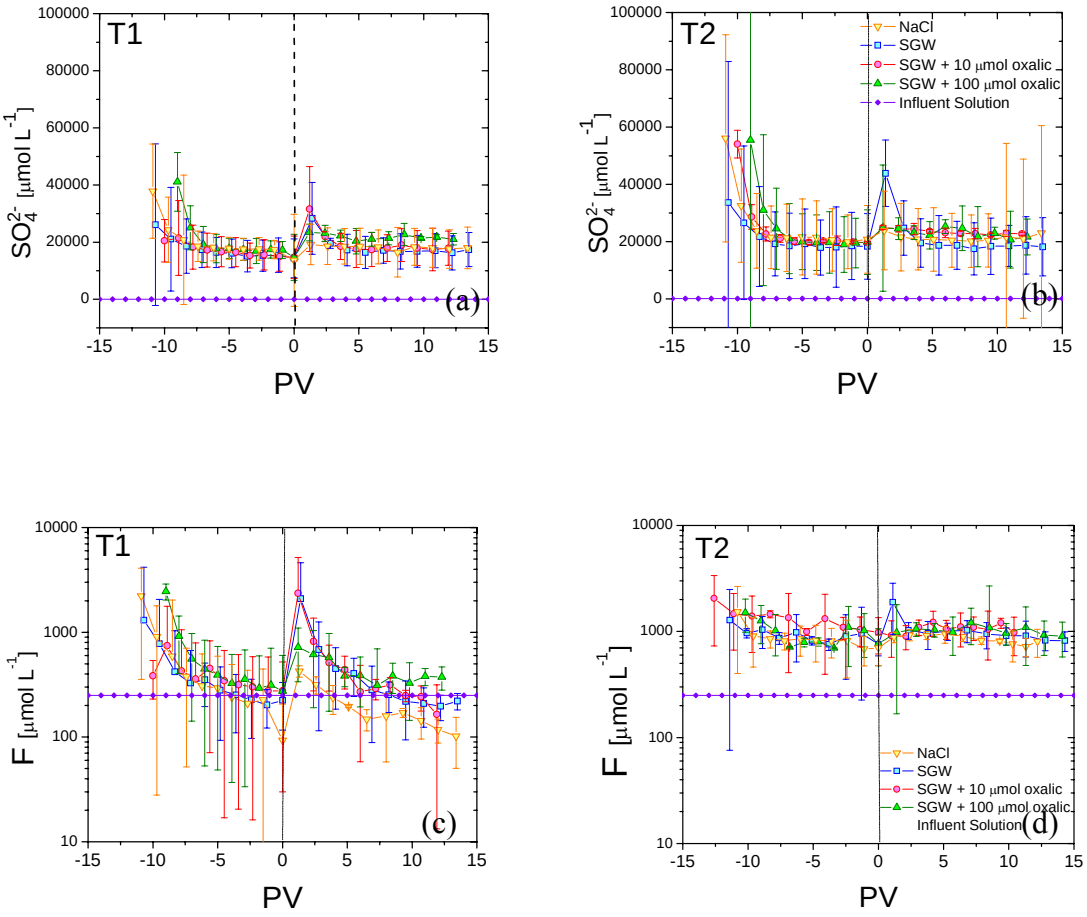

Figure 3-3 Effects of NaCl, SGW, SGW+10 and SGW+100 treatments on anion mobilization during and after the stopped-flow experiment. Negative PV values represent the constant flow pore volumes preceding the stopped flow period (phase 1), dashed line indicates the stopped flow period (phase 2), and positive PV values represent re-application of the constant flow (phase 3). Error bars represent 95% confidence limit.

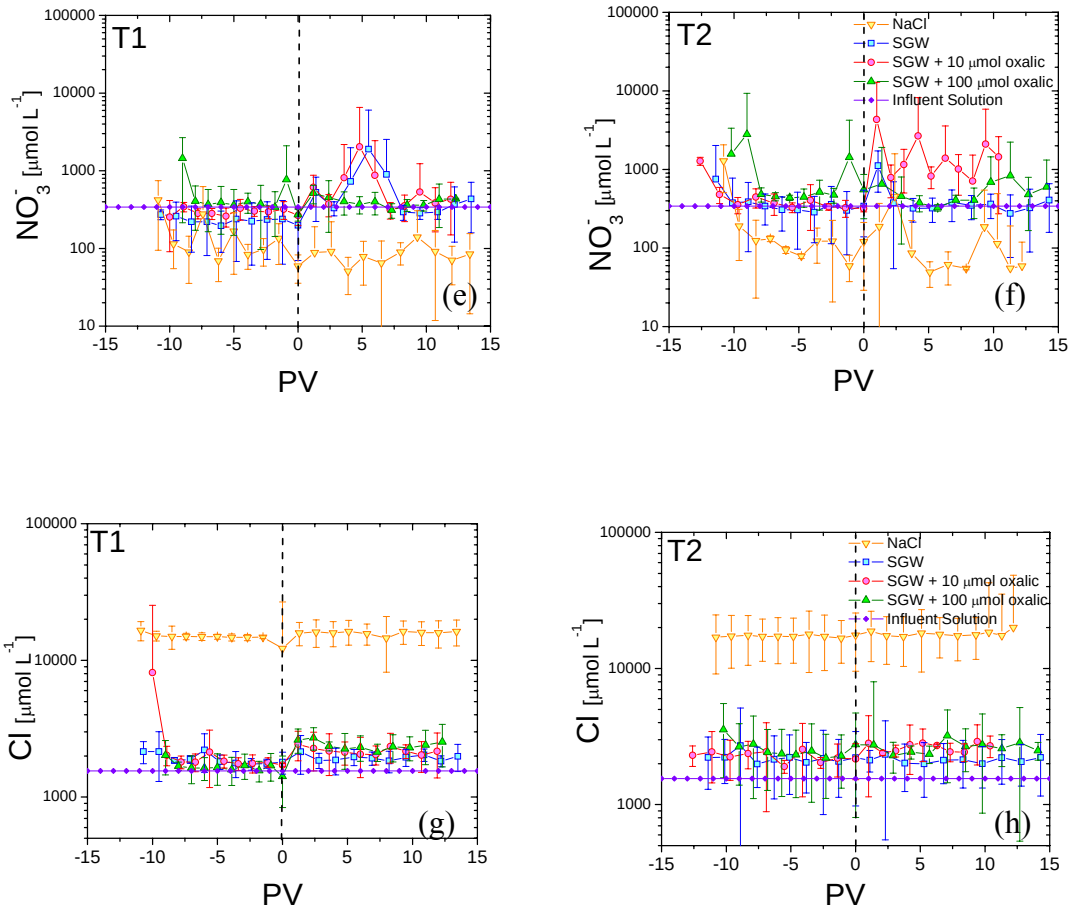

Figure 3-3 – *Continued* Effects of NaCl, SGW, SGW+10 and SGW+100 treatments on anion mobilization during and after the stopped-flow experiment. Negative PV values represent the constant flow pore volumes preceding the stopped flow period (phase 1), dashed line indicates the stopped flow period (phase 2), and positive PV values represent re-application of the constant flow (phase 3). Error bars represent 95% confidence limit.

3.3.4 Metal(loid) Release

In T1 and T2, Pb mobilization decreased with increasing PV in phase 1 (Figures 3-4a and 3-4b). The higher mobilization of Pb was observed during the first pore volumes in both tailings. An increase in lead mobilization was observed right after the equilibration period (phase 2) in T1 and T2, suggesting that minerals containing Pb exhibit kinetically-limited dissolution. In T1, during pore volume 9 (phase 1), Pb mobilization exhibited statistically significant difference between NaCl and SGW+10 treatments. In addition, during pore volumes 3 and 4 (phase 3) of NaCl, Pb mobilization exhibited statistically significant differences between this treatment and SGW+10 and SGW+100 treatments. Finally, during pore volume 7 (phase 3) of NaCl, a statistically significant difference in Pb mobilization was observed between this treatment and SGW+10.

In T2, the NaCl treatment significantly increased Pb mobilization relative to other treatments (Figure 3-4b) with some exceptions. During pore volume 1 (phase 1), Pb mobilization exhibited a statistically significant difference between NaCl and SGW+10. Also, during pore volumes 1 and 9 (phase 3) of NaCl, Pb mobilization did not exhibit statistically significant differences between this treatment and SGW, SGW+10 and SGW+100 treatments. Although T1 contains only 1/3 the total mass of Pb that is contained in T2 (Table 3-2), it exhibited a higher mass efflux from the column as reflected in higher concentrations throughout the experiment.

In T1 and T2, the highest amounts of Zn were released early in phase 1 (Figures 3-4c and 3-4d). An increase in Zn mobilization was observed after the equilibration

period (phase 2) in both tailings, suggesting that minerals containing Zn exhibit kinetically-limited dissolution. In T1 and T2, the amount of Zn released was found to decrease over the course of both phases 1 and 3.

In T1, during pore volume 2 (phase 1) of SGW+10, Zn mobilization exhibited statistically significant differences between this treatment and SGW, NaCl, and SGW+100 treatments. In addition, during pore volumes 4, 5, and 6 (phase 1) of NaCl, Zn mobilization exhibited statistically significant differences between this treatment and SGW, SGW+10, and SGW+100 treatments. During pore volume 7 (phase 1) of NaCl, statistically significant differences in Zn mobilization were observed between this treatment and SGW+10, and SGW+100 treatments. Finally, during the first pore volume (phase 1) of SGW, a statistically significant differences in Zn mobilization was observed between this treatment and NaCl, SGW+10, and SGW+100 treatments. In T2, Zn mobilization exhibited a statistically difference between NaCl and SGW+10.

Most importantly, although Klondyke tailings contain higher total concentrations of Pb than Zn, the relative amount of Zn mobilized is much higher, suggesting that minerals containing lead are more recalcitrant to dissolution under the conditions of the study.

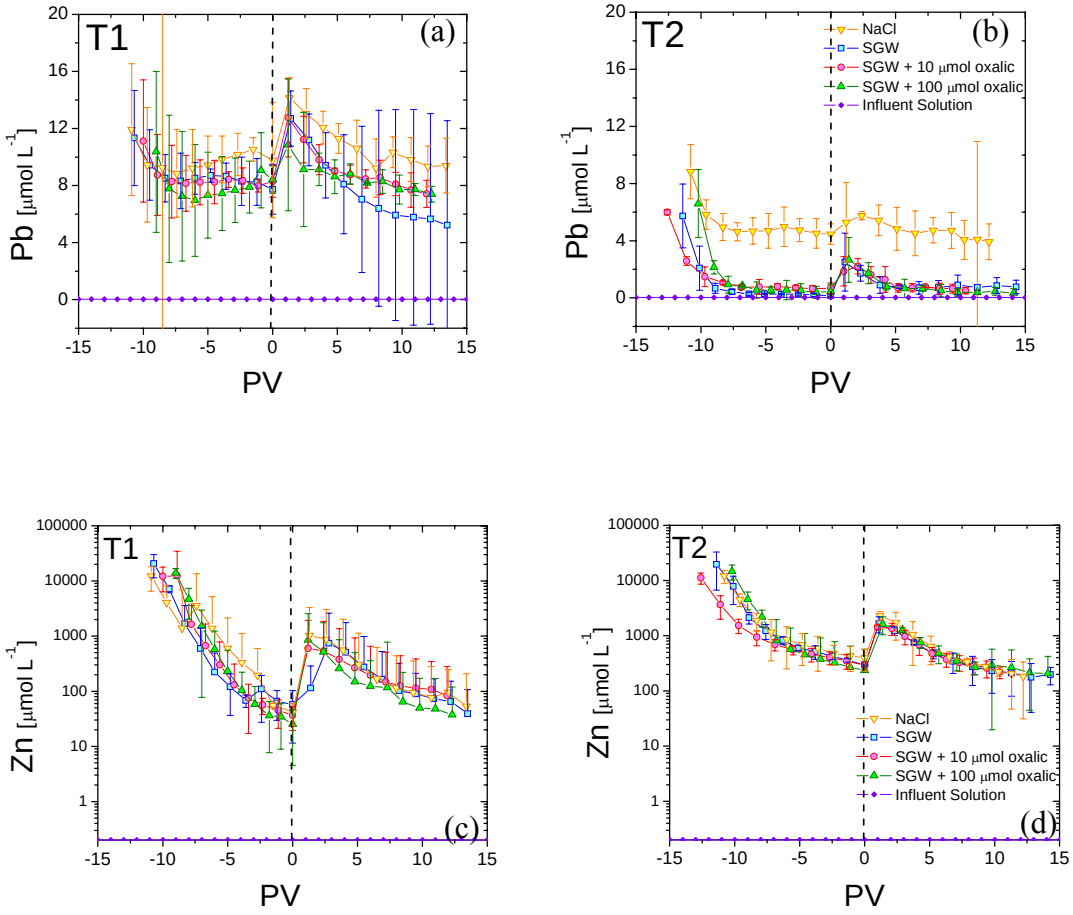

Figure 3-4 Effects of NaCl, SGW, SGW+10 and SGW+100 treatments on zinc and lead mobilization during and after the stopped-flow experiment. Negative PV values represent the constant flow pore volumes preceding the stopped flow period (phase 1), dashed line indicates the stopped flow period (phase 2), and positive PV values represent re-application of the constant flow (phase 3). Error bars represent 95% confidence limit.

A large amount of Ca was mobilized from T1 and T2, reflecting the prevalence of gypsum in both tailings materials (Figure 3-5a, b). In T1, during pore volume 2 (phase 1), Ca mobilization exhibited a statistically significant difference between NaCl and SGW+10. During pore volume 2 (T1) (phase 3) of NaCl, Ca mobilization exhibited statistically significant differences between this treatment and SGW and SGW+10 treatments. The following treatments, during phase 3 (T1), exhibited statistically significant differences in Ca mobilization: NaCl and SGW+10 (PV 3), NaCl and SGW (PV 4), NaCl and SGW+10 (PV 4), NaCl and SGW (PV 7), NaCl and SGW+100 (PV 7), NaCl and SGW+100 (PV 8), SGW and SGW+10 (PV 9), and NaCl and SGW (PV 10). In T2, calcium mobilization did not show a statistically significant effect, regardless of the treatment used (Figure 3-5b).

In T1 and T2, the highest amounts of Mn were released early in phase 1 (Figures 3-5c and 3-5d). An increase in Mn mobilization was observed after the equilibration time (phase 2) in both tailings, with the exception of SGW+10 treatment (T1), suggesting that minerals containing Mn exhibit kinetically-limited dissolution. In T1 and T2, the amount of Mn released was found to decrease over the course of phase 1 and phase 3. In T1, during the last pore volumes of SGW+10 treatment (phases 1 and 3), Mn mobilization was higher than in other treatments.

In T1, during pore volumes 1, 2, 3, and 4 (phase 1) of SGW, Mn mobilization exhibited statistically significant differences between this treatment and NaCl, SGW+10, and SGW+100. During pore volume 5 (T1) (phase 1) of NaCl, Mn mobilization exhibited statistically significant differences between this treatment and SGW and

SGW+100 treatments. During pore volumes 7, 8, 9, and 10 (T1) (phase 1) of SGW+10, Mn mobilization exhibited statistically significant differences between this treatment and NaCl, SGW, and SGW+100 treatments. During the first eluted pore volume (T1) (phase 3) of SGW+100, Mn mobilization exhibited statistically significant differences between this treatment and NaCl, SGW, and SGW+10 treatments. Also, during pore volume 5 (T1) (phase 3), a statistically significant difference between NaCl and SGW was observed. In addition, during pore volumes 6, 7, 8, 9, and 10 (T1) (phase 3) of SGW+10, Mn mobilization exhibited statistically significant differences between this treatment and NaCl, SGW, and SGW+100 treatments.

In T2 (phase 1), Mn mobilization exhibited a statistically significant difference between SGW and SGW+10 treatments during pore volumes 8, 9, and 10. During phase 3 (T2), Mn mobilization did not show a significant effect, regardless of the treatment used.

In T1 and T2, the highest amounts of K were released early in phase 1 (Figure 3-5e, f). The amount of K released was found to decrease over the course of phases 1 for both tailings. In T1 and T2, the lowest amount of released K was reported during the last pore volumes of NaCl treatment (phase 1). In T1, during pore volume 3 (phase 1), K mobilization exhibited a statistically significant difference between NaCl and SGW+10. Also, during pore volume 6 (T1) (phase 1), K mobilization exhibited a statistically significant difference between NaCl and SGW. During pore volumes 7, 8, and 9 (T1) (phase 1) of NaCl, K mobilization exhibited statistically significant differences between this treatment and SGW, SGW+10, and SGW+100 treatments. In addition, during pore

volume 1 (T1) (phase 3) of NaCl, K mobilization exhibited statistically significant differences between this treatment and SGW, SGW+10, and SGW+100 treatments.

In T2, during pore volume 2 (phase 1), K mobilization exhibited a statistically significant difference between SGW and SGW+10. Also, during pore volume 4 (T2, phase 1), a significant difference was observed between NaCl and SGW. During pore volumes 5, 6, 8, 9, and 19 (T2, phase 1) of NaCl, K mobilization exhibited statistically significant differences between this treatment and SGW, SGW+10, and SGW+100 treatments. In addition, during pore volumes 2, 3, 6, and 9 (T2, phase 3) of NaCl, K mobilization exhibited statistically significant differences between this treatment and SGW, SGW+10, and SGW+100 treatments.

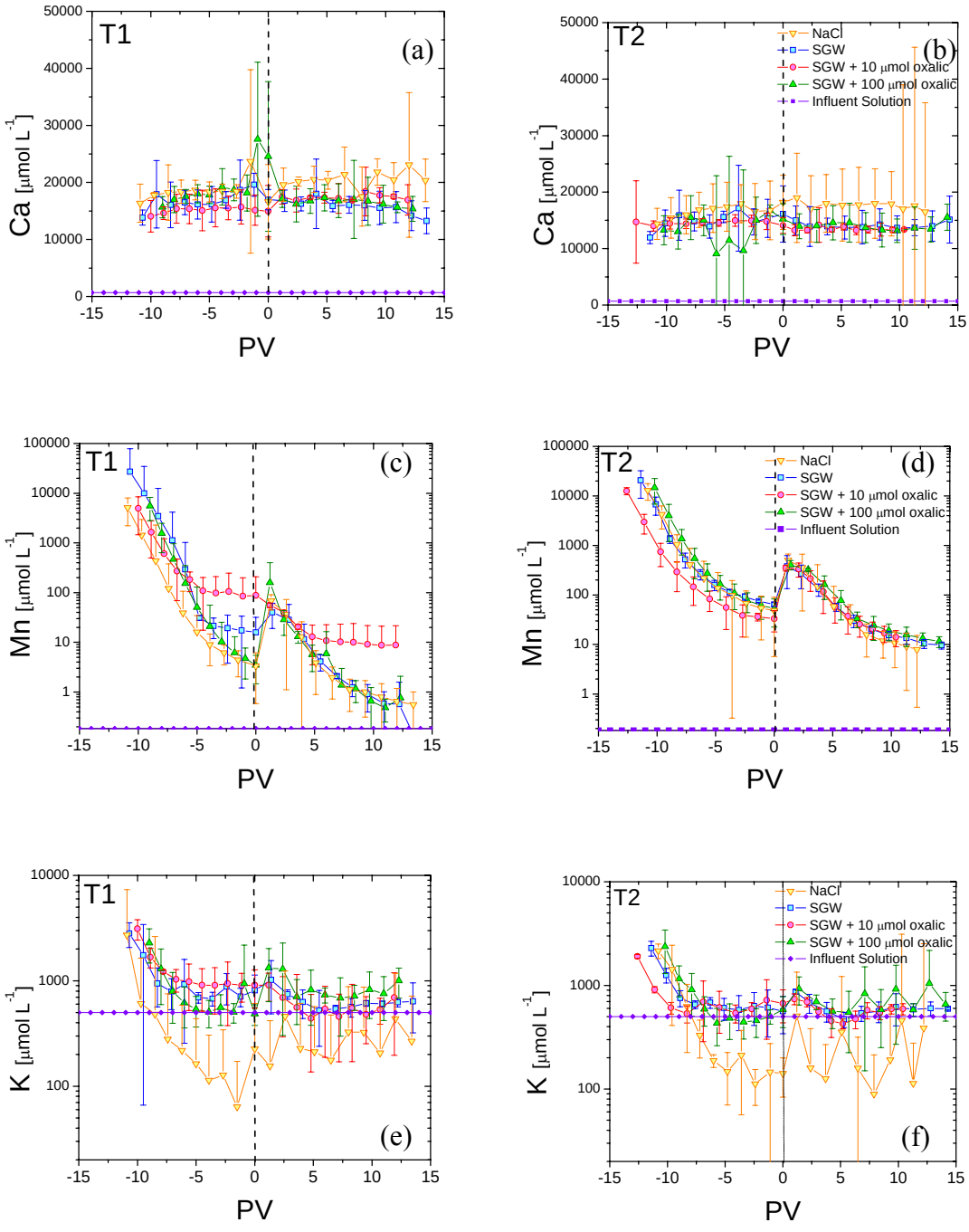

Figure 3-5 Effects of NaCl, SGW, SGW+10 and SGW+100 treatments on Ca, Mn, and K mobilization during and after the stopped-flow experiment. Negative PV values represent the constant flow pore volumes preceding the stopped flow period (phase 1), dashed line indicates the stopped flow period (phase 2), and positive PV values represent re-application of the constant flow (phase 3). Error bars represent 95% confidence limit.

Total copper concentration in T1 and T2 was 650 mg kg^{-1} and 1,600 mg kg^{-1}, respectively (Table 3-2). Regardless the fact that T1 contained less total Cu than T2, a high concentration of Cu was released from T1, suggesting its presence in more soluble phases and/or a strong impact of pH on Cu solubility (Figure 3-6a, b). Cu mobilization was high during the first eluted pore volumes (early phase 1) in T1 and T2. While kinetic effects are apparent in T2, they are less evident in T1.

In T1 (phases 1 and 3), Cu mobilization did not show a statistically significant effect, regardless of the treatment used. In T2, during pore volume 1 (phase 1), Cu mobilization exhibited a statistically significant difference between NaCl and SGW+10. During pore volumes 5 and 6 (T2, phase 3) of NaCl, Cu mobilization exhibited a statistically significant differences between this treatment and SGW and SGW+100. Also, during pore volumes 7, 8, and 9 (T2, phase 3) of NaCl, Cu mobilization exhibited a statistically significant differences between this treatment and SGW, SGW+10 and SGW+100 treatments. Finally, during pore volume 10 (T2, phase 3) of NaCl, Cu mobilization exhibited a statistically significant differences between this treatment and SGW and SGW+10 treatments.

Total aluminum concentration in T1 and T2 was 22,600 mg kg^{-1} and 14,500 mg kg^{-1}, respectively (Table 3-2). Large differences in Al release were observed between T1 and T2 (Figures 3-6c, d). The highest Al release in T1 was observed during the elution of the first pore volumes (phase 1). In T1, the amount of Al released was found to decrease over the course of both phases 1 and 3. An increase in Al mobilization was observed after the equilibration time (phase 2) in T1, suggesting that minerals containing Al exhibit

kinetically-limited dissolution. In T2, the highest amount of Al was released during the elution of the first pore volumes (phase 1). After the equilibration time (phase 2), aluminum mobilization remained low and comparable to the preceding values. While kinetic effects are apparent in T1, there is not evidence in T2.

In T1, during pore volumes 1, 2, 3, 4, 5, 6, and 7 (phase 1) of SGW, Al mobilization exhibited statistically significant differences between this treatment and NaCl, SGW+10, SGW+100 treatments. In T1 (phase 3), Al mobilization did not show a statistically significant effect, regardless of the treatment used. In T2, during pore volume 2 (phase 1), Al mobilization exhibited a statistically significant difference between SGW+10 and SGW+100. In T2, during pore volumes 3 and 4 (phase 1) of NaCl, Al mobilization exhibited statistically significant differences between this treatment and SGW and SGW+100 treatments. During pore volume 10 (T2, phase 1) of SGW+100, Al mobilization exhibited statistically significant differences between this treatment and NaCl, SGW and SGW+10 treatments. The following treatments, during phase 3 (T2), exhibited statistically significant differences in Al mobilization: NaCl and SGW (PV 1), SGW+10 and NaCl (PV 6), SGW+10 and SGW+10 (PV 6), SGW+10 and SGW, and SGW+10 and SGW+100.

In T1 and T2, high amounts of Mg were released early in phase 1 (Figures 3-6e, f). An increase in Mg mobilization was observed after the equilibration time (phase 2) in both tailings, with the exception of NaCl treatment (T1), suggesting that minerals containing Mg exhibit kinetically-limited dissolution. In T1 and T2, the amount of Mg released was found to decrease over the course of both phases 1 and 3.

In T1, during pore volumes 4 and 5 (phase 1) of NaCl, Mg mobilization exhibited statistically significant differences between this treatment and SGW, SGW+10, SGW+100 treatments. In T1 (phase 3), Mg mobilization did not show a statistically significant difference between SGW and SGW+100. Also, during all pore volumes (T1, phase 3) of SGW+10, Mg mobilization exhibited statistically significant differences between this treatment and SGW and SGW+100 treatments. In T1 (phase 3), during all pore volumes, but PV 5 and 10, Mg mobilization exhibited statistically significant difference between NaCl and SGW+10 treatments.

In T2 (phase 1), during pore volumes 7, 8, 9, and 10 of NaCl, Mg mobilization exhibited statistically significant difference between this treatment and SGW, SGW+10, SGW+100 treatments. Also, during pore volumes 6, 7, 8, 9, and 10 of NaCl (T2, phase 3), Mg mobilization exhibited statistically significant difference between this treatment and SGW, SGW+10, SGW+100 treatments.

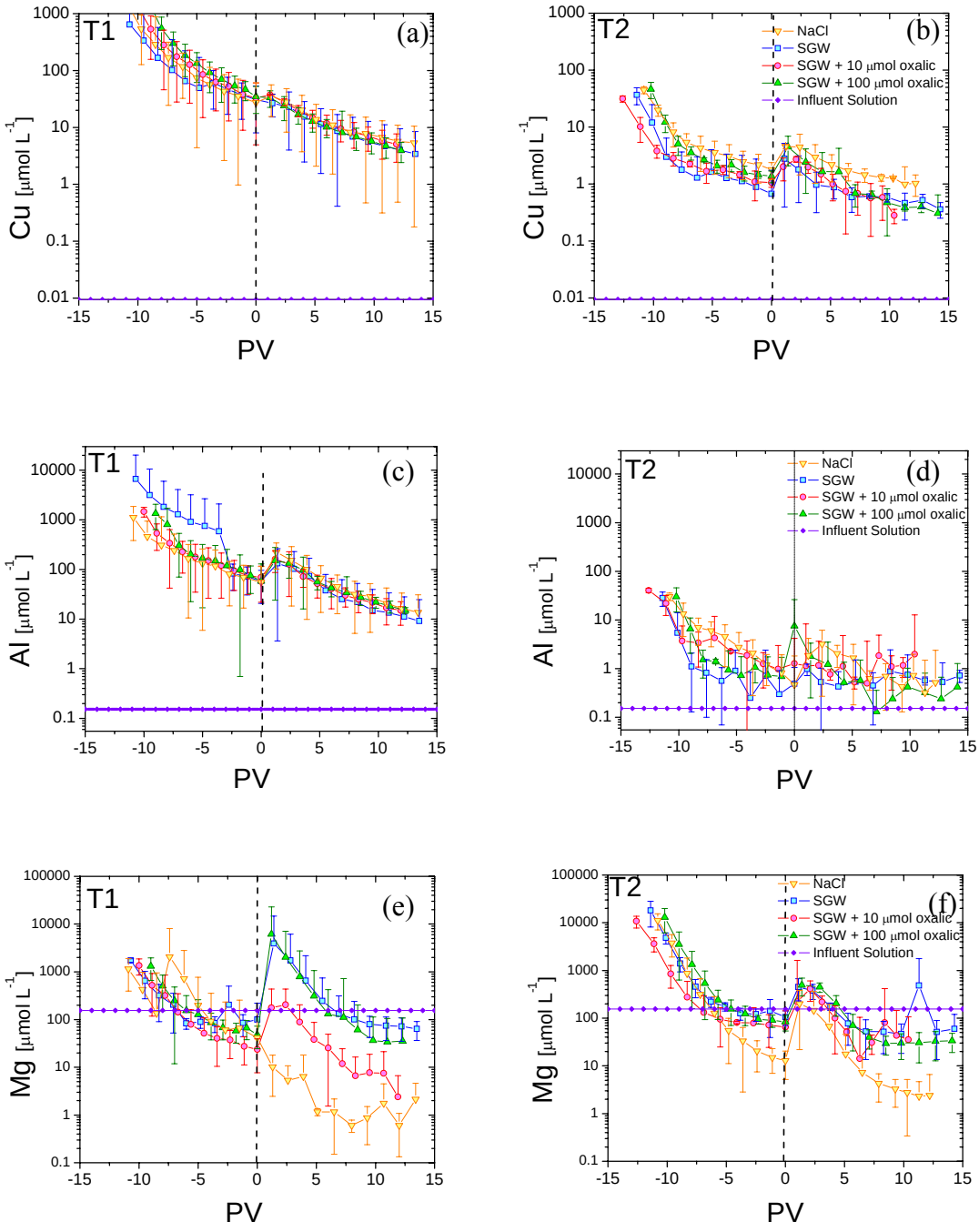

Figure 3-6 Effects of NaCl, SGW, SGW+10 and SGW+100 treatments on Cu, Al, and Mg mobilization during and after the stopped-flow experiment. Negative PV values represent the constant flow pore volumes preceding the stopped flow period (phase 1), dashed line indicates the stopped flow period (phase 2), and positive PV values represent re-application of the constant flow (phase 3). Error bars represent 95% confidence limit.

In T1 and T2, silica mobilization remained relatively constant and comparable during phase 1, with the exception of NaCl treatment (T1) (Figures 3-7a, b). An increase in Si mobilization was observed after the equilibration time (phase 2) in both tailings, suggesting that minerals containing Si exhibit kinetically-limited dissolution. In T1 and T2, the amount of Si released was found to decrease over the course of phase 3.

In T1, during pore volumes 4 through 10 (phase 1) of NaCl, Si mobilization exhibited statistically significant differences between this treatment and SGW, SGW+10, SGW+100 treatments. Also, during pore volumes 6 through 10 (T1, phase 3) of NaCl, Si mobilization exhibited statistically significant differences between this treatment and SGW, SGW+10, SGW+100 treatments.

In T2, during pore volumes 4 through 10 (phase 1), Si mobilization exhibited statistically significant difference between NaCl and SGW+10 treatments. In addition, during all pore volumes (T2, phase 3), Si mobilization exhibited statistically significant difference between SGW+10 and SGW+100 treatments.

SGW, SGW+10 and SGW+100 treatments contain about of 2,200 μM of sodium and in most cases the amount of mobilized Na was less than this concentration, suggesting Na retention in the column system (Figures 3-7c, d). A decrease in Na mobilization was observed after the equilibration time (phase 2) in both tailings. NaCl treatment introduced a high concentration of Na, which affected the Na concentration in effluent solution.

In T1 and T2 (phase 1), Na mobilization did not show a statistically significant difference between the following treatments: SGW, SGW+10 and SGW+100. In T1,

during pore volume 4 (phase 3), Na mobilization exhibited a statistically significant difference between SGW and SGW+100. In T2, during pore volume 4 (phase 3), Na mobilization exhibited a statistically significant difference between SGW and SGW+10. Also, Na mobilization exhibited a statistically significant difference between SGW and SGW+100 during pore volume 4 (T2, phase 3).

In T1 and T2, the highest amounts of Cd were released early in phase 1 (Figures 3-7e, f). An increase in Cd mobilization was observed after the equilibration time (phase 2) in both tailings, suggesting that minerals containing Cd exhibit kinetically-limited dissolution. The amount of Cd released was found to decrease over the course of both phases 1 and 3.

In T1 (phase 1), Cd mobilization did not show a statistically significant difference between the following treatments: NaCl, SGW, SGW+10 and SGW+100. Also, during the first eluted pore volume (T1, phase 3) of SGW+100, Cd mobilization exhibited statistically significant differences between SGW and SGW+10 treatments. In T2 (phases 1 and 3), Cd mobilization did not show a statistically significant difference between the following treatments: NaCl, SGW, SGW+10 and SGW+100.

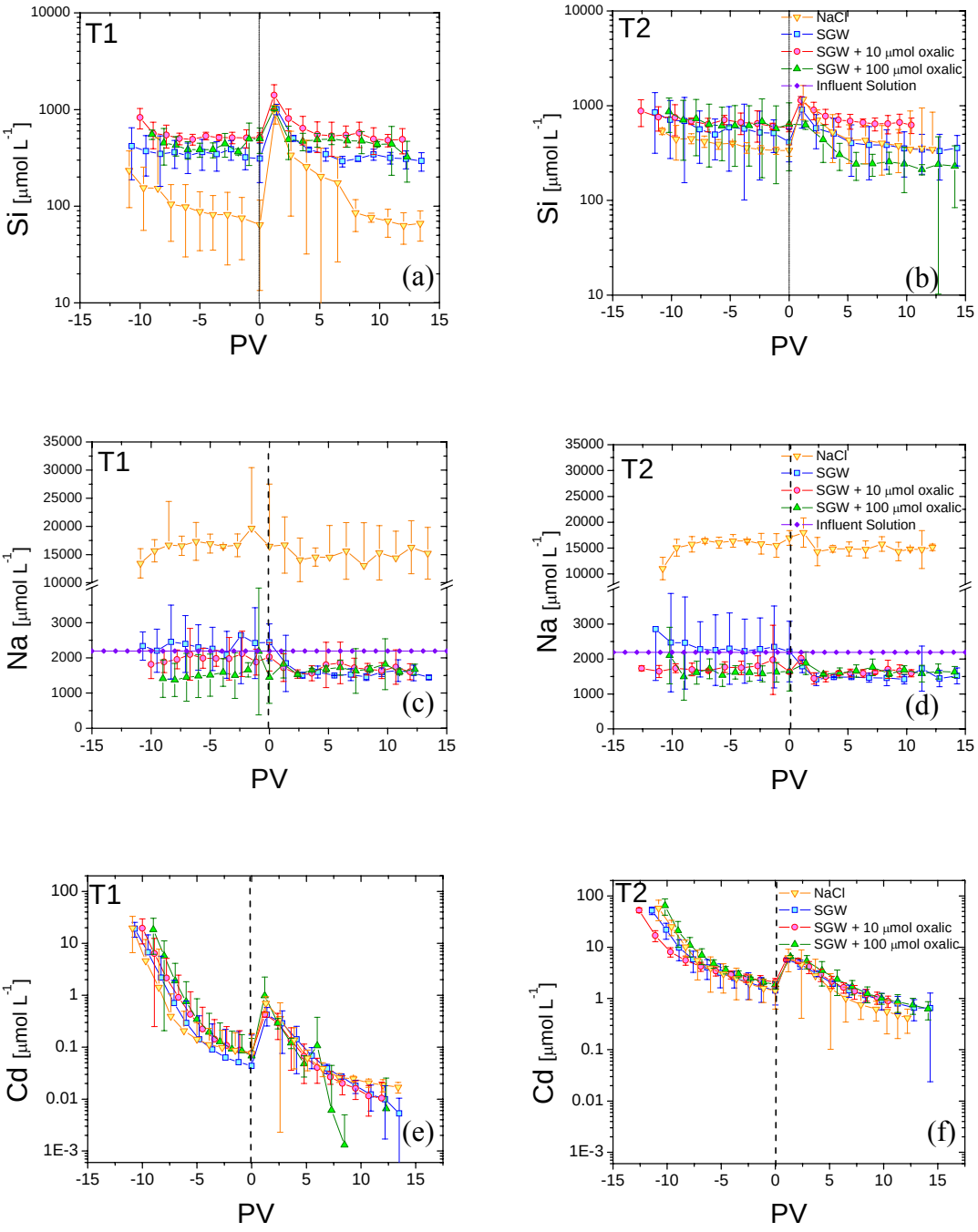

Figure 3-7 Effects of NaCl, SGW, SGW+10 and SGW+100 treatments on Si, Na, and Cd mobilization during and after the stopped-flow experiment. Negative PV values represent the constant flow pore volumes preceding the stopped flow period (phase 1), dashed line indicates the stopped flow period (phase 2), and positive PV values represent re-application of the constant flow (phase 3). Error bars represent 95% confidence limit.

In T1 and T2, the highest amounts of As were released early in phase 1 (Figures 3-8a, b). An increase in As mobilization was observed after the equilibration time (phase 2) in both tailings, suggesting that minerals containing As exhibit kinetically-limited dissolution. The amount of As released was found to decrease over the course of both phases 1 and 3.

In T1 (phases 1 and 3), As mobilization did not show a statistically significant difference between the following treatments: NaCl, SGW, SGW+10 and SGW+100. In T2 (phase 1), As mobilization did not show a statistically significant difference between the following treatments: NaCl, SGW, SGW+10 and SGW+100. In T2, during pore volumes 1, 2, 3, and 5 (phase 3) of SGW+10, As mobilization exhibited statistically significant differences between this treatment and SGW and SGW+100. Also, during pore volume 4 (T2, phase 3) of SGW+10, As mobilization exhibited statistically significant differences between this treatment and NaCl, SGW and SGW+100. The following treatments, during phase 3 (T2), exhibited statistically significant differences in As mobilization: SGW+10 and SGW+100 (PV 8), and SGW and SGW+10 (PV 10).

Klondyke tailings contain a substantial amount of iron (Table 3-2). A low and relatively constant concentration of iron was mobilized from T1 and T2, consistent with the low solubility of Fe(III) minerals (Figures 3-8c, d).

In T1, during pore volumes 2 and 3 (phase 1) of SGW+100, Fe mobilization exhibited statistically significant difference between this treatment and NaCl. Also, during pore volumes 8 and 9 (T1, phase 3) of SGW+100, Fe mobilization exhibited statistically significant differences between this treatment and SGW and NaCl. During

pore volume 10 (T1, phase 3) of SGW+100, Fe mobilization exhibited statistically significant differences between this treatment and SGW and SGW+100. The following treatments, in T2, exhibited statistically significant differences in Fe mobilization: NaCl and SGW+10 (PV 2, phase 1), and NaCl and SGW+10 (PV 1, phase 3).

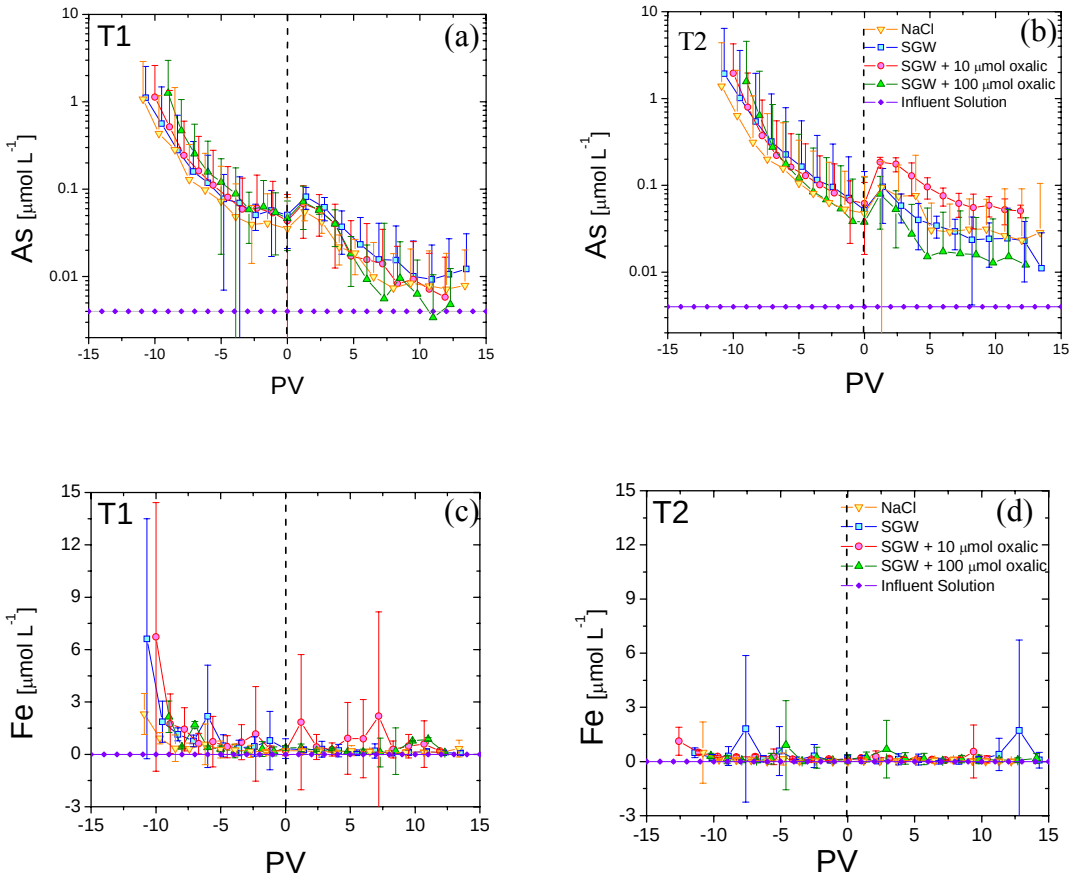

Figure 3-8 Effects of NaCl, SGW, SGW+10 and SGW+100 treatments on As and Fe mobilization during and after the stopped-flow experiment. Negative PV values represent the constant flow pore volumes preceding the stopped flow period (phase 1), dashed line indicates the stopped flow period (phase 2), and positive PV values represent re-application of the constant flow (phase 3). Error bars represent 95% confidence limit.

CHAPTER 4: DISCUSSION

Geochemical modeling was conducted to help test the hypothesis that irrigation with groundwater solutions would promote the dissolution of sulfate mineral phases and lead to the formation of Fe and Al (oxyhdyr)oxides phases. The fate of metals, then, might be expected to shift from sulfate mineral control to metal (oxyhydr)oxide sorbent control. The formation of (oxyhydr)oxide products is also hypothesized to sequester some of the Pb, Zn, Al, and Fe that might be otherwise released from the columns. Chemical data from pore volumes one (phase 1), ten (phase 1), one (phase 3), and ten (phase 3) for NaCl, SGW, SGW+10, and SGW+100 treatments were entered into MinteqA2 for Windows (Version 1.50, Allison Geoscience Consultants, Inc.) in order to calculate solution phase speciation and saturation indices, and to interpret dissolution-precipitation reactions in the column experiments.

Values of log Ω, where Ω is IAP/K_{SO} (section 2.5.4), were calculated to examine potential controls on solute behavior. The log Ω values for relevant minerals are shown in Table A-19. Given the known mineralogy of the tailings (orthoclase ($KAlSi_3O_8$), quartz (SiO_2), gypsum ($CaSO_4 \cdot 2H_2O$), jarosite ($KFe_3(SO_4)_2(OH)_6$), plumbojarosite ($PbFe_6(SO_4)_4(OH)_{12}$), goslarite ($ZnSO_4 \cdot 7H_2O$), Zn-talc ($Zn_xMg_{3-x}Si_4O_{10}(OH)_2$), anglesite (PbSO4)) and the expected solid phase products from dissolution reactions of these minerals (goethite (FeOOH), hematite (Fe_2O_3), ferrihydrite ($Fe(OH)_3$), kaolinite ($Al_2Si_2O_5(OH)_4$), and gibbsite ($Al(OH)_3$)), MINTEQA2 was used to measure the tendency of these minerals to contribute to precipitation-dissolution reactions, and hence metal retention and release, under the experimental conditions.

4.1 Anions and Metal(loids)

High amounts of sulfate were mobilized from T1 and T2. MINTEQA2 predicted that log Ω values for gypsum fluctuated around zero, which implies effluent solutions were near to equilibrium conditions with respect to this mineral. Hence, gypsum ($CaSO_4 \cdot 2H_2O$) dissolution may be exerting the primary control on sulfate concentration in the effluent solution. The following reaction describes gypsum dissolution-precipitation reaction:

$$CaSO_4 \cdot 2H_2O_{(s)} \leftrightarrow Ca^{2+} + SO_4^{2-} + 2H_2O \qquad (4.1)$$

Regardless of the treatment applied, MINTEQA2 indicated that solutions were undersaturated with respect to anglesite ($PbSO_4$) at all studied pore volumes for both tailings. Therefore, if anglesite is present in the tailings, this solid contributed to SO_4^{2-} and Pb^{2+} mobilization from the columns. Another mineral possibly contributing to SO_4^{2-} and Pb^{2+} concentration in the effluent solution was Pb-jarosite ($PbFe_6(SO_4)_4(OH)_{12}$). Nearly all effluent solutions were undersaturated with respect to Pb-jarosite. The following reactions describe anglesite and Pb-jarosite dissolution:

$$PbSO_{4(s)} \rightarrow Pb^{2+} + SO_4^{2-} \qquad (4.2)$$

$$PbFe_6(SO_4)_4(OH)_{12(s)} + 12H^+ \rightarrow Pb^{2+} + 6Fe^{3+} + 2SO_4^{2-} + 12H_2O \qquad (4.3)$$

Despite the fact that effluent solutions were undersaturated with respect to anglesite and Pb-jarosite, low concentrations of lead were mobilized from the columns. Because of the higher solubility of gypsum relative to anglesite and Pb-jarosite, it seems that rapid equilibrium saturation of the solutions with respect to gypsum could be preventing Pb dissolution from Pb-sulfate minerals.

For NaCl, SGW, SGW+10, and SGW+100 treatments, Fe concentrations were consistently low in effluent solutions from both columns. A possible explanation for this result is that Fe-sulfate minerals were undergoing an incongruent dissolution and forming low solubility Fe(III)-(oxyhydr)oxides minerals. Values of log Ω indicate that all effluent solutions were supersaturated with respect to goethite (FeOOH) and hematite (Fe_2O_3), regardless of the treatment. Incongruent dissolution of Na-jarosite and goethite/hematite precipitation will be used as models to explain SO_4^{2-} and Fe^{3+} mobilization from the column systems. Equation 4.4 represents Na-jarosite dissolution and goethite precipitation and equation 4.5 represents Na-jarosite dissolution and hematite precipitation.

$$NaFe_3(SO_4)_2(OH)_{6(s)} \rightarrow 3FeOOH_{(s)} + Na^+ + 2SO_4^{2-} + 3H^+ \quad (4.4)$$

$$NaFe_3(SO_4)_2(OH)_{6(s)} \rightarrow 1.5Fe_2O_{3(s)} + Na^+ + 2SO_4^{2-} + 3H^+ + 1.5H_2O \quad (4.5)$$

Other minerals possibly contributing to iron concentration in the effluent solutions were ferrihydrite ($Fe(OH)_3$) and schwertmannite ($Fe_8O_8(OH)_6SO_4$). In most cases, effluent solutions were undersaturated with respect to ferrihydrite and schwertmannite in

T1 for NaCl, SGW, SGW+10, and SGW+100 treatments. In T2, effluent solutions were supersaturated with respect to ferrihydrite and schwertmannite for SGW, SGW+10, and SGW+100 treatments. Figures 3-8c and 3-8d show a slightly higher concentration of Fe in T1 which can potentially be attributed to the dissolution of ferrihydrite and schwertmannite. Equations 4.6 and 4.7 represent ferrihydrite and schwertmannite dissolution/precipitation reactions, respectively:

$$Fe(OH)_{3(s)} + 3H^{+} \leftrightarrow Fe^{3+} + 3H_2O \quad (4.6)$$

$$Fe_8O_8(OH)_6SO_{4(s)} + 22H^{+} \leftrightarrow 8Fe^{3+} + SO_4^{2-} + 14H_2O \quad (4.7)$$

In most cases, MINTEQA2 predicted that effluent solutions were undersaturated with respect to hydronium-jarosite (H_3O-$Fe_3(SO_4)_2(OH)_6$) and Na-jarosite ($NaFe_3(SO_4)_2(OH)_6$). Even though effluent solutions were undersaturated with respect to hydronium-jarosite and Na-jarosite, a low amount of iron was mobilized from both tailings, suggesting low contribution of these minerals in iron concentration in the effluent solution. The apparent equilibrium of the effluent solution with gypsum can also be affecting the dissolution of hydronium-jarosite and Na-jarosite.

Large amounts of Zn were mobilized from both tailings. Possible minerals contributing to Zn concentration in the effluent solution were Zn-talc ($Zn_3Si_4O_{10}(OH)_2$) and goslarite ($ZnSO_4 \cdot 7H_2O$). The following equations describe Zn-talc and goslarite dissolution reactions, respectively:

$$Zn_3Si_4O_{10}(OH)_{2(s)} + 6H^+ + 4H_2O \rightarrow 3Zn^{2+} + 4H_4SiO_4 \quad (4.8)$$

$$ZnSO_4 \cdot 7H_2O_{(s)} \rightarrow Zn^{2+} + SO_4^{2-} + 7H_2O \quad (4.9)$$

In T1, effluent solutions were undersaturated with respect to Zn-talc, suggesting that this mineral was undergoing dissolution, regardless of the treatment. In contrast, in T2, effluent solutions were supersaturated with respect to Zn-talc in all treatments, suggesting the precipitation of this mineral is favored by water infusion. MINTEQA2 indicated that effluent solutions were undersaturated with respect to goslarite at all times in both tailings, for NaCl, SGW, SGW+10, and SGW+100 treatments. Goslarite dissolution may contribute to the mobilization of Zn^{2+} and SO_4^{2-}.

Higher mobilization of aluminum was observed in T1 than in T2. Possible minerals controlling Al concentration in the effluent solution were $AlOHSO_4$, $Al_4(OH)_{10}SO_4$, alunite ($KAl_3(OH)3(SO4)_2$), gibbsite ($Al(OH)_3$), orthoclase ($KAlSi_3O_8$), and kaolinite ($Al_2Si_2O_5(OH)_4$). Dissolution reactions of gibbsite, orthoclase, and kaolinite are shown in equations 4.10, 4.11, and 4.12, respectively.

$$Al(OH)_{3(s)} + 3H^+ \rightarrow Al^{3+} + 3H_2O \quad (4.10)$$

$$KAlSi_3O_{8(s)} + 4H_2O + 4H^+ \rightarrow K^+ + Al^{3+} + 3H_4SiO_4 \quad (4.11)$$

$$Al_2Si_2O_5(OH)_{4(s)} + 6\,H^+ \rightarrow 2Al^{3+} + 2H_4SiO_4 + H_2O \quad (4.12)$$

Effluent solutions were undersaturated with respect to $AlOHSO_4$, $Al_4(OH)_{10}SO_4$, and alunite during all pore volumes with the exception of $AlOHSO_4$ during pore volume

one in SGW treatment (T1). In T1, effluent solutions were undersaturated with respect to gibbsite, suggesting that this mineral is dissolving under experimental conditions. In T2, saturation indices of gibbsite vary depending on the treatment and collection time. For instance, during pore volume 10 (phase 3, T2) of SWG treatment, the effluent solution was supersaturated with respect to gibbsite. Lower concentrations of Al in T2 can potentially be attributed to the precipitation of Al-hydroxide minerals such as gibbsite. Effluent solutions in NaCl (T1 and T2), SGW+10 (T1), and SGW+100 (T1) treatments were always undersaturated with respect to kaolinite, suggesting kaolinite as a possible source of Al and Si into the effluent solution.

Significant amounts of calcium were released from both tailings. On average, calcium mobilization remained constant throughout all the experiments. Again, the effluent solutions were near to equilibrium conditions with respect to gypsum, suggesting that this mineral was controlling the concentration of calcium and sulfate in the effluent solutions.

The presence of oxalic acid was hypothesized to increase metal mobilization. Calcium cations have a tendency to interact with oxalate anions, forming Ca-oxalate precipitates (Ca-$C_2O_4 \cdot H_2O$ and Ca-$C_2O_4 \cdot 3H_2O$). This interaction can result in less metal mobilization from the tailing material. During SGW+10 treatment in T1, effluent solutions were undersaturated with respect to Ca-$C_2O_4 \cdot H_2O$ in all pore volumes with the exception of pore volume 10 (phase 3). Also, during the same treatment (T1), effluent solutions were undersaturated with respect to Ca-$C_2O_4 \cdot 3H_2O$ in all pore volumes. In the case of SGW+10 in T2, effluent solutions were undersaturated with respect to Ca-

$C_2O_4 \cdot H_2O$ in pore volumes 10 (phase 1) and 10 (phase 3) and with respect to Ca-$C_2O_4 \cdot 3H_2O$ in all pore volumes. During SGW+100 in T1 and T2, effluent solutions were undersaturated with respect to Ca-$C_2O_4 \cdot H_2O$ and Ca-$C_2O_4 \cdot 3H_2O$ only during the first eluted pore volume (phase 1) and supersaturated during the other pore volumes.

CHAPTER 5: CONCLUSIONS

Effluent solutions from column experiments were collected and characterized after the application of sodium chloride (NaCl), synthetic ground water (SGW), and SGW plus 10 μM and 100 μM oxalic acid treatments. Chemical data from selected pore volumes were entered into MINTEQA2 for Windows in order to predict geochemical process controls in the column systems.

Sulfate minerals (gypsum, jarosites, anglesite, goslarite, and Al-sulfates), which are kinetically labile minerals, are expected to dissolve in the columns, therefore playing a significant role in metal release. In fact, MINTEQA2 modeling indicated that these sulfate-bearing minerals were indeed dissolving and releasing metal(loid)s and sulfate anions into the effluent solution. Iron, in particular, could have been re-precipitated as Fe (oxyhydr)oxides (goethite, hematite, ferrihydrite) and Al could also have being re-precipitated as gibbsite.

Relative Zn mobilization was higher than Pb, suggesting the presence of more kinetically labile Zn phases. Lead mobilization was also lower because effluent solutions were near to equilibrium conditions with respect to gypsum, preventing Pb dissolution from Pb-sulfate minerals. In order to determine whether the presence of gypsum was affecting Pb mobilization, a constant flow should be applied to the columns for a long period of time. Lead mobilization would be expected to increase after most of the gypsum has been removed from the system. The release of lead and zinc both exhibit kinetic limitations which imply important time-dependence in mineral dissolution.

Large amounts of sulfate were released from both tailings for NaCl, SGW, SGW+10 and SGW+100 treatments. Geochemical modeling indicated that gypsum dissolution could be controlling the sulfate concentration in the effluent solution. Geochemical modeling also indicates that lead release was controlled by anglesite and plumbojarosite dissolution. Zinc release appears to be controlled by Zn-talc and goslarite.

Even though effluent solutions were undersaturated with respect to Fe-bearing sulfates, low concentrations of Fe were mobilized from both tailings, regardless of the treatment. In other words, dissolution of Fe-bearing sulfates was non-stoichiometric. The low solubilization of Fe was attributed to the precipitation of goethite and hematite. The formation of Fe-(oxyhydr)oxide products sequestered a fraction of the Fe that might otherwise be released from the columns. The solubility of Al appears to be controlled by three mineral phases: gibbsite, orthoclase, and kaolinite. Possible minerals controlling the dissolution of calcium were gypsum and calcium oxalate precipitates.

In general, metal contaminant dissolution was not affected by the presence of oxalic acid. This is likely because the precipitation of Ca-oxalates minimized the interaction of oxalic acid with the contaminant metals found in Klondyke tailings, resulting in less metal mobilization from the tailings. This was surprising because the expected result would otherwise be an incremental increase in metal mobilization in the presence of oxalic acid as a result of the high stability of transition metal oxalate complexes that could enhance metal solubilization. This effect was not observed.

APPENDIX A: CHEMICAL DATA AND SATURATION INDEX DATA

Table A-1 pH values of collected pore volumes in T1 after being treated with NaCl, SWG, 10 μmoles Oxalic Acid, 100 μmoles Oxalic Acid.

	NaCl		SGW		10 μmoles Oxalic Acid		100 μmoles Oxalic Acid	
PV	pH	s.d.	pH	s.d.	pH	s.d.	pH	s.d.
1 - phase 1	3.83	0.10	3.78	0.03	3.23	0.95	3.57	0.16
2 - phase 1	3.94	0.11	3.90	0.08	3.35	0.99	3.84	0.06
3 -phase 1	4.03	0.13	4.01	0.05	3.50	0.89	3.93	0.05
4 -phase 1	4.09	0.13	4.08	0.01	4.03	0.11	4.00	0.05
5 -phase 1	4.13	0.14	4.15	0.14	4.08	0.08	4.04	0.04
6 -phase 1	4.15	0.13	4.17	0.09	3.68	0.75	4.09	0.03
7 -phase 1	4.21	0.13	4.18	0.09	3.40	1.30	4.11	0.02
8 -phase 1	4.23	0.12	4.15	0.10	3.73	0.74	4.15	0.03
9 -phase 1	4.24	0.11	4.21	0.06	4.21	0.04	4.23	0.08
10 -phase 1	4.26	0.14	4.25	0.10	4.22	0.06	4.20	0.02
1 -phase 3	4.32	0.08	4.43	0.15	4.13	0.11	4.24	0.07
2 -phase 3	4.36	0.10	4.50	0.17	4.15	0.11	4.23	0.13
3 -phase 3	4.41	0.07	4.60	0.18	4.21	0.10	4.31	0.11
4 -phase 3	4.44	0.08	4.85	0.42	4.29	0.03	4.42	0.02
5 -phase 3	4.47	0.09	5.07	0.78	4.36	0.03	4.41	0.12
6 -phase 3	4.50	0.08	5.25	0.98	4.39	0.01	4.41	0.08
7 -phase 3	4.51	0.07	5.34	1.10	4.41	0.03	4.48	0.07
8 -phase 3	4.54	0.08	5.40	1.22	4.46	0.02	4.51	0.06
9 -phase 3	4.56	0.11	5.48	1.21	4.54	0.06	4.56	0.07
10 -phase 3	4.57	0.09	5.53	1.21	4.55	0.08	4.63	0.03

Table A-2 pH values of collected pore volumes in T2 after being treated with NaCl, SWG, 10 μmoles Oxalic Acid, 100 μmoles Oxalic Acid.

	NaCl		SGW		10 μmoles Oxalic Acid		100 μmoles Oxalic Acid	
PV	pH	s.d.	pH	s.d.	pH	s.d.	pH	s.d.
1 - phase 1	5.58	0.24	5.85	0.36	6.04	0.14	5.28	0.45
2 - phase 1	5.69	0.07	6.23	0.19	6.40	0.03	6.21	0.16
3 -phase 1	5.80	0.04	6.57	0.11	6.70	0.05	6.44	0.10
4 -phase 1	5.90	0.04	6.84	0.27	6.91	0.19	6.72	0.08
5 -phase 1	5.94	0.11	6.89	0.26	7.08	0.13	6.84	0.04
6 -phase 1	5.98	0.11	6.98	0.20	7.13	0.25	6.94	0.04
7 -phase 1	6.01	0.13	7.03	0.18	7.13	0.08	7.02	0.04
8 -phase 1	6.06	0.13	7.07	0.17	7.13	0.12	7.08	0.03
9 -phase 1	6.06	0.15	7.13	0.11	7.12	0.08	7.14	0.04
10 -phase 1	6.05	0.12	7.18	0.10	7.11	0.09	7.19	0.05
1 -phase 3	5.77	0.81	6.78	0.34	6.47	0.13	6.78	0.24
2 -phase 3	5.66	0.82	6.79	0.39	6.56	0.09	6.90	0.16
3 -phase 3	5.67	0.82	6.99	0.40	6.67	0.05	7.02	0.18
4 -phase 3	5.65	0.72	7.12	0.30	6.77	0.04	7.16	0.13
5 -phase 3	5.65	0.79	7.20	0.23	6.88	0.09	7.26	0.11
6 -phase 3	5.64	0.79	7.30	0.21	6.90	0.09	7.33	0.07
7 -phase 3	5.50	0.55	7.38	0.19	6.97	0.05	7.33	0.09
8 -phase 3	5.81	0.85	7.46	0.26	6.97	0.02	7.39	0.11
9 -phase 3	5.92	1.22	7.42	0.17	7.00	0.02	7.43	0.08
10 -phase 3	5.73	0.75	7.51	0.28	7.13	0.19	7.45	0.09

Table A-3 Inorganic anions of collected pore volumes in T1 after being treated with NaCl.

PV	F- (μM)	s.d.	Cl- (μM)	s.d.	NO3- (μM)	s.d.	SO4- (μM)	s.d.
1 - phase 1	2,226	1,107	16,545	1,559	421	193	37,883	9,769
2 - phase 1	910	522	15,105	736	114	35	24,338	6,743
3 -phase 1	593	323	14,951	647	90	12	20,841	5,078
4 -phase 1	379	194	14,964	472	277	206	18,560	3,161
5 -phase 1	308	186	14,942	568	69	19	18,216	2,810
6 -phase 1	294	176	14,926	369	167	71	17,871	2,265
7 -phase 1	240	150	14,755	522	83	18	17,537	2,296
8 -phase 1	210	133	14,724	461	97	22	17,647	2,343
9 -phase 1	227	130	14,800	221	135	43	17,410	1,893
10 -phase 1	93	25	12,224	3,260	59	5	13,644	3,610
1 -phase 3	426	32	15,878	1,833	89	60	19,220	4,203
2 -phase 3	316	35	16,107	2,166	91	76	18,613	3,807
3 -phase 3	238	43	15,886	1,953	51	15	18,540	3,675
4 -phase 3	195	2	16,249	1,978	79	27	18,550	3,759
5 -phase 3	148	20	15,677	1,639	65	35	18,342	3,502
6 -phase 3	159	60	14,567	3,775	90	17	16,473	5,131
7 -phase 3	170	10	16,260	1,867	140	98	18,352	3,829
8 -phase 3	144	28	16,023	1,861	91	47	18,032	4,009
9 -phase 3	118	18	15,919	2,132	70	22	17,607	3,985
10 -phase 3	102	31	16,241	2,065	85	42	18,002	4,301

Table A-4 Inorganic anions of collected pore volumes in T2 after being treated with NaCl.

PV	F- (μM)	s.d.	Cl- (μM)	s.d.	NO3- (μM)	s.d.	SO4- (μM)	s.d.
1 - phase 1	1,531	668	16,970	4,639	1,283	459	56,084	21,408
2 - phase 1	909	265	17,309	4,292	191	72	32,545	11,701
3 -phase 1	854	94	17,497	4,109	124	60	23,784	7,711
4 -phase 1	817	88	17,182	3,483	132	7	21,500	6,497
5 -phase 1	855	161	17,255	3,802	95	6	21,320	6,946
6 -phase 1	829	185	17,206	3,699	79	3	21,632	7,847
7 -phase 1	818	151	17,878	5,044	122	34	21,486	7,562
8 -phase 1	823	271	17,172	4,455	123	60	20,622	6,453
9 -phase 1	687	127	16,718	3,418	59	13	19,952	5,561
10 -phase 1	699	132	17,548	4,736	121	54	20,825	6,998
1 -phase 3	885	61	18,791	4,455	188	108	23,881	8,104
2 -phase 3	928	65	17,391	3,928	455	670	21,607	6,981
3 -phase 3	916	45	17,140	4,015	86	82	20,853	6,351
4 -phase 3	944	100	18,242	5,225	49	11	20,773	6,568
5 -phase 3	899	55	17,810	3,453	61	16	20,481	5,564
6 -phase 3	821	39	17,391	3,555	55	1	20,174	5,444
7 -phase 3	812	20	17,670	3,551	186	213	20,445	5,523
8 -phase 3	763	55	18,457	5,440	114	85	21,651	7,328
9 -phase 3	720	32	17,453	3,965	55	30	21,034	6,234
10 -phase 3	808	53	20,039	6,363	59	14	23,076	8,398

Table A-5 Inorganic anions of collected pore volumes in T1 after being treated with SGW.

PV	F- (μM)	s.d.	Cl- (μM)	s.d.	NO3- (μM)	s.d.	SO4- (μM)	s.d.
1 - phase 1	1,305	1,712	2,153	235	273	24	26,124	16,744
2 - phase 1	780	757	2,156	506	260	79	21,052	10,752
3 -phase 1	420	364	1,857	52	220	77	18,601	5,641
4 -phase 1	327	203	1,888	75	220	82	17,345	3,672
5 -phase 1	353	93	2,214	412	196	63	16,388	3,125
6 -phase 1	281	111	1,817	131	239	101	16,081	2,955
7 -phase 1	253	85	1,772	226	224	96	15,105	3,268
8 -phase 1	227	77	1,746	102	235	97	15,304	3,242
9 -phase 1	203	48	1,762	78	238	104	15,465	3,538
10 -phase 1	224	63	1,801	194	198	76	14,358	4,016
1 -phase 3	2,100	1,487	2,148	401	526	179	28,351	7,422
2 -phase 3	685	337	1,854	141	331	41	19,596	1,065
3 -phase 3	449	157	1,867	246	730	741	17,276	3,267
4 -phase 3	404	95	1,969	158	1,894	2,458	16,436	3,320
5 -phase 3	282	115	1,925	128	898	964	17,106	2,618
6 -phase 3	254	49	1,838	195	294	38	16,765	3,645
7 -phase 3	218	74	1,957	166	286	29	16,803	3,292
8 -phase 3	210	50	2,034	126	294	34	16,976	3,519
9 -phase 3	197	32	1,837	100	369	147	16,273	3,536
10 -phase 3	221	23	1,986	263	434	163	17,385	3,534

Table A-6 Inorganic anions of collected pore volumes in T2 after being treated with SGW.

PV	F- (μM)	s.d.	Cl- (μM)	s.d.	NO3- (μM)	s.d.	SO4- (μM)	s.d.
1 - phase 1	1,279	712	2,219	545	752	753	33,671	29,145
2 - phase 1	966	59	2,226	471	377	238	26,582	15,883
3 -phase 1	1,038	205	2,713	1,428	388	176	21,805	10,309
4 -phase 1	868	66	1,990	386	342	86	19,252	6,606
5 -phase 1	979	274	2,153	621	307	84	18,511	6,760
6 -phase 1	820	43	2,221	610	306	124	19,250	7,185
7 -phase 1	757	55	2,044	487	287	100	17,922	5,703
8 -phase 1	897	321	2,183	791	360	146	18,098	8,289
9 -phase 1	958	433	2,074	558	303	131	18,522	6,936
10 -phase 1	759	101	2,212	732	343	120	18,350	6,768
1 -phase 3	1,890	215	2,117	86	1,121	136	43,870	2,598
2 -phase 3	1,026	110	2,339	1,057	376	190	24,796	5,624
3 -phase 3	960	167	2,017	454	320	63	19,539	5,035
4 -phase 3	1,009	111	1,996	510	323	65	18,699	6,158
5 -phase 3	1,024	143	2,118	410	383	98	18,717	4,963
6 -phase 3	950	155	2,141	484	348	70	17,505	5,398
7 -phase 3	911	100	1,999	399	362	74	18,385	5,822
8 -phase 3	913	200	2,213	472	276	118	18,551	4,242
9 -phase 3	824	98	2,071	415	325	140	18,703	5,933
10 -phase 3	820	101	2,220	629	408	56	18,210	6,019

Table A-7 Inorganic anions of collected pore volumes in T1 after being treated with 10 μmoles Oxalic Acid.

PV	F- (μM)	s.d.	Cl- (μM)	s.d.	NO3- (μM)	s.d.	SO4- (μM)	s.d.
1 - phase 1	385	91	8,137	10,171	253	96	20,523	4,383
2 - phase 1	745	609	2,025	195	343	28	21,470	7,766
3 -phase 1	429	371	1,806	113	281	25	18,254	4,579
4 -phase 1	359	257	1,801	157	281	27	17,220	3,515
5 -phase 1	452	225	2,135	568	260	42	16,632	3,116
6 -phase 1	345	194	1,829	117	329	58	16,494	3,026
7 -phase 1	316	175	1,752	109	302	26	15,303	2,598
8 -phase 1	301	169	1,768	157	295	32	15,595	3,131
9 -phase 1	276	180	1,795	84	319	49	14,978	3,027
10 -phase 1	276	145	1,715	28	265	40	14,742	4,403
1 -phase 3	2,366	1,673	2,436	354	613	155	31,622	8,791
2 -phase 3	820	322	2,267	422	375	71	21,938	1,027
3 -phase 3	514	142	2,172	435	813	810	18,545	2,715
4 -phase 3	439	89	2,126	242	2,031	2,677	17,633	3,867
5 -phase 3	271	126	2,060	399	873	929	17,387	3,527
6 -phase 3	291	38	2,045	191	314	44	17,921	2,790
7 -phase 3	315	32	2,349	341	353	78	18,974	3,384
8 -phase 3	248	18	2,164	147	531	414	17,940	3,636
9 -phase 3	242	39	2,033	307	385	131	17,443	4,422
10 -phase 3	164	89	2,164	462	430	166	17,891	3,545

Table A-8 Inorganic anions of collected pore volumes in T2 after being treated with 10 μmoles Oxalic Acid.

PV	F- (μM)	s.d.	Cl- (μM)	s.d.	NO3- (μM)	s.d.	SO4- (μM)	s.d.
1 - phase 1	2,053	783	2,306	236	1,280	88	54,077	2,870
2 - phase 1	1,471	476	2,445	593	480	67	28,642	2,547
3 -phase 1	1,398	452	2,239	432	357	50	22,681	1,448
4 -phase 1	1,457	67	2,374	321	445	72	21,136	775
5 -phase 1	1,346	554	2,444	920	374	68	20,190	676
6 -phase 1	994	44	1,906	121	329	28	19,763	432
7 -phase 1	1,319	548	2,547	830	405	141	20,220	246
8 -phase 1	1,097	155	2,035	111	334	19	20,324	990
9 -phase 1	1,043	194	2,191	350	326	47	19,880	233
10 -phase 1	980	218	2,167	378	319	18	19,669	185
1 -phase 3	916	205	2,820	991	4,340	5,089	24,898	406
2 -phase 3	902	137	2,396	59	790	209	24,521	671
3 -phase 3	1,097	110	2,487	147	1,154	386	24,391	1,168
4 -phase 3	1,224	194	2,754	644	2,669	3,269	23,614	395
5 -phase 3	1,058	128	2,831	451	823	150	23,085	1,015
6 -phase 3	1,105	230	2,722	31	1,391	1,304	22,875	486
7 -phase 3	1,096	161	2,442	227	1,012	320	22,819	1,074
8 -phase 3	1,047	302	2,430	214	716	478	22,359	353
9 -phase 3	1,203	78	2,909	564	2,101	2,227	22,904	618
10 -phase 3	978	230	2,704	291	1,447	695	22,714	308

Table A-9 Inorganic anions of collected pore volumes in T1 after being treated with 100 μmoles Oxalic Acid.

PV	F- (μM)	s.d.	Cl- (μM)	s.d.	NO3- (μM)	s.d.	SO4- (μM)	s.d.
1 - phase 1	2,464	251	2,023	338	1,444	728	41,091	6,071
2 - phase 1	918	305	1,683	70	405	138	25,034	4,570
3 -phase 1	557	246	1,631	224	368	121	19,200	3,751
4 -phase 1	447	233	1,635	184	391	141	17,765	2,963
5 -phase 1	391	203	1,646	253	360	126	17,844	2,083
6 -phase 1	326	171	1,586	220	399	68	17,436	2,257
7 -phase 1	357	191	1,704	210	374	164	16,897	2,605
8 -phase 1	293	179	1,562	160	340	117	17,452	1,796
9 -phase 1	313	231	1,700	231	769	790	17,245	1,762
10 -phase 1	274	194	1,417	343	272	28	14,709	4,769
1 -phase 3	719	225	2,623	315	512	82	23,409	1,712
2 -phase 3	614	251	2,713	300	453	172	23,114	1,672
3 -phase 3	575	236	2,358	105	402	79	22,208	1,170
4 -phase 3	384	48	2,257	391	370	55	20,344	2,611
5 -phase 3	388	115	2,314	287	398	76	21,060	1,420
6 -phase 3	312	86	2,132	70	310	15	21,377	512
7 -phase 3	384	73	2,332	312	362	38	22,672	2,320
8 -phase 3	328	109	2,298	272	359	33	21,398	352
9 -phase 3	381	42	2,403	401	429	144	21,767	505
10 -phase 3	374	55	2,533	516	433	5	21,040	1,180

Table A-10 Inorganic anions of collected pore volumes in T2 after being treated with 100 μmoles Oxalic Acid.

PV	F- (μM)	s.d.	Cl- (μM)	s.d.	NO3- (μM)	s.d.	SO4- (μM)	s.d.
1 - phase 1	1,502	306	3,554	1,173	1,576	1,062	55,448	40,839
2 - phase 1	1,262	294	2,659	751	2,803	3,849	31,001	15,566
3 -phase 1	1,018	254	2,789	994	485	59	24,517	8,375
4 -phase 1	713	6	2,416	677	453	32	21,065	7,258
5 -phase 1	790	44	2,360	719	437	20	19,991	5,787
6 -phase 1	797	41	2,327	712	447	69	19,661	5,753
7 -phase 1	696	1	2,483	852	517	126	19,733	6,354
8 -phase 1	1,094	371	2,199	643	474	60	18,995	5,746
9 -phase 1	1,020	267	2,285	571	1,429	1,677	19,531	5,114
10 -phase 1	769	174	2,761	1,158	551	186	19,833	6,684
1 -phase 3	978	182	2,746	1,180	651	282	24,752	4,947
2 -phase 3	1,056	91	2,289	347	457	204	24,522	2,246
3 -phase 3	1,035	90	2,430	162	376	51	23,171	1,417
4 -phase 3	981	229	2,349	203	326	18	22,229	2,830
5 -phase 3	1,207	270	3,207	1,041	407	38	25,257	1,412
6 -phase 3	1,085	360	2,678	209	408	38	24,657	1,751
7 -phase 3	965	131	2,756	1,119	692	450	21,738	6,213
8 -phase 3	1,090	362	2,584	402	833	826	22,945	1,235
9 -phase 3	927	196	2,855	1,370	481	186	20,711	5,871
10 -phase 3	901	193	2,494	222	600	427	21,652	3,695

Table A-11 Cations and metals concentration of collected pore volumes in T1 after being treated with NaCl.

PV	Pb (μM)	s.d.	Zn (μM)	s.d.	Fe (μM)	s.d.	Mg (μM)	s.d.	Ca (μM)	s.d.
1 - phase 1	11.92	2.73	12305	3437	2.32	0.70	1152	448	16366	1986
2 - phase 1	9.45	2.37	4068	2579	0.93	0.19	425	325	17789	275
3 -phase 1	9.25	2.91	1400	1208	0.35	0.17	136	182	18229	1086
4 -phase 1	8.85	1.82	3577	5904	0.32	0.19	2061	3545	18379	1209
5 -phase 1	9.22	1.61	1387	2233	0.58	0.69	719	1239	18659	1016
6 -phase 1	9.43	1.20	599	909	0.28	0.29	200	340	18348	1040
7 -phase 1	9.83	0.97	331	460	0.24	0.21	92	156	18441	759
8 -phase 1	10.18	0.88	195	238	0.17	0.21	61	103	18434	694
9 -phase 1	10.53	0.48	55	3	0.15	0.04	66	112	23688	9513
10 -phase 1	9.78	2.39	42	11	0.22	0.06	41	70	16612	3861
1 -phase 3	14.14	0.84	1026	1349	0.19	0.08	10	5	19608	1728
2 -phase 3	13.05	1.04	871	1286	0.18	0.11	5.33	3.22	20158	486
3 -phase 3	12.07	0.68	557	868	0.12	0.04	6.42	6.95	20539	1365
4 -phase 3	11.30	0.61	305	487	0.21	0.17	1.16	0.12	20392	926
5 -phase 3	10.61	1.17	167	270	0.15	0.09	1.16	0.60	21415	2836
6 -phase 3	9.22	1.22	115	192	0.08	0.01	0.61	0.11	17543	3067
7 -phase 3	10.33	0.64	95	153	0.13	0.08	0.87	0.37	21835	1370
8 -phase 3	9.82	0.91	77	121	0.13	0.06	1.76	1.62	20447	1788
9 -phase 3	9.34	0.85	96	89	0.13	0.03	0.61	0.28	23074	7507
10 -phase 3	9.40	1.13	53	91	0.33	0.28	2.13	1.50	20364	2204

Table A-11 *(Continued)*

PV	Na (μM)	s.d.	Al (μM)	s.d.	Si (μM)	s.d.	K (μM)	s.d.	Ti (μM)	s.d.
1 - phase 1	13430	1542	1124	438	234	82	4075	2723	0.140	0.089
2 - phase 1	15672	1165	462	282	155	58	1168	610	0.073	0.041
3 -phase 1	16669	1740	309	190	153	80	706	483	0.069	0.033
4 -phase 1	16546	1010	242	163	105	37	392	280	0.043	0.004
5 -phase 1	17334	2006	165	91	99	41	277	218	0.054	0.007
6 -phase 1	16930	997	133	75	88	32	219	163	0.051	0.022
7 -phase 1	16438	188	117	78	82	28	180	113	0.074	0.047
8 -phase 1	16627	1198	82	37	82	34	186	127	0.057	0.024
9 -phase 1	19669	6378	69	31	76	28	237	64	0.053	0.016
10 -phase 1	16457	6547	55	35	65	30	204	227	0.052	0.035
1 -phase 3	16686	2959	222	71	908	118	409	156	0.188	0.083
2 -phase 3	14057	2299	154	80	338	153	426	461	0.095	0.074
3 -phase 3	14552	963	101	54	257	133	244	228	0.073	0.034
4 -phase 3	14523	3333	67	31	204	115	229	212	0.086	0.045
5 -phase 3	15629	2985	45	19	174	88	213	176	0.073	0.035
6 -phase 3	13052	4503	32	16	86	18	255	327	0.086	0.047
7 -phase 3	15305	2855	29	14	77	5	327	324	0.071	0.043
8 -phase 3	14410	2808	21	13	70	13	219	207	0.073	0.036
9 -phase 3	16300	2793	16	10	63	13	360	436	0.072	0.044
10 -phase 3	15223	2729	14	10	67	14	262	267	0.070	0.046

Table A-11 *(Continued)*

PV	Cr (μM)	s.d.	Mn (μM)	s.d.	Co (μM)	s.d.	Ni (μM)	s.d.	Cu (μM)	s.d.
1 - phase 1	0.020	0.011	5125	1720	13.94	0.91	13.27	6.64	1496	225
2 - phase 1	0.009	0.016	1439	891	4.00	1.89	5.46	3.47	539	244
3 -phase 1	0.005	0.007	438	414	1.52	0.94	3.19	2.14	289	133
4 -phase 1	0.003	0.005	122	151	0.69	0.37	1.89	0.93	169	86
5 -phase 1	0.003	0.005	39	40	0.46	0.16	1.71	0.73	117	50
6 -phase 1	0.014	0.018	16	11	0.39	0.05	1.47	0.44	74	41
7 -phase 1	0.005	0.009	9.0	3.4	0.36	0.04	1.53	0.42	57	34
8 -phase 1	0.003	0.006	6.2	1.6	0.34	0.02	1.44	0.45	44	24
9 -phase 1	0.004	0.006	4.4	1.4	0.35	0.04	1.75	0.78	36	21
10 -phase 1	0.012	0.022	3.4	1.6	0.31	0.08	1.28	0.57	27	20
1 -phase 3	0.039	0.067	68	14	0.60	0.03	0.78	0.09	36	12
2 -phase 3	0.037	0.063	37	21	0.50	0.10	0.63	0.11	28	12
3 -phase 3	0.034	0.059	13	8	0.39	0.06	0.54	0.15	20	10
4 -phase 3	0.035	0.061	3.9	1.8	0.36	0.06	0.48	0.19	13.8	6.9
5 -phase 3	0.034	0.058	2.0	0.7	0.36	0.03	0.47	0.19	11.0	5.6
6 -phase 3	0.039	0.067	1.11	0.42	0.31	0.10	0.38	0.20	8.2	5.0
7 -phase 3	0.035	0.060	1.00	0.41	0.32	0.05	0.48	0.16	7.8	4.3
8 -phase 3	0.034	0.059	0.80	0.40	0.32	0.06	0.47	0.12	6.7	3.8
9 -phase 3	0.035	0.060	0.65	0.31	0.32	0.06	0.45	0.15	5.7	3.1
10 -phase 3	0.046	0.057	0.56	0.26	0.32	0.09	0.49	0.13	5.4	3.1

Table A-11 *(Continued)*

PV	As (μM)	s.d.	Se (μM)	s.d.	Mo (μM)	s.d.	Ag (μM)	s.d.
1 - phase 1	1.070	1.074	3.621	0.155	0.0013	0.0023	0.090	0.041
2 - phase 1	0.433	0.438	1.682	0.045	0.0340	0.0589	0.071	0.014
3 -phase 1	0.283	0.264	1.024	0.273	0.0019	0.0027	0.041	0.041
4 -phase 1	0.128	0.116	0.663	0.125	0.0013	0.0022	0.032	0.032
5 -phase 1	0.098	0.094	0.477	0.061	0.0012	0.0021	0.030	0.026
6 -phase 1	0.073	0.065	0.325	0.061	<3.76 E-4		0.022	0.021
7 -phase 1	0.048	0.039	0.238	0.037	<3.76 E-4		0.016	0.019
8 -phase 1	0.040	0.015	0.186	0.035	<3.76 E-4		0.011	0.017
9 -phase 1	0.041	0.028	0.160	0.038	<3.76 E-4		0.009	0.013
10 -phase 1	0.036	0.027	0.124	0.034	<3.76 E-4		0.009	0.010
1 -phase 3	0.055	0.007	0.745	0.068	0.0013	0.0013	0.004	0.005
2 -phase 3	0.042	0.007	0.576	0.094	0.0015	0.0007	0.005	0.003
3 -phase 3	0.022	0.005	0.345	0.101	0.0009	0.0011	0.005	0.004
4 -phase 3	0.019	0.005	0.203	0.043	0.0010	0.0014	0.003	0.004
5 -phase 3	0.010	0.009	0.135	0.031	0.0007	0.0010	0.004	0.004
6 -phase 3	0.0074	0.0065	0.096	0.016	0.0006	0.0010	0.003	0.003
7 -phase 3	0.0084	0.0073	0.087	0.006	0.0004	0.0007	0.002	0.003
8 -phase 3	0.0078	0.0070	0.081	0.006	0.0063	0.0109	0.003	0.003
9 -phase 3	0.0072	0.0067	0.074	0.011	0.0009	0.0015	0.0025	0.003
10 -phase 3	0.0079	0.0073	0.075	0.003	0.0013	0.0012	0.0024	0.003

Table A-11 *(Continued)*

PV	Cd (μM)	s.d.	Ba (μM)	s.d.	Bi (μM)	s.d.	U (μM)	s.d.
1 - phase 1	19.790	7.798	0.1170	0.1828	0.0022	0.0038	0.2429	0.0745
2 - phase 1	4.616	4.310	0.0573	0.0981	0.0020	0.0034	0.1052	0.0568
3 -phase 1	1.421	1.421	0.0476	0.0637	0.0046	0.0065	0.0671	0.0362
4 -phase 1	0.393	0.398	0.0240	0.0380	0.0023	0.0040	0.0420	0.0225
5 -phase 1	0.206	0.168	0.0184	0.0265	0.0009	0.0015	0.0310	0.0161
6 -phase 1	0.141	0.092	0.0109	0.0171	0.0010	0.0017	0.0242	0.0057
7 -phase 1	0.112	0.070	0.0142	0.0219	0.0010	0.0018	0.0231	0.0142
8 -phase 1	0.098	0.067	0.0104	0.0162	0.0024	0.0041	0.0186	0.0090
9 -phase 1	0.087	0.060	0.0105	0.0176	0.0020	0.0035	0.0180	0.0111
10 -phase 1	0.075	0.064	0.0120	0.0144	0.0040	0.0060	0.0222	0.0121
1 -phase 3	0.699	0.142	0.1002	0.1000	0.0077	0.0101	0.0181	0.0071
2 -phase 3	0.359	0.211	0.0521	0.0228	0.0067	0.0100	0.0161	0.0043
3 -phase 3	0.138	0.059	0.0578	0.0325	0.0022	0.0019	0.0114	0.0041
4 -phase 3	0.062	0.016	0.0664	0.0506	0.0032	0.0028	0.0111	0.0029
5 -phase 3	0.039	0.007	0.0764	0.0559	0.1519	0.2594	0.0104	0.0018
6 -phase 3	0.026	0.003	0.0678	0.0488	0.0251	0.0385	0.0081	0.0037
7 -phase 3	0.025	0.002	0.0934	0.0706	0.0037	0.0050	0.0064	0.0036
8 -phase 3	0.021	0.002	0.3178	0.4265	0.0119	0.0199	0.0054	0.0033
9 -phase 3	0.019	0.003	0.1009	0.0809	0.0033	0.0042	0.0058	0.0033
10 -phase 3	0.017	0.002	0.1122	0.0903	0.0041	0.0050	0.0046	0.0047

Table A-12 Cations and metals concentration of collected pore volumes in T2 after being treated with NaCl.

PV	Pb (μM)	s.d.	Zn (μM)	s.d.	Fe (μM)	s.d.	Mg (μM)	s.d.	Ca (μM)	s.d.
1 - phase 1	8.84	1.12	12037	1915	0.49	0.38	11254	2481	14380	1627
2 - phase 1	5.83	0.61	4561	694	0.11	0.02	3773	1101	15434	2118
3 -phase 1	4.96	0.56	1876	396	0.10	0.05	870	566	15992	2001
4 -phase 1	4.63	0.37	1156	476	0.08	0.03	315	213	16857	1844
5 -phase 1	4.68	0.55	853	357	0.01	0.02	127	93	17153	2543
6 -phase 1	4.69	0.72	689	236	0.14	0.20	55.1	26.0	17393	2578
7 -phase 1	4.98	0.82	598	219	0.02	0.02	33.4	18.1	17942	2000
8 -phase 1	4.75	0.48	477	112	0.04	0.05	20.5	7.7	16559	2928
9 -phase 1	4.52	0.61	434	124	0.01	0.02	15.0	4.8	16755	3074
10 -phase 1	4.46	0.42	396	97	0.00	0.00	12.8	4.5	18188	2834
1 -phase 3	5.29	1.64	2313	238	0.03	0.04	201	106	18987	4674
2 -phase 3	5.76	0.17	1737	538	0.02	0.03	146	128	17046	3472
3 -phase 3	5.43	0.63	1045	447	0.03	0.03	67	75	17987	3031
4 -phase 3	4.83	0.89	638	202	0.08	0.03	18	17	17696	3769
5 -phase 3	4.52	0.93	415	56	0.06	0.10	7.27	4.49	17750	3928
6 -phase 3	4.73	0.53	336	28	0.09	0.09	4.30	1.51	17983	3645
7 -phase 3	4.72	0.75	276	16	0.04	0.04	3.28	1.14	17922	3361
8 -phase 3	4.06	0.31	223	9	0.02	0.03	2.77	0.54	17015	4930
9 -phase 3	4.10	1.53	206	36	0.02	0.02	2.32	0.53	17585	6295
10 -phase 3	3.93	0.28	183	34	0.02	0.02	2.40	0.94	16506	4332

Table A-12 *(Continued)*

PV	Na (μM)	s.d.	Al (μM)	s.d.	Si (μM)	s.d.	K (μM)	s.d.	Ti (μM)	s.d.
1 - phase 1	11052	1284	30.44	3.20	540	26	2162	203	0.145	0.096
2 - phase 1	15074	968	13.46	5.25	443	104	1426	601	0.088	0.023
3 -phase 1	15752	888	7.00	2.35	450	32	625	237	0.083	0.021
4 -phase 1	16405	275	6.01	1.88	420	34	330	78	0.076	0.028
5 -phase 1	16050	628	4.56	2.05	393	27	188	16	0.077	0.013
6 -phase 1	16392	725	2.75	1.65	402	6	147	46	0.071	0.029
7 -phase 1	16399	154	2.10	1.08	361	27	212	92	0.067	0.022
8 -phase 1	15854	1175	1.20	0.44	343	21	112	25	0.064	0.030
9 -phase 1	15517	1352	0.82	0.65	336	17	146	77	0.070	0.031
10 -phase 1	16976	847	0.47	0.81	339	28	141	34	0.064	0.015
1 -phase 3	18021	1681	1.86	1.38	1174	274	508	495	0.179	0.057
2 -phase 3	14326	1605	3.21	1.74	707	114	159	133	0.122	0.052
3 -phase 3	14861	382	2.04	0.58	527	164	126	84	0.098	0.038
4 -phase 3	14840	805	1.67	0.88	436	113	356	510	0.090	0.036
5 -phase 3	14753	957	0.63	0.16	431	111	159	93	0.080	0.026
6 -phase 3	15793	838	0.70	0.33	402	128	89	74	0.092	0.021
7 -phase 3	14331	1057	0.43	0.17	379	108	191	247	0.091	0.031
8 -phase 3	14815	65	0.73	0.28	347	120	458	598	0.080	0.031
9 -phase 3	14729	825	0.32	0.26	357	132	113	37	0.084	0.033
10 -phase 3	15157	138	0.52	0.42	345	114	388	482	0.084	0.034

Table A-12 *(Continued)*

PV	Ag (μM)	s.d.	Mn (μM)	s.d.	Co (μM)	s.d.	Ni (μM)	s.d.
1 - phase 1	0.0146	0.0100	12937	2814	4.76	0.32	4.34	0.33
2 - phase 1	0.0099	0.0052	4217	1225	1.83	0.29	2.24	0.27
3 -phase 1	0.0046	0.0044	1051	353	0.82	0.08	1.52	0.25
4 -phase 1	0.0045	0.0039	408	274	0.57	0.07	1.31	0.31
5 -phase 1	0.0009	0.0015	216	155	0.48	0.06	1.19	0.31
6 -phase 1	<5.61 E-4		137	87	0.45	0.04	1.17	0.36
7 -phase 1	<5.61 E-4		98	58	0.45	0.06	1.16	0.41
8 -phase 1	0.00018	0.00032	67	32	0.42	0.02	1.07	0.40
9 -phase 1	0.00033	0.00057	54	25	0.41	0.01	1.03	0.38
10 -phase 1	<5.61 E-4		48	25	0.43	0.02	1.06	0.38
1 -phase 3	0.0013	0.0007	503	99	3.03	4.21	1.10	0.31
2 -phase 3	0.0021	0.0008	356	183	5.00	7.78	0.92	0.35
3 -phase 3	0.0014	0.0011	149	155	1.81	2.48	0.76	0.21
4 -phase 3	0.0007	0.0004	59	54	0.61	0.54	0.64	0.16
5 -phase 3	0.0006	0.0003	29	20	0.38	0.14	0.66	0.27
6 -phase 3	0.0006	0.0005	15.8	6.0	4.97	8.11	0.58	0.11
7 -phase 3	0.0006	0.0003	11.9	3.9	0.38	0.17	0.58	0.08
8 -phase 3	0.0003	0.0005	10.7	1.6	0.44	0.18	0.58	0.06
9 -phase 3	0.0005	0.0007	9.1	1.8	0.72	0.61	0.58	0.12
10 -phase 3	0.0001	0.0002	7.9	1.7	0.60	0.20	0.57	0.09

Table A-12 *(Continued)*

PV	Cu (μM)	s.d.	As (μM)	s.d.	Se (μM)	s.d.	Mo (μM)	s.d.
1 - phase 1	44.76	3.68	1.390	1.780	2.239	0.224	0.0052	0.0047
2 - phase 1	19.91	2.63	0.638	0.875	0.583	0.122	0.0034	0.0030
3 -phase 1	8.21	2.21	0.313	0.448	0.176	0.016	0.0030	0.0009
4 -phase 1	5.38	1.34	0.200	0.278	0.112	0.006	0.0032	0.0012
5 -phase 1	4.30	1.56	0.157	0.219	0.085	0.005	0.0041	0.0026
6 -phase 1	3.57	1.23	0.106	0.134	0.073	0.003	0.0025	0.0006
7 -phase 1	3.10	1.07	0.081	0.100	0.064	0.006	0.0039	0.0007
8 -phase 1	2.48	0.76	0.063	0.072	0.057	0.004	0.0038	0.0009
9 -phase 1	2.18	0.68	0.053	0.055	0.054	0.005	0.0037	0.0023
10 -phase 1	1.79	0.35	0.048	0.047	0.051	0.002	0.0033	0.0010
1 -phase 3	4.56	0.23	0.095	0.055	0.318	0.084	0.0036	0.0014
2 -phase 3	4.47	1.79	0.075	0.057	0.141	0.067	0.0037	0.0005
3 -phase 3	2.97	1.15	0.076	0.087	0.068	0.003	0.0036	0.0018
4 -phase 3	2.19	0.65	0.031	0.019	0.044	0.009	0.0040	0.0004
5 -phase 3	1.72	0.34	0.029	0.019	0.041	0.014	0.0037	0.0007
6 -phase 3	1.46	0.23	0.031	0.023	0.039	0.011	0.0055	0.0028
7 -phase 3	1.30	0.10	0.031	0.023	0.035	0.007	0.0052	0.0024
8 -phase 3	1.27	0.00	0.026	0.015	0.033	0.012	0.0035	0.0011
9 -phase 3	0.99	0.23	0.023	0.015	0.032	0.011	0.0040	0.0001
10 -phase 3	1.03	0.09	0.029	0.017	0.035	0.006	0.0038	0.0005

Table A-12 *(Continued)*

PV	Cd (μM)	s.d.	Ba (μM)	s.d.	Bi (μM)	s.d.	U (μM)	s.d.
1 - phase 1	57.849	14.751	0.0011	0.0003	0.0008	0.0014	0.0007	0.0003
2 - phase 1	25.141	4.958	0.0014	0.0012	0.0012	0.0021	0.0002	0.0002
3 -phase 1	10.189	2.157	0.0007	0.0004	0.0005	0.0008	0.0001	0.0001
4 -phase 1	5.519	1.905	0.0011	0.0010	0.0006	0.0010	0.0001	0.0000
5 -phase 1	3.910	1.527	0.0013	0.0016	0.0005	0.0009	0.0001	0.0001
6 -phase 1	3.016	1.027	0.0022	0.0022	0.0006	0.0010	0.0001	0.0001
7 -phase 1	2.430	0.879	0.0034	0.0037	0.0013	0.0022	0.0001	0.0001
8 -phase 1	1.918	0.578	0.0018	0.0016	0.0010	0.0017	0.0001	0.0001
9 -phase 1	1.587	0.448	0.0012	0.0010	0.0009	0.0015	0.0001	0.0001
10 -phase 1	1.418	0.471	0.0013	0.0010	0.0016	0.0014	0.0003	0.0004
1 -phase 3	6.224	1.727	0.1120	0.1089	0.0049	0.0042	0.0010	0.0015
2 -phase 3	4.640	2.503	0.0794	0.0668	0.0023	0.0012	0.0001	0.00001
3 -phase 3	2.777	1.815	0.0948	0.0821	0.0028	0.0025	0.0001	0.00001
4 -phase 3	1.575	0.872	0.1069	0.0925	0.0153	0.0199	0.0001	0.00001
5 -phase 3	1.007	0.391	0.1187	0.1030	0.0028	0.0026	0.00003	0.00001
6 -phase 3	0.758	0.218	0.1285	0.1113	0.0347	0.0472	0.00003	0.00001
7 -phase 3	0.622	0.154	0.1388	0.1204	0.0076	0.0112	0.00003	0.00001
8 -phase 3	0.561	0.080	0.1151	0.1628	0.0077	0.0102	0.00002	0.00002
9 -phase 3	0.476	0.070	0.1210	0.1711	0.0016	0.0023	0.00002	0.00001
10 -phase 3	0.416	0.046	0.1215	0.1718	0.0031	0.0044	0.0099	0.0140

Table A-13 Cations and metals concentration of collected pore volumes in T1 after being treated with SWG.

PV	Pb (μM)	s.d.	Zn (μM)	s.d.	Fe (μM)	s.d.	Mg (μM)	s.d.	Ca (μM)	s.d.
1 - phase 1	11.33	1.98	20673	5485	6.620	4.067	1729	89	13844	786
2 - phase 1	9.44	1.46	7168	641	1.871	0.693	647	222	17918	3506
3 -phase 1	8.51	0.98	1679	1137	1.147	0.219	319	136	16068	2363
4 -phase 1	8.33	1.15	596	476	0.765	0.198	204	90	16502	1263
5 -phase 1	8.51	0.66	223	161	2.181	1.737	83	12	16148	1512
6 -phase 1	8.71	0.27	121	50	0.483	0.377	90	14	16166	1839
7 -phase 1	8.66	0.54	68	10	0.370	0.262	84	18	16922	867
8 -phase 1	8.30	1.01	110	49	0.451	0.330	203	176	18666	3111
9 -phase 1	8.25	0.97	66	22	0.795	0.988	85	24	19592	1201
10 -phase 1	7.74	1.03	57	27	0.328	0.335	100	71	17007	1046
1 -phase 3	12.70	1.15	114	102	0.257	0.092	3928	6417	16786	1116
2 -phase 3	11.20	1.07	743	1103	0.295	0.271	1730	2627	16259	733
3 -phase 3	9.42	1.35	510	737	0.217	0.210	651	901	18022	3605
4 -phase 3	8.09	2.06	275	418	0.090	0.044	245	293	15871	602
5 -phase 3	7.03	3.03	165	213	0.198	0.240	131	107	16072	868
6 -phase 3	6.40	4.06	103	129	0.067	0.012	101	82	15970	1544
7 -phase 3	5.93	4.37	90	72	0.107	0.090	80	22	15548	1731
8 -phase 3	5.78	4.47	73	56	0.155	0.095	74	23	15669	1602
9 -phase 3	5.66	4.37	65	52	0.091	0.067	72	22	14182	1537
10 -phase 3	5.22	4.34	39	40	0.075	0.076	64	16	13267	1337

Table A-13 *(Continued)*

PV	Na (μM)	s.d.	Al (μM)	s.d.	Si (μM)	s.d.	K (μM)	s.d.	Ti (μM)	s.d.
1 - phase 1	2336	237	6671	8105	418	136	2810	439	0.127	0.020
2 - phase 1	2201	363	3162	4381	371	98	1747	994	0.144	0.094
3 -phase 1	2451	621	1827	2457	348	111	944	224	0.068	0.007
4 -phase 1	2394	479	1302	1645	363	69	789	152	0.102	0.011
5 -phase 1	2295	380	915	1353	334	69	925	396	0.117	0.033
6 -phase 1	2254	363	753	1125	363	76	695	48	0.070	0.018
7 -phase 1	2087	395	590	880	347	69	677	60	0.068	0.043
8 -phase 1	2641	812	83	27	388	53	881	172	0.062	0.038
9 -phase 1	2418	597	71	24	320	48	709	84	0.097	0.018
10 -phase 1	2444	309	58	22	311	80	812	191	0.080	0.023
1 -phase 3	1843	472	133	77	1008	74	1020	316	0.357	0.149
2 -phase 3	1505	47	102	75	504	20	746	46	0.113	0.029
3 -phase 3	1599	101	74	56	385	9	630	113	0.089	0.008
4 -phase 3	1501	4	38	25	345	31	524	169	0.190	0.176
5 -phase 3	1524	102	25	22	291	22	541	27	0.086	0.015
6 -phase 3	1457	58	22	18	311	12	565	67	0.071	0.023
7 -phase 3	1595	71	15	15	344	27	612	23	0.237	0.255
8 -phase 3	1640	183	14	12	317	26	605	21	0.101	0.034
9 -phase 3	1571	131	11	10	308	38	624	35	0.103	0.013
10 -phase 3	1445	32	9	9	294	38	639	188	0.084	0.035

Table A-13 *(Continued)*

PV	Cu (μM)	s.d.	Cr (μM)	s.d.	Mn (μM)	s.d.	Co (μM)	s.d.
1 - phase 1	647.93	837.02	0.063	0.021	27138.19	30633.93	14.01	2.10
2 - phase 1	337.84	487.19	0.048	0.037	9937.14	14749.17	5.46	2.64
3 -phase 1	167.39	238.90	0.029	0.010	3464.57	5374.70	2.00	1.33
4 -phase 1	102.19	147.33	0.030	0.008	1132.00	1795.96	0.91	0.45
5 -phase 1	65.29	92.77	0.139	0.187	293.72	432.03	0.61	0.17
6 -phase 1	49.46	71.26	0.027	0.018	31.23	2.06	0.47	0.11
7 -phase 1	60.52	23.44	0.019	0.011	21.38	5.63	0.43	0.05
8 -phase 1	46.73	17.60	0.020	0.018	19.43	9.26	0.42	0.04
9 -phase 1	37.21	13.76	0.024	0.007	17.40	9.58	0.52	0.21
10 -phase 1	30.89	13.55	0.029	0.033	15.90	9.49	0.41	0.03
1 -phase 3	26.75	6.79	0.036	0.055	40.07	12.43	0.55	0.07
2 -phase 3	23.07	11.28	0.039	0.054	28.40	17.42	0.47	0.05
3 -phase 3	15.53	7.73	0.040	0.055	11.56	6.96	0.38	0.03
4 -phase 3	11.43	5.85	0.035	0.057	4.12	0.87	0.35	0.01
5 -phase 3	8.67	4.89	0.038	0.059	2.08	0.13	0.37	0.01
6 -phase 3	6.90	4.82	0.038	0.061	1.25	0.26	0.35	0.02
7 -phase 3	5.60	4.30	0.036	0.055	0.91	0.30	0.36	0.05
8 -phase 3	4.70	3.84	0.050	0.055	0.58	0.25	0.34	0.03
9 -phase 3	4.03	3.24	0.035	0.053	0.57	0.60	0.34	0.03
10 -phase 3	3.42	2.99	0.036	0.058	0.12	0.20	0.32	0.06

Table A-13 *(Continued)*

PV	Ni (μM)	s.d.	As (μM)	s.d.	Se (μM)	s.d.	Mo (μM)	s.d.
1 - phase 1	14.75	3.99	1.113	0.840	4.478	0.523	0.010	0.017
2 - phase 1	6.03	4.17	0.562	0.541	2.165	0.522	0.017	0.015
3 -phase 1	2.49	2.50	0.280	0.250	1.278	0.198	0.005	0.009
4 -phase 1	1.28	1.58	0.159	0.114	0.862	0.011	0.003	0.004
5 -phase 1	2.20	1.71	0.118	0.075	0.632	0.024	0.026	0.036
6 -phase 1	0.72	0.89	0.077	0.042	0.440	0.012	0.005	0.009
7 -phase 1	0.66	0.81	0.070	0.041	0.324	0.028	0.006	0.010
8 -phase 1	0.60	0.83	0.051	0.010	0.276	0.038	0.004	0.007
9 -phase 1	0.76	0.78	0.057	0.024	0.226	0.050	0.002	0.004
10 -phase 1	0.59	0.88	0.051	0.018	0.180	0.056	0.001	0.001
1 -phase 3	0.81	0.28	0.082	0.014	0.798	0.059	0.006	0.006
2 -phase 3	0.71	0.21	0.062	0.011	0.717	0.202	0.003	0.005
3 -phase 3	0.55	0.18	0.037	0.011	0.445	0.155	0.007	0.009
4 -phase 3	0.41	0.06	0.023	0.014	0.248	0.051	0.003	0.003
5 -phase 3	0.42	0.03	0.016	0.015	0.181	0.031	0.003	0.002
6 -phase 3	0.45	0.17	0.015	0.013	0.144	0.029	0.002	0.002
7 -phase 3	0.45	0.15	0.010	0.009	0.127	0.016	0.003	0.004
8 -phase 3	0.68	0.56	0.009	0.008	0.109	0.016	0.004	0.002
9 -phase 3	0.43	0.11	0.011	0.010	0.102	0.012	0.002	0.001
10 -phase 3	0.33	0.07	0.012	0.011	0.095	0.009	0.002	0.001

Table A-13 *(Continued)*

PV	Cd (μM)	s.d.	Ba (μM)	s.d.	Bi (μM)	s.d.	U (μM)	s.d.
1 - phase 1	19.194	3.590	0.32	0.17	0.0505	0.0558	0.2589	0.0286
2 - phase 1	6.742	4.614	0.22	0.05	0.0165	0.0097	0.1274	0.0391
3 -phase 1	2.192	2.063	0.22	0.11	0.0218	0.0174	0.0766	0.0215
4 -phase 1	0.710	0.724	0.26	0.17	0.0232	0.0227	0.0526	0.0111
5 -phase 1	0.291	0.290	0.34	0.30	0.0339	0.0201	0.0439	0.0075
6 -phase 1	0.142	0.154	0.20	0.14	0.0105	0.0125	0.0375	0.0054
7 -phase 1	0.090	0.112	0.19	0.13	0.0102	0.0060	0.0324	0.0052
8 -phase 1	0.063	0.093	0.20	0.14	0.0062	0.0012	0.0256	0.0060
9 -phase 1	0.051	0.089	0.19	0.14	0.0058	0.0045	0.0231	0.0072
10 -phase 1	0.044	0.075	0.21	0.16	0.0066	0.0081	0.0203	0.0054
1 -phase 3	0.419	0.096	0.11	0.10	0.0075	0.0106	0.0151	0.0058
2 -phase 3	0.288	0.126	0.11	0.09	0.0030	0.0027	0.0126	0.0050
3 -phase 3	0.142	0.066	0.19	0.19	0.0017	0.0015	0.0080	0.0052
4 -phase 3	0.068	0.018	0.11	0.08	0.0061	0.0056	0.0056	0.0039
5 -phase 3	0.039	0.005	0.12	0.10	0.0015	0.0014	0.0055	0.0058
6 -phase 3	0.027	0.002	0.19	0.16	0.0023	0.0022	0.0039	0.0040
7 -phase 3	0.018	0.003	0.18	0.18	0.0041	0.0058	0.0040	0.0036
8 -phase 3	0.012	0.004	0.18	0.15	0.0031	0.0033	0.0039	0.0036
9 -phase 3	0.010	0.005	0.17	0.14	0.0020	0.0017	0.0028	0.0035
10 -phase 3	0.005	0.003	0.14	0.12	0.0066	0.0109	0.0024	0.0038

Table A-14 Cations and metals concentration of collected pore volumes in T2 after being treated with SWG.

PV	Pb (μM)	s.d.	Zn (μM)	s.d.	Fe (μM)	s.d.	Mg (μM)	s.d.	Ca (μM)	s.d.
1 - phase 1	5.73	1.32	19691	7671	0.488	0.159	18152	5933	11948	642
2 - phase 1	2.08	0.92	7803	2443	0.210	0.110	4840	757	14486	1383
3 -phase 1	0.67	0.21	2129	297	0.304	0.313	1399	275	15896	2629
4 -phase 1	0.42	0.09	1224	218	1.810	2.402	458	112	14815	986
5 -phase 1	0.27	0.05	825	80	0.149	0.100	221	31	13922	1223
6 -phase 1	0.28	0.02	601	38	0.579	0.804	176	21	15613	599
7 -phase 1	0.25	0.02	517	85	0.079	0.020	127	21	17133	4496
8 -phase 1	0.27	0.04	427	35	0.305	0.377	121	21	14711	1367
9 -phase 1	0.20	0.07	358	16	0.068	0.066	142	61	15353	1997
10 -phase 1	0.16	0.04	295	7	0.165	0.120	106	21	16135	2950
1 -phase 3	2.51	1.20	1657	314	0.121	0.129	452	131	14981	1525
2 -phase 3	1.72	0.33	1227	125	0.027	0.023	377	78	13903	2082
3 -phase 3	0.90	0.34	750	32	0.123	0.180	177	18	13921	880
4 -phase 3	0.76	0.05	469	50	0.111	0.178	77	30	13708	1202
5 -phase 3	0.70	0.26	346	82	0.019	0.020	53	23	13806	1745
6 -phase 3	0.72	0.30	273	88	0.004	0.005	52	20	14275	1631
7 -phase 3	0.90	0.42	230	83	0.092	0.101	47	17	13660	1266
8 -phase 3	0.73	0.13	212	78	0.393	0.530	485	767	13719	846
9 -phase 3	0.86	0.33	177	80	1.718	2.967	51	22	13992	1590
10 -phase 3	0.77	0.10	197	15	0.075	0.097	60	13	15140	929

Table A-14 *(Continued)*

PV	Na (μM)	s.d.	Al (μM)	s.d.	Si (μM)	s.d.	K (μM)	s.d.	Ti (μM)	s.d.
1 - phase 1	2853	868	28.41	5.43	847	315	2293	222	0.126	0.033
2 - phase 1	2471	833	5.45	5.14	706	254	1256	120	0.092	0.014
3 -phase 1	2461	780	1.11	0.58	687	316	755	80	0.104	0.030
4 -phase 1	2277	467	0.82	0.43	562	187	653	33	0.090	0.026
5 -phase 1	2254	597	0.56	0.29	496	135	682	47	0.095	0.054
6 -phase 1	2297	603	0.91	0.87	591	229	605	86	0.096	0.033
7 -phase 1	2224	542	0.25	0.35	571	278	580	127	0.145	0.126
8 -phase 1	2285	527	0.71	1.00	520	210	632	131	0.073	0.011
9 -phase 1	2346	694	0.30	0.36	514	115	610	173	0.077	0.017
10 -phase 1	2213	512	0.49	0.34	412	92	563	132	0.074	0.018
1 -phase 3	1793	107	0.98	0.15	908	194	868	27	0.242	0.077
2 -phase 3	1419	105	0.53	0.30	578	135	679	84	0.116	0.005
3 -phase 3	1481	3	0.43	0.26	507	135	563	72	0.115	0.033
4 -phase 3	1482	16	0.54	0.58	403	132	470	47	0.082	0.005
5 -phase 3	1462	75	0.45	0.23	384	130	538	52	0.144	0.103
6 -phase 3	1460	133	0.88	0.92	384	102	564	76	0.101	0.032
7 -phase 3	1418	76	0.75	0.69	353	105	620	126	0.076	0.010
8 -phase 3	1728	382	0.57	0.06	344	92	585	48	0.072	0.023
9 -phase 3	1442	138	0.53	0.47	331	99	600	54	0.074	0.014
10 -phase 3	1520	51	0.72	0.04	358	29	596	3	0.077	0.020

Table A-14 *(Continued)*

PV	Cr (μM)	s.d.	Mn (μM)	s.d.	Co (μM)	s.d.	Ni (μM)	s.d.
1 - phase 1	0.025	0.021	20591.09	6887.25	4.83	0.56	4.49	0.25
2 - phase 1	0.015	0.013	6742.49	1586.30	1.96	0.21	1.80	0.50
3 -phase 1	0.027	0.032	1340.07	141.50	0.97	0.09	0.81	0.39
4 -phase 1	0.034	0.038	523.96	103.14	0.67	0.04	0.55	0.30
5 -phase 1	0.015	0.014	263.10	37.08	0.56	0.02	0.42	0.28
6 -phase 1	0.075	0.119	159.63	22.29	0.50	0.04	0.47	0.19
7 -phase 1	0.006	0.006	113.52	9.37	0.47	0.03	0.37	0.21
8 -phase 1	0.062	0.099	91.99	8.07	0.51	0.02	0.32	0.26
9 -phase 1	0.007	0.007	74.77	2.40	0.48	0.06	0.25	0.28
10 -phase 1	0.022	0.028	64.57	3.41	0.44	0.04	0.40	0.14
1 -phase 3	0.003	0.002	379.75	144.86	4.65	6.77	1.18	0.29
2 -phase 3	0.003	0.004	268.04	79.46	0.66	0.09	0.98	0.19
3 -phase 3	0.002	0.002	130.62	21.54	0.87	0.63	0.83	0.22
4 -phase 3	0.009	0.013	57.29	6.22	0.62	0.31	0.81	0.11
5 -phase 3	0.001	0.001	30.30	4.97	0.70	0.48	0.62	0.11
6 -phase 3	0.013	0.022	20.46	2.15	1.48	1.86	0.56	0.17
7 -phase 3	0.013	0.012	15.39	1.87	0.44	0.08	0.63	0.02
8 -phase 3	0.012	0.016	13.54	2.07	0.80	0.66	0.61	0.13
9 -phase 3	0.053	0.084	10.45	1.26	0.67	0.49	0.90	0.66
10 -phase 3	0.012	0.008	9.64	0.34	0.39	0.02	0.45	0.01

Table A-14 *(Continued)*

PV	As (μM)	s.d.	Se (μM)	s.d.	Mo (μM)	s.d.	Cd (μM)	s.d.
1 - phase 1	1.932	2.656	2.027	0.113	0.012	0.008	52.020	5.332
2 - phase 1	1.015	1.515	0.541	0.145	0.007	0.007	21.819	4.484
3 -phase 1	0.543	0.834	0.148	0.032	0.006	0.005	9.779	2.552
4 -phase 1	0.320	0.478	0.075	0.014	0.008	0.002	5.807	1.514
5 -phase 1	0.227	0.330	0.051	0.010	0.004	0.005	4.042	1.007
6 -phase 1	0.164	0.230	0.039	0.018	0.003	0.005	3.166	0.915
7 -phase 1	0.115	0.155	0.027	0.008	0.002	0.003	2.505	0.532
8 -phase 1	0.096	0.120	0.021	0.009	0.002	0.003	2.072	0.665
9 -phase 1	0.071	0.084	0.019	0.013	0.003	0.004	1.700	0.508
10 -phase 1	0.052	0.055	0.017	0.014	0.003	0.003	1.429	0.404
1 -phase 3	0.096	0.036	0.296	0.076	0.011	0.004	5.671	0.245
2 -phase 3	0.058	0.013	0.108	0.010	0.009	0.001	4.653	0.543
3 -phase 3	0.040	0.013	0.045	0.005	0.009	0.001	3.045	0.233
4 -phase 3	0.034	0.006	0.029	0.006	0.010	0.001	1.945	0.124
5 -phase 3	0.029	0.007	0.024	0.005	0.009	0.001	1.434	0.230
6 -phase 3	0.024	0.012	0.023	0.005	0.010	0.002	1.159	0.191
7 -phase 3	0.024	0.008	0.020	0.003	0.008	0.001	0.933	0.195
8 -phase 3	0.025	0.018	0.017	0.004	0.011	0.004	0.800	0.175
9 -phase 3	0.023	0.009	0.019	0.003	0.009	0.002	0.659	0.172
10 -phase 3	0.011	0.004	0.014	0.003	0.0109	0.0002	0.650	0.140

Table A-14 *(Continued)*

PV	Cu (μM)	s.d.	Ba (μM)	s.d.	Bi (μM)	s.d.	U (μM)	s.d.
1 - phase 1	36.88	7.26	0.10	0.09	0.0122	0.0157	0.0006	0.0006
2 - phase 1	11.99	7.53	0.15	0.13	0.0023	0.0016	0.0002	0.0002
3 -phase 1	3.01	2.03	0.16	0.14	0.0081	0.0047	0.0002	0.0002
4 -phase 1	1.79	1.10	0.22	0.19	0.0065	0.0036	0.0003	0.0002
5 -phase 1	1.30	1.02	0.23	0.20	0.0038	0.0025	0.0004	0.0001
6 -phase 1	1.63	1.41	0.25	0.22	0.0090	0.0090	0.0004	0.0001
7 -phase 1	1.28	1.23	0.28	0.24	0.0279	0.0430	0.0004	0.0000
8 -phase 1	1.12	1.22	0.25	0.22	0.0108	0.0129	0.0005	0.0001
9 -phase 1	0.89	1.10	0.27	0.23	0.0159	0.0167	0.0005	0.0001
10 -phase 1	0.67	0.64	0.31	0.27	0.0023	0.0033	0.0003	0.0004
1 -phase 3	2.78	1.42	0.27	0.01	0.0082	0.0096	0.0004	0.0005
2 -phase 3	1.80	0.79	0.15	0.13	0.0052	0.0018	0.0004	0.0005
3 -phase 3	0.97	0.38	0.16	0.14	0.0067	0.0049	0.0004	0.0005
4 -phase 3	0.88	0.19	0.21	0.18	0.0040	0.0006	0.0005	0.0004
5 -phase 3	0.59	0.16	0.21	0.18	0.0148	0.0199	0.0005	0.0005
6 -phase 3	0.61	0.01	0.23	0.19	0.0040	0.0035	0.0006	0.0004
7 -phase 3	0.58	0.06	0.27	0.23	0.0031	0.0008	0.0007	0.0004
8 -phase 3	0.46	0.13	0.28	0.24	0.0052	0.0045	0.0007	0.0004
9 -phase 3	0.52	0.08	0.29	0.26	0.0064	0.0064	0.0005	0.0004
10 -phase 3	0.36	0.02	0.48	0.02	0.0061	0.0066	0.0007	0.0006

Table A-15 Cations and metals concentration of collected pore volumes in T1 after being treated with 10 μmoles Oxalic Acid.

PV	Pb (μM)	s.d.	Zn (μM)	s.d.	Fe (μM)	s.d.	Mg (μM)	s.d.
1 - phase 1	11.12	2.53	12112.08	3417.33	6.73	4.55	1357.0	295.9
2 - phase 1	8.75	1.68	12458.25	13242.84	1.76	1.01	520.9	238.0
3 -phase 1	8.28	1.51	1638.97	1156.36	1.44	0.73	320.6	318.0
4 -phase 1	8.16	1.15	667.37	581.85	0.62	0.35	143.7	121.4
5 -phase 1	8.23	0.93	301.07	287.60	0.73	0.86	79.2	47.9
6 -phase 1	8.25	0.90	130.50	108.16	0.44	0.37	52.0	33.2
7 -phase 1	8.42	0.32	75.80	34.67	0.70	0.59	40.5	17.8
8 -phase 1	8.35	0.53	56.22	10.97	1.17	1.60	37.2	13.0
9 -phase 1	7.98	0.26	45.33	14.27	0.23	0.15	27.4	9.6
10 -phase 1	8.30	0.66	36.47	10.13	0.22	0.17	23.5	9.4
1 -phase 3	12.76	1.63	596.29	783.48	1.85	2.29	176.9	152.9
2 -phase 3	11.23	0.97	534.39	778.46	0.42	0.42	204.1	137.7
3 -phase 3	9.81	0.62	381.08	583.44	0.28	0.22	88.5	68.4
4 -phase 3	9.03	0.11	265.31	391.64	0.92	1.22	38.1	29.2
5 -phase 3	8.76	0.39	195.84	271.38	0.90	1.32	25.5	14.2
6 -phase 3	8.46	0.38	147.23	214.83	2.18	3.54	11.8	7.5
7 -phase 3	8.57	0.72	125.55	185.23	0.28	0.29	6.7	5.7
8 -phase 3	8.11	0.48	113.72	162.24	0.47	0.40	7.7	6.6
9 -phase 3	7.69	0.71	108.65	140.10	0.59	0.79	7.5	8.1
10 -phase 3	7.42	0.56	83.39	116.18	0.19	0.06	2.4	2.5

Table A-15 *(Continued)*

PV	Ca (μM)	s.d.	Na (μM)	s.d.	Al (μM)	s.d.	K (μM)	s.d.	Si (μM)	s.d.
1 - phase 1	14072	1640	1818	240	1466.86	193.98	3120	404	828	117
2 - phase 1	14609	656	1885	180	536.35	173.58	1681	212	566	103
3 -phase 1	15391	1501	1955	158	339.85	176.11	5056	6670	546	86
4 -phase 1	15360	1525	2100	435	227.61	84.52	1032	148	502	41
5 -phase 1	15088	2104	1992	167	178.48	85.01	983	272	492	37
6 -phase 1	15556	1973	1983	131	150.12	73.28	910	235	533	29
7 -phase 1	15525	1232	1976	357	120.69	55.73	908	251	513	21
8 -phase 1	15695	1774	2116	382	94.60	33.47	942	335	512	41
9 -phase 1	15151	1573	1881	219	75.26	25.87	904	163	509	64
10 -phase 1	14972	2674	2029	238	69.42	28.17	911	213	516	35
1 -phase 3	17465	744	1724	234	161.25	44.01	911	161	1410	235
2 -phase 3	16846	1194	1539	71	128.50	59.11	695	237	807	121
3 -phase 3	17358	159	1563	127	72.05	16.89	558	349	641	124
4 -phase 3	17346	567	1800	381	51.82	14.89	440	180	553	114
5 -phase 3	17206	1547	1858	350	40.95	14.64	539	208	534	122
6 -phase 3	16885	85	1718	161	30.19	7.55	458	170	543	80
7 -phase 3	18418	2530	1677	99	25.11	6.87	549	224	571	99
8 -phase 3	17764	782	1637	133	21.74	5.24	480	135	495	90
9 -phase 3	17532	228	1737	289	16.77	5.39	536	88	482	42
10 -phase 3	16945	1577	1606	136	15.02	4.42	695	295	492	85

Table A-15 *(Continued)*

PV	Ti (μM)	s.d.	Cr (μM)	s.d.	Co (μM)	s.d.	Mn (μM)	s.d.
1 - phase 1	0.206	0.152	0.273	0.343	10.95	2.65	4975.33	2080.32
2 - phase 1	0.073	0.050	0.069	0.011	3.57	2.06	1645.06	677.41
3 -phase 1	0.077	0.023	0.101	0.042	1.25	1.15	609.49	362.93
4 -phase 1	0.125	0.121	0.052	0.035	0.55	0.64	271.32	119.65
5 -phase 1	0.039	0.019	0.482	0.778	0.44	0.32	182.67	46.10
6 -phase 1	0.204	0.283	0.134	0.168	0.19	0.23	109.57	54.42
7 -phase 1	0.064	0.005	0.282	0.408	0.16	0.15	98.65	65.87
8 -phase 1	0.054	0.015	0.571	0.912	0.22	0.18	104.93	83.23
9 -phase 1	0.042	0.014	0.061	0.011	0.17	0.26	85.20	67.31
10 -phase 1	0.040	0.005	0.063	0.054	0.11	0.15	88.20	71.45
1 -phase 3	0.221	0.050	0.311	0.408	0.43	0.08	56.07	3.48
2 -phase 3	0.127	0.045	0.102	0.060	0.40	0.11	39.40	2.80
3 -phase 3	0.093	0.032	0.075	0.041	0.32	0.11	20.54	1.41
4 -phase 3	0.086	0.036	0.210	0.237	0.33	0.11	12.87	5.52
5 -phase 3	0.084	0.049	0.212	0.244	0.27	0.07	10.78	7.01
6 -phase 3	0.074	0.051	0.445	0.647	0.29	0.06	10.22	7.74
7 -phase 3	0.080	0.062	0.071	0.056	0.28	0.07	10.01	8.12
8 -phase 3	0.081	0.032	0.119	0.053	0.25	0.07	9.13	7.50
9 -phase 3	0.068	0.044	0.133	0.123	0.26	0.09	8.75	7.39
10 -phase 3	0.075	0.052	0.057	0.052	0.24	0.09	8.80	7.58

Table A-15 *(Continued)*

PV	Ni (μM)	s.d.	Cu (μM)	s.d.	As (μM)	s.d.	Se (μM)	s.d.
1 phase1	17.82	4.52	1296.39	433.17	1.1277	0.8750	1.1793	2.0426
2 phase1	6.00	3.45	537.13	224.24	0.5177	0.4914	0.5944	0.8709
3 phase 1	2.81	2.15	280.65	138.80	0.2434	0.2111	0.7854	0.0723
4 phase 1	2.11	1.45	175.95	87.60	0.1612	0.1426	0.6998	0.2240
5 phase 1	12.57	19.06	127.61	59.77	0.1115	0.0990	0.5527	0.2065
6 phase 1	2.47	2.16	85.02	41.49	0.0808	0.0595	0.4076	0.1452
7 phase 1	3.81	4.46	63.08	25.74	0.0592	0.0442	0.3183	0.1224
8 phase 1	11.03	17.13	52.81	23.57	0.0604	0.0502	0.2653	0.1077
9 phase 1	0.92	0.62	38.07	17.26	0.0537	0.0411	0.2210	0.1085
10 phase1	1.39	0.85	32.76	16.46	0.0435	0.0257	0.2018	0.0948
1 phase1	0.94	0.59	37.35	0.26	0.0682	0.0242	0.6641	0.0765
2 phase1	0.62	0.31	28.02	2.31	0.0577	0.0170	0.6308	0.0412
3 phase 1	0.51	0.26	19.92	2.58	0.0400	0.0162	0.4030	0.0343
4 phase 1	0.53	0.23	14.82	3.06	0.0171	0.0157	0.2462	0.0480
5 phase 1	0.61	0.41	11.87	2.71	0.0156	0.0147	0.1486	0.0184
6 phase 1	0.81	0.78	9.47	2.29	0.0140	0.0123	0.1120	0.0193
7 phase 1	0.54	0.40	8.29	2.36	0.0083	0.0083	0.1006	0.0156
8 phase 1	0.52	0.25	6.99	1.87	0.0093	0.0093	0.0912	0.0126
9 phase 1	0.53	0.37	5.84	1.82	0.0072	0.0067	0.0714	0.0075
10 phase3	0.42	0.18	5.07	1.55	0.0058	0.0064	0.0724	0.0114

Table A-15 *(Continued)*

Cd (μM)	s.d.	Ba (μM)	s.d.	Bi (μM)	s.d.	U (μM)	s.d.
19.6562	5.8598	0.2235	0.0964	0.0025	0.0014	0.2904	0.0370
6.3808	3.6287	0.2293	0.0791	0.0062	0.0058	0.1323	0.0315
2.1503	1.7762	0.2174	0.1157	0.0156	0.0085	0.0770	0.0178
0.9128	0.9064	0.1880	0.1032	0.0046	0.0034	0.0560	0.0118
0.4287	0.4379	0.1920	0.1205	0.0142	0.0157	0.0447	0.0073
0.2238	0.2168	0.1695	0.1059	0.0040	0.0021	0.0394	0.0069
0.1424	0.1167	0.1773	0.1219	0.0183	0.0266	0.0333	0.0039
0.1081	0.0835	0.1712	0.1217	0.0084	0.0070	0.0294	0.0048
0.0876	0.0714	0.1507	0.1050	0.0015	0.0009	0.0243	0.0050
0.0762	0.0614	0.1544	0.1085	0.0092	0.0112	0.0207	0.0075
0.4264	0.0284	0.0695	0.0506	3.5983	6.2299	0.0230	0.0187
0.2941	0.0914	0.0648	0.0545	3.3684	5.8316	0.0174	0.0151
0.1361	0.0594	0.0616	0.0539	3.0254	5.2375	0.0131	0.0115
0.0674	0.0281	0.0775	0.0706	2.9982	5.1879	0.0095	0.0087
0.0406	0.0121	0.0955	0.0838	2.9907	5.1744	0.0083	0.0073
0.0266	0.0044	0.0993	0.0860	2.8846	4.9720	0.0068	0.0061
0.0201	0.0047	0.1001	0.0867	2.9738	5.1446	0.0066	0.0057
0.0161	0.0038	0.1125	0.0988	2.8643	4.9579	0.0055	0.0047
0.0115	0.0040	0.1188	0.1032	2.8194	4.8664	0.0052	0.0036
0.0104	0.0063	0.1256	0.1079	5.4620	4.7360	0.0013	0.0015

Table A-16 Cations and metals concentration of collected pore volumes in T2 after being treated with 10 μmoles Oxalic Acid.

PV	Pb (μM)	s.d.	Zn (μM)	s.d.	Fe (μM)	s.d.	Mg (μM)	s.d.	Ca (μM)	s.d.
1 - phase1	5.99	0.11	11156	1547	1.12	0.46	16.0	0.6	14715	4316
2 - phase1	2.58	0.18	3639	978	0.50	0.06	14.1	4.3	14001	527
3 -phase 1	1.48	0.41	1535	266	0.28	0.04	13.0	3.5	14443	581
4 -phase 1	1.07	0.07	944	170	0.25	0.07	8.9	5.5	14396	498
5 -phase 1	0.75	0.10	690	92	0.26	0.08	11.0	1.6	14683	372
6 -phase 1	0.76	0.31	555	61	0.26	0.26	9.1	5.6	14546	348
7 -phase 1	0.79	0.12	463	75	0.12	0.01	0.1	0.0	14977	604
8 -phase 1	0.71	0.11	399	61	0.12	0.05	0.2	0.1	14911	587
9 -phase 1	0.66	0.12	350	60	0.13	0.05	0.9	1.4	14833	866
10 phase1	0.67	0.23	288	30	0.08	0.04	0.2	0.2	14095	822
1 -phase 3	1.86	0.61	1427	77	0.19	0.03	529.5	25.3	13245	585
2 -phase 3	2.21	0.32	1347	194	0.28	0.18	553.4	24.6	13254	267
3 -phase 3	1.61	0.34	972	170	0.16	0.05	424.2	57.3	14151	1806
4 -phase 3	1.28	0.53	683	144	0.11	0.07	235.7	105.1	13363	244
5 -phase 3	0.69	0.17	474	79	0.13	0.03	77.2	16.4	13865	324
6 -phase 3	0.71	0.17	373	62	0.11	0.07	42.4	6.4	13234	449
7 -phase 3	0.77	0.03	330	61	0.08	0.02	29.8	5.2	13360	348
8 -phase 3	0.65	0.23	294	58	0.11	0.07	23.3	2.8	13364	685
9 -phase 3	0.65	0.18	258	52	0.55	0.87	20.2	3.1	13313	271
10 phase3	0.50	0.13	218	30	0.12	0.12	17.2	2.0	13384	110

Table A-16 *(Continued)*

PV	Na (μM)	s.d.	Al (μM)	s.d.	Si (μM)	s.d.	K (μM)	s.d.	Ti (μM)	s.d.
1 - phase1	1733	43	24.92	1.79	879	164	1902	48	0.162	0.029
2 - phase1	1645	101	20.81	2.75	757	129	911	38	0.122	0.006
3 -phase 1	1738	74	20.23	3.57	751	160	607	47	0.110	0.019
4 -phase 1	1699	107	22.38	2.34	688	33	533	59	0.097	0.008
5 -phase 1	1664	18	21.46	2.01	632	61	694	241	0.129	0.035
6 -phase 1	1769	90	21.55	2.21	710	48	612	158	0.085	0.017
7 -phase 1	1748	115	22.52	1.89	666	101	540	63	0.081	0.018
8 -phase 1	1804	169	23.20	0.65	647	139	592	52	0.082	0.004
9 -phase 1	1975	586	21.39	1.06	604	28	719	247	0.086	0.005
10 phase1	1635	35	22.02	1.91	586	33	670	139	0.066	0.020
1 -phase 3	2021	90	1.22	0.59	1137	68	739	53	0.172	0.034
2 -phase 3	1447	96	2.60	1.80	899	112	693	43	0.146	0.019
3 -phase 3	1494	86	1.26	0.22	775	84	557	31	0.097	0.014
4 -phase 3	1595	35	0.90	0.30	709	65	454	83	0.072	0.017
5 -phase 3	1599	66	7.08	10.25	688	73	427	27	0.081	0.014
6 -phase 3	1589	63	2.17	1.75	663	37	473	54	0.083	0.043
7 -phase 3	1621	29	0.77	0.11	642	59	577	61	0.061	0.029
8 -phase 3	1706	155	0.92	0.39	646	84	543	45	0.063	0.029
9 -phase 3	1660	102	1.18	0.52	665	89	592	37	0.062	0.039
10 phase3	1593	60	1.37	1.44	625	69	592	43	0.047	0.007

Table A-16 *(Continued)*

PV	Cr (μM)	s.d.	Mn (μM)	s.d.	Co (μM)	s.d.	Ni (μM)	s.d.	Cu (μM)	s.d.
1 - phase1	0.155	0.248	12570	1205	4.92	0.39	5.22	0.24	31.46	2.37
2 - phase1	0.005	0.002	2980	756	1.89	0.20	2.81	0.19	10.11	2.79
3 –phase 1	0.004	0.007	741	217	1.11	0.10	2.07	0.17	3.81	0.57
4 –phase 1	0.000	0.000	292	104	0.93	0.05	1.83	0.07	2.83	0.45
5 –phase 1	0.007	0.012	146	50.41	0.90	0.03	1.69	0.12	2.26	0.15
6 -phase 1	0.003	0.002	83	21.81	0.80	0.05	1.64	0.03	1.68	0.38
7 -phase 1	0.000	0.000	55	21.18	0.81	0.01	1.63	0.06	1.79	0.19
8 -phase 1	0.004	0.004	38	14.39	0.77	0.03	1.53	0.03	1.46	0.11
9 -phase 1	0.001	0.002	36	3.76	0.75	0.03	1.56	0.08	1.10	0.35
10 phase1	0.001	0.002	33	8.94	0.73	0.04	1.54	0.07	1.06	0.11
1 -phase 3	0.005	0.001	350	27.34	0.76	0.07	1.85	0.15	2.01	0.51
2 -phase 3	0.012	0.012	334	62.64	0.73	0.09	1.78	0.14	2.73	0.18
3 -phase 3	0.005	0.001	213	56.77	0.62	0.05	1.63	0.13	1.98	0.27
4 -phase 3	0.003	0.003	116	44.06	0.54	0.05	1.47	0.12	1.48	0.23
5 -phase 3	0.004	0.003	57	18.03	0.48	0.03	1.42	0.11	1.00	0.29
6 -phase 3	0.000	0.000	37	12.33	0.44	0.03	1.27	0.06	0.74	0.36
7 -phase 3	0.005	0.005	25	6.85	0.43	0.06	1.34	0.18	0.68	0.24
8 -phase 3	0.004	0.003	20	4.71	0.42	0.02	1.32	0.18	0.57	0.27
9 -phase 3	0.008	0.004	17	3.63	0.38	0.05	1.46	0.09	0.58	0.21
10 phase3	0.008	0.007	14	2.99	0.36	0.02	1.27	0.10	0.28	0.05

Table A-16 *(Continued)*

PV	As (μM)	s.d.	Se (μM)	s.d.	Cd (μM)	s.d.
1 phase1	1.9573	1.3690	3.5752	0.5804	52.7129	3.2445
2 phase1	0.7969	0.6944	0.7416	0.1852	16.9376	2.4519
3 phase 1	0.3727	0.3506	0.2467	0.0483	8.1013	0.9851
4 phase 1	0.2212	0.1972	0.1335	0.0034	5.5635	0.6701
5 phase 1	0.1621	0.1361	0.0934	0.0107	4.2301	0.5005
6 phase 1	0.1292	0.1018	0.0703	0.0142	3.4312	0.4049
7 phase 1	0.1012	0.0691	0.0592	0.0029	2.9227	0.3077
8 phase 1	0.0816	0.0567	0.0466	0.0083	2.5243	0.2684
9 phase 1	0.0672	0.0271	0.0412	0.0077	2.3114	0.2915
10 phase1	0.0620	0.0272	0.0327	0.0056	2.0893	0.2266
1 phase1	0.1846	0.0153	0.2870	0.0345	5.6834	0.1220
2 phase1	0.1752	0.0190	0.2391	0.0426	5.4251	0.3503
3 phase 1	0.1284	0.0311	0.1306	0.0068	4.1680	0.6607
4 phase 1	0.0960	0.0156	0.0759	0.0190	2.9338	0.4664
5 phase 1	0.0755	0.0105	0.0581	0.0042	2.1353	0.3421
6 phase 1	0.0620	0.0114	0.0440	0.0029	1.6416	0.2232
7 phase 1	0.0555	0.0141	0.0302	0.0040	1.3821	0.2447
8 phase 1	0.0588	0.0092	0.0285	0.0048	1.1970	0.1844
9 phase 1	0.0525	0.0103	0.0296	0.0054	1.0481	0.1664
10 phase3	0.0507	0.0050	0.0248	0.0143	0.8905	0.1314

Table A-16 *(Continued)*

PV	Ba (μM)	s.d.	Bi (μM)	s.d.	U (μM)	s.d.
1 phase1	0.1152	0.1105	0.0029	0.0022	0.0008	0.0006
2 phase1	0.1346	0.1170	0.0007	0.0004	0.0002	0.0002
3 phase 1	0.1396	0.1208	0.0039	0.0062	0.0002	0.0001
4 phase 1	0.1648	0.1428	0.0092	0.0146	0.0002	0.0002
5 phase 1	0.2386	0.2166	0.0075	0.0124	0.0002	0.0001
6 phase 1	0.2021	0.1749	0.0071	0.0110	0.0002	0.0001
7 phase 1	0.2129	0.1847	0.0023	0.0024	0.0002	0.0001
8 phase 1	0.2264	0.1974	0.0010	0.0004	0.0002	0.0000
9 phase 1	0.2299	0.1993	0.0014	0.0022	0.0002	0.0001
10 phase1	0.2396	0.2091	0.0040	0.0060	0.0004	0.0002
1 phase1	0.1230	0.1061	2.6507	4.5864	0.0002	0.0002
2 phase1	0.0916	0.0805	0.0033	0.0009	0.0001	0.0000
3 phase 1	0.1008	0.0892	0.0031	0.0010	0.0001	0.0001
4 phase 1	0.0926	0.0825	0.0024	0.0008	0.0001	0.0001
5 phase 1	0.1190	0.1088	0.0038	0.0015	0.0001	0.0001
6 phase 1	0.1479	0.1297	0.0033	0.0020	0.0001	0.0001
7 phase 1	0.1419	0.1239	0.0111	0.0140	0.0002	0.0002
8 phase 1	0.1640	0.1435	0.0020	0.0004	0.0001	0.0001
9 phase 1	0.1827	0.1584	0.0028	0.0020	0.0002	0.0001
10 phase3	0.1762	0.1534	0.0014	0.0017	0.0002	0.0001

Table A-17 Cations and metals concentration of collected pore volumes in T1 after being treated with 100 μmoles Oxalic Acid.

PV	Pb (μM)	s.d.	Zn (μM)	s.d.	Fe (μM)	s.d.	Mg (μM)	s.d.	Ca (μM)	s.d.
1 phase1	10.37	3.34	14044	1694	1.69	0.90	1309	384	15660	1097
2 phase1	7.77	3.05	4695	1574	0.39	0.06	505	209	17009	1359
3 phase 1	7.25	2.69	1522	854	0.31	0.20	247	139	17548	721
4 phase 1	6.96	2.32	572	392	0.19	0.09	154	96	18022	931
5 phase 1	7.32	1.78	229	190	0.21	0.17	127	80	17819	897
6 phase 1	7.44	1.53	103	70.37	0.31	0.38	86	29	19229	1890
7 phase 1	7.67	1.34	58.18	38.21	0.17	0.13	68	18	18688	1128
8 phase 1	7.89	1.08	36.15	16.86	0.37	0.42	58	15	18146	1873
9 phase 1	9.07	1.56	34.29	15.00	0.38	0.25	67	17	27585	7995
10 phase1	8.41	0.57	25.31	12.29	0.22	0.13	48	14	24565	7782
1 phase1	10.85	2.73	853	1004	0.27	0.22	6151	9955	17124	890
2 phase1	9.13	2.37	517	722.42	0.15	0.04	2021	3006	16225	1852
3 phase 1	9.13	0.67	257	356.47	0.13	0.04	793	1145	16762	1279
4 phase 1	8.62	0.70	148	208.75	0.12	0.01	309	446	17321	1359
5 phase 1	8.82	0.42	122	138.77	0.19	0.16	132	173	16788	1752
6 phase 1	8.18	0.00	115	148.96	0.77	0.83	111	137	17011	1535
7 phase 1	8.28	0.49	63.89	92.47	0.87	1.34	61	84	16704	2483
8 phase 1	7.72	0.60	50.03	72.28	0.09	0.02	37	45	16196	1968
9 phase 1	7.73	0.25	48.21	73.09	0.13	0.09	34	43	15645	551
10 phase3	7.40	0.33	37.31	48.40	0.08	0.06	35	42	15365	1291

Table A-17*(Continued)*

PV	Na (μM)	s.d.	Al (μM)	s.d.	Si (μM)	s.d.	K (μM)	s.d.	Ti (μM)	s.d.
1 phase1	1409	315	1351	423	551	36	2292	485	0.094	0.025
2 phase1	1372	280	804	535	452	110	1300	418	0.055	0.022
3 phase 1	1448	402	302	137	427	57	797	238	0.053	0.031
4 phase 1	1484	361	201	106	385	47	616	153	0.045	0.009
5 phase 1	1508	355	168	89	384	38	538	102	0.052	0.003
6 phase 1	1588	233	150	92	385	39	505	87	0.052	0.008
7 phase 1	1501	386	118	80	443	72	558	107	0.053	0.012
8 phase 1	1659	120	99.0	58.2	365	16	503	62	0.054	0.008
9 phase 1	2183	1066	75.2	25.0	495	136	941	737	0.068	0.004
10 phase1	1448	439	58.3	42.2	498	87	486	64	0.047	0.014
1 phase1	1822	231	151.1	75.1	1031	37	1329	411	0.196	0.081
2 phase1	1530	30	133.6	39.5	489	112	1292	585	0.087	0.077
3 phase 1	1653	26	97.0	47.9	470	60	706	190	0.058	0.057
4 phase 1	1684	54	55.9	10.1	487	48	821	261	0.065	0.099
5 phase 1	1725	127	42.7	8.6	498	36	737	71	0.063	0.072
6 phase 1	1629	142	34.1	8.5	474	40	685	87	0.083	0.077
7 phase 1	1685	56	27.5	5.1	471	71	716	113	0.065	0.058
8 phase 1	1821	427	21.9	3.3	437	17	826	229	0.054	0.055
9 phase 1	1603	52	18.1	2.9	439	141	758	200	0.065	0.079
10 phase3	1668	91	15.0	1.2	324	91	1002	188	0.058	0.087

Table A-17*(Continued)*

PV	Cr (μM)	s.d.	Mn (μM)	s.d.	Co (μM)	s.d.	Ni (μM)	s.d.	Cu (μM)	s.d.
1 phase1	0.144	0.161	5517	1615	11.64	1.13	14.20	5.34	1506	347.21
2 phase1	0.008	0.006	1565	547	3.75	1.24	5.54	2.93	550	187.15
3 phase 1	0.035	0.046	469	291	1.42	0.63	2.57	1.92	298	105.22
4 phase 1	0.006	0.005	153	115	0.66	0.30	1.59	1.35	184	62.62
5 phase 1	0.007	0.005	50.52	46	0.46	0.24	1.18	1.07	133	42.78
6 phase 1	0.004	0.004	20.99	20	0.33	0.08	1.05	0.83	91.54	29.89
7 phase 1	0.014	0.019	10.26	8.90	0.35	0.09	0.97	0.79	70.13	25.05
8 phase 1	0.063	0.101	6.20	4.00	0.28	0.03	0.93	0.68	53.46	15.76
9 phase 1	0.054	0.028	4.74	1.72	0.30	0.07	0.97	0.64	46.63	10.16
10 phase1	0.006	0.011	3.48	1.19	0.27	0.01	0.88	0.69	34.99	10.31
1 phase1	0.132	0.029	158	141	0.64	0.08	0.68	0.45	33.33	6.35
2 phase1	0.062	0.040	28.65	8.78	0.51	0.01	0.30	0.11	24.06	6.42
3 phase 1	0.053	0.051	13.02	2.06	0.42	0.02	0.17	0.06	16.90	3.21
4 phase 1	0.042	0.061	5.69	1.84	0.37	0.03	0.13	0.04	12.75	2.63
5 phase 1	0.049	0.051	5.93	6.17	0.36	0.01	0.14	0.06	10.18	2.15
6 phase 1	0.083	0.079	1.38	0.36	0.35	0.01	0.23	0.25	8.10	2.50
7 phase 1	0.057	0.050	1.15	0.32	0.36	0.05	0.17	0.14	6.81	1.71
8 phase 1	0.047	0.046	0.65	0.34	0.36	0.01	0.15	0.10	5.75	1.36
9 phase 1	0.070	0.090	0.48	0.14	0.40	0.04	0.14	0.12	4.73	1.09
10 phase3	0.039	0.054	0.77	0.78	0.36	0.04	0.21	0.11	3.94	0.90

Table A-17*(Continued)*

PV	As (μM)	s.d.	Se (μM)	s.d.	Cd (μM)	s.d.
1 phase1	1.255	1.027	3.735	0.186	18.288	7.192
2 phase1	0.467	0.351	1.832	0.280	5.707	3.253
3 phase 1	0.254	0.178	1.124	0.396	1.887	1.322
4 phase 1	0.157	0.117	0.834	0.358	0.752	0.633
5 phase 1	0.120	0.060	0.621	0.279	0.343	0.304
6 phase 1	0.088	0.052	0.451	0.210	0.196	0.151
7 phase 1	0.058	0.020	0.350	0.166	0.128	0.098
8 phase 1	0.063	0.037	0.283	0.133	0.092	0.066
9 phase 1	0.054	0.022	0.283	0.186	0.085	0.053
10 phase1	0.047	0.016	0.207	0.097	0.068	0.047
1 phase1	0.071	0.022	0.728	0.122	0.980	0.742
2 phase1	0.058	0.003	0.637	0.062	0.290	0.039
3 phase 1	0.040	0.011	0.402	0.030	0.121	0.016
4 phase 1	0.018	0.006	0.218	0.022	0.047	0.012
5 phase 1	0.009	0.008	0.158	0.026	0.106	0.160
6 phase 1	0.006	0.008	0.112	0.009	0.006	0.009
7 phase 1	0.010	0.009	0.102	0.016	0.001	0.002
8 phase 1	0.006	0.005	0.098	0.018	0.000	0.000
9 phase 1	0.003	0.004	0.093	0.023	0.000	0.000
10 phase3	0.005	0.004	0.080	0.013	0.006	0.011

Table A-17*(Continued)*

PV	Ba (μM)	s.d.	Bi (μM)	s.d.	U (μM)	s.d.
1 phase1	0.198	0.116	0.0030	0.0021	0.2198	0.1704
2 phase1	0.153	0.006	0.0022	0.0018	0.1158	0.0457
3 phase 1	0.155	0.052	0.0044	0.0040	0.0674	0.0300
4 phase 1	0.180	0.095	0.0014	0.0006	0.0493	0.0194
5 phase 1	0.145	0.077	0.0022	0.0023	0.0403	0.0144
6 phase 1	0.151	0.093	0.0013	0.0006	0.0362	0.0078
7 phase 1	0.147	0.093	0.0019	0.0012	0.0312	0.0079
8 phase 1	0.150	0.101	0.0018	0.0017	0.0283	0.0067
9 phase 1	0.154	0.110	0.0019	0.0004	0.0314	0.0069
10 phase1	0.149	0.106	0.0077	0.0131	0.0299	0.0016
1 phase1	0.032	0.032	<5.42 E-4		0.0245	0.0081
2 phase1	0.038	0.037	<5.42 E-4		0.0175	0.0081
3 phase 1	0.022	0.010	<5.42 E-4		0.0161	0.0054
4 phase 1	0.066	0.046	<5.42 E-4		0.0107	0.0041
5 phase 1	0.091	0.072	0.0005	0.0008	0.0100	0.0023
6 phase 1	0.046	0.048	0.0000	0.0000	0.0081	0.0039
7 phase 1	0.089	0.069	0.0012	0.0021	0.0079	0.0042
8 phase 1	0.079	0.061	0.0000	0.0000	0.0052	0.0035
9 phase 1	0.118	0.103	<5.42 E-4		0.0054	0.0038
10 phase3	0.121	0.099	0.0023	0.0040	0.0043	0.0039

Table A-18 Cations and metals concentration of collected pore volumes in T2 after being treated with 100 μmoles Oxalic Acid.

PV	Pb (μM)	s.d.	Zn (μM)	s.d.	Fe (μM)	s.d.	Mg (μM)	s.d.	Ca (μM)	s.d.
1 phase1	6.59	1.41	14590	2622.95	0.31	0.08	12990	4056	13253	1531
2 phase1	2.14	0.28	4560	960.96	0.11	0.13	3519	1709	12981	1819
3 phase 1	0.93	0.35	2171	434.68	0.06	0.03	1335	695	15478	2301
4 phase 1	0.85	0.03	815	678.13	0.05	0.05	534	261	15013	1610
5 phase 1	0.55	0.34	570	476.50	0.16	0.18	239	86	9085	8180
6 phase 1	0.54	0.13	453	380.42	0.90	1.46	156	51	11440	8806
7 phase 1	0.55	0.40	377	316.18	0.01	0.00	124	32	9638	8460
8 phase 1	0.52	0.28	321	270.73	0.21	0.34	95	12	15011	2432
9 phase 1	0.39	0.25	267	224.50	0.05	0.05	90	15	16767	567
10 phase1	0.46	0.30	235	197.43	0.13	0.15	84	18	15233	1615
1 phase1	2.66	0.93	1618	340.84	0.25	0.16	491	118	13956	1302
2 phase1	1.72	0.44	1270	70.89	0.68	0.94	446	60	14017	1718
3 phase 1	0.78	0.14	756	99.90	0.17	0.19	203	55	14577	1788
4 phase 1	0.66	0.38	480	100.69	0.15	0.19	71	30	14583	2047
5 phase 1	0.66	0.12	349	70.02	0.04	0.04	40	10	13712	1567
6 phase 1	0.50	0.26	266	41.14	0.14	0.12	29	7	13290	1780
7 phase 1	0.38	0.16	294	162.66	0.12	0.14	30	10	13145	1231
8 phase 1	0.38	0.07	265	168.81	0.08	0.08	31	11	13629	2209
9 phase 1	0.45	0.16	212	99.68	0.07	0.08	33	12	13426	1313
10 phase3	0.34	0.18	207	128.13	0.17	0.16	34	9	15540	1369

Table A-18 *(Continued)*

PV	Na (μM)	s.d.	Al (μM)	s.d.	Si (μM)	s.d.	K (μM)	s.d.	Ti (μM)	s.d.
1 phase1	2103	479	30.22	9.23	863	202	2362	629	0.115	0.045
2 phase1	1498	399	6.57	2.66	704	259	1159	227	0.066	0.039
3 phase 1	1613	194	1.52	0.52	730	257	905	238	0.093	0.034
4 phase 1	1723	167	1.41	0.09	633	241	591	110	0.070	0.039
5 phase 1	1532	187	0.93	0.83	614	208	432	101	0.068	0.042
6 phase 1	1620	112	0.72	0.62	616	229	481	107	0.058	0.038
7 phase 1	1615	149	1.06	0.33	615	227	443	83	0.062	0.034
8 phase 1	1577	134	0.74	0.60	678	299	456	84	0.060	0.037
9 phase 1	1621	167	0.69	0.61	572	250	502	48	0.065	0.031
10 phase1	1651	336	7.53	11.11	640	256	585	115	0.060	0.032
1 phase1	1881	192	1.79	0.91	624	60	925	165	0.182	0.013
2 phase1	1566	25	1.22	1.36	437	186	695	66	0.105	0.034
3 phase 1	1604	84	0.52	0.49	303	97	563	106	0.099	0.008
4 phase 1	1657	106	0.57	0.56	242	79	550	193	0.073	0.026
5 phase 1	1763	141	0.13	0.13	244	64	830	402	0.075	0.019
6 phase 1	1579	48	0.24	0.25	256	67	581	195	0.079	0.019
7 phase 1	1685	71	0.42	0.36	243	122	920	385	0.068	0.050
8 phase 1	1584	140	0.32	0.29	212	27	582	50	0.077	0.012
9 phase 1	1645	127	0.24	0.25	240	56	1042	673	0.068	0.039
10 phase3	1629	93	0.42	0.50	231	123	655	120	0.060	0.043

Table A-18 *(Continued)*

PV	Cr (μM)	s.d.	Mn (μM)	s.d.	Co (μM)	s.d.	Ni (μM)	s.d.	Cu (μM)	s.d.
1 phase1	0.032	0.032	14622	4612	4.34	1.64	4.95	0.37	46.19	8.64
2 phase1	0.013	0.012	3962	1640	1.43	0.62	1.72	0.10	12.13	2.43
3 phase 1	0.011	0.010	1364	427	0.75	0.24	1.23	0.05	5.04	1.10
4 phase 1	0.012	0.010	541	195	0.54	0.18	0.91	0.07	3.56	0.55
5 phase 1	0.034	0.044	271	90.30	0.40	0.09	0.82	0.10	2.68	0.13
6 phase 1	0.011	0.009	163	50.49	0.37	0.11	0.65	0.05	2.08	0.32
7 phase 1	0.011	0.009	108	34.28	0.34	0.10	0.65	0.10	2.17	0.31
8 phase 1	0.049	0.070	77	19.58	0.32	0.08	0.60	0.06	1.59	0.27
9 phase 1	0.014	0.014	61	17.38	0.31	0.07	0.55	0.02	1.46	0.12
10 phase1	0.015	0.013	52	17.87	0.33	0.11	0.54	0.04	1.37	0.19
1 phase1	0.112	0.097	406	51.30	0.88	0.10	1.21	0.28	4.50	1.42
2 phase1	0.054	0.049	322	11.79	6.51	9.90	0.87	0.12	2.42	1.03
3 phase 1	0.059	0.051	162	47.87	0.78	0.11	0.70	0.09	1.66	1.14
4 phase 1	0.038	0.037	76.93	26.99	0.58	0.08	0.59	0.08	1.65	1.53
5 phase 1	0.040	0.035	33.35	6.83	0.55	0.06	0.50	0.17	0.69	0.17
6 phase 1	0.045	0.042	24.45	7.31	0.49	0.03	0.43	0.16	0.65	0.06
7 phase 1	0.033	0.049	18.90	4.15	0.57	0.07	0.52	0.16	0.47	0.21
8 phase 1	0.043	0.038	15.72	3.92	0.46	0.04	0.46	0.14	0.39	0.03
9 phase 1	0.036	0.039	13.22	2.29	0.49	0.01	0.44	0.16	0.40	0.05
10 phase3	0.028	0.039	11.53	1.69	0.54	0.18	0.43	0.13	0.31	0.20

Table A-18 *(Continued)*

PV	As (μM)	s.d.	Se (μM)	s.d.	Cd (μM)	s.d.
1 phase1	1.573	1.761	2.577	0.751	64.765	13.373
2 phase1	0.638	0.845	0.519	0.205	21.004	6.491
3 phase 1	0.276	0.341	0.195	0.044	10.904	2.684
4 phase 1	0.175	0.217	0.121	0.017	6.975	1.407
5 phase 1	0.122	0.157	0.078	0.010	4.785	0.527
6 phase 1	0.084	0.110	0.071	0.008	3.604	0.352
7 phase 1	0.068	0.083	0.055	0.011	2.998	0.269
8 phase 1	0.054	0.068	0.045	0.008	2.456	0.096
9 phase 1	0.038	0.047	0.049	0.009	2.118	0.157
10 phase1	0.038	0.051	0.037	0.013	1.844	0.196
1 phase1	0.079	0.028	0.340	0.054	6.545	0.231
2 phase1	0.053	0.020	0.175	0.072	5.333	0.914
3 phase 1	0.027	0.020	0.089	0.043	3.512	1.045
4 phase 1	0.015	0.024	0.060	0.035	2.359	0.721
5 phase 1	0.017	0.019	0.048	0.016	1.703	0.316
6 phase 1	0.016	0.020	0.035	0.014	1.249	0.253
7 phase 1	0.016	0.016	0.036	0.019	1.009	0.144
8 phase 1	0.013	0.017	0.028	0.012	0.861	0.192
9 phase 1	0.015	0.022	0.029	0.006	0.748	0.153
10 phase3	0.012	0.018	0.026	0.008	0.625	0.143

Table A-18 *(Continued)*

PV	Ba (μM)	s.d.	Bi (μM)	s.d.	U (μM)	s.d.
1 phase1	0.088	0.075	0.0014	0.0012	0.00088	0.00092
2 phase1	0.105	0.096	0.0015	0.0016	0.00007	0.00004
3 phase 1	0.141	0.122	0.0024	0.0030	0.00009	0.00008
4 phase 1	0.179	0.155	0.0055	0.0006	0.00016	0.00011
5 phase 1	0.193	0.167	0.0021	0.0020	0.00025	0.00017
6 phase 1	0.207	0.181	0.0031	0.0029	0.00029	0.00012
7 phase 1	0.213	0.184	0.0020	0.0018	0.00039	0.00029
8 phase 1	0.227	0.196	0.0024	0.0022	0.00036	0.00022
9 phase 1	0.247	0.213	0.0031	0.0023	0.00032	0.00027
10 phase1	0.249	0.217	0.0019	0.0016	0.00047	0.00027
1 phase1	0.153	0.132	0.0055	0.0014	0.00030	0.00024
2 phase1	0.087	0.075	0.0030	0.0025	0.00036	0.00037
3 phase 1	0.098	0.090	0.0033	0.0016	0.00052	0.00022
4 phase 1	0.129	0.111	0.0052	0.0026	0.00042	0.00035
5 phase 1	0.159	0.137	0.0018	0.0002	0.00037	0.00042
6 phase 1	0.184	0.165	0.0022	0.0005	0.00042	0.00046
7 phase 1	0.211	0.187	0.0032	0.0016	0.00037	0.00038
8 phase 1	0.248	0.218	0.0019	0.0010	0.00043	0.00044
9 phase 1	0.266	0.232	0.0039	0.0014	0.00037	0.00039
10 phase3	0.293	0.256	0.0012	0.0017	0.00033	0.00044

Table A-19 Saturation indices at pore volumes one (phase 1), ten (phase 1), one (phase 3), ten (phase 3) for NaCl, SWG, 10 µmoles Oxalic Acid, 100 µmoles Oxalic Acid treatments.

NaCl T1							
1 PV (phase 1)		10 PV (phase 1)		1 PV (phase 3)		10 PV (phase 3)	
Mineral Name	SI	Mineral Name	SI	Mineral Name	SI	Mineral Name	SI
Zn talc	-6.019	Zn talc	-12.521	Zn talc	-3.572	Zn talc	-10.426
quartz	0.385	quartz	-0.183	quartz	0.966	quartz	-0.169
gibbsite	-3.381	gibbsite	-2.452	gibbsite	-2.229	gibbsite	-3.78
ferrihydrite	-0.613	ferrihydrite	-1.099	ferrihydrite	1.591	ferrihydrite	-0.613
goethite	2.087	goethite	1.601	goethite	1.591	goethite	2.088
hematite	6.576	hematite	5.603	hematite	5.583	hematite	6.576
anglesite	-0.122	anglesite	-0.308	anglesite	-0.109	anglesite	-0.298
goslarite	-2.693	goslarite	-5.293	goslarite	-3.845	goslarite	-5.141
Orthoclase	-1.794	Orthoclase	-3.403	Orthoclase	0.622	Orthoclase	-4.277
schwertmannite	0.382	schwertmannite	-4.698	schwertmannite	-4.78	schwertmannite	-1.334
H-Jarosite	0.339	H-Jarosite	-3.5	H-Jarosite	-3.535	H-Jarosite	-3.095
Na-Jarosite	1.265	Na-Jarosite	-2.022	Na-Jarosite	-1.999	Na-Jarosite	-1.348
Pb-Jarosite	0.578	Pb-Jarosite	-2.759	Pb-Jarosite	-2.693	Pb-Jarosite	-2.086
K-Jarosite	4.341	K-Jarosite	-0.332	K-Jarosite	-0.013	K-Jarosite	0.484
AlOHSO4	-1.605	AlOHSO4	-1.869	AlOHSO4	-1.647	AlOHSO4	-3.724
$Al_4(OH)_{10}SO4$	-12.804	$Al_4(OH)_{10}SO4$	-10.283	$Al_4(OH)_{10}SO4$	-9.39	$Al_4(OH)_{10}SO4$	-16.12
alunite	-25.04	alunite	-28.051	alunite	-27.392	alunite	-34.537
gypsum	0.063	gypsum	-0.086	gypsum	0.051	gypsum	0.053
kaolinite	-4.844	kaolinite	-4.124	kaolinite	-1.377	kaolinite	-6.751

Table A-19 *(Continued)*

NaCl T2							
1 PV (phase 1)		10 PV (phase 1)		1 PV (phase 3)		10 PV (phase 3)	
Mineral Name	SI	Mineral Name	SI	Mineral Name	SI	Mineral Name	SI
Zn talc	5.59	Zn talc	3.781	Zn talc	6.489	Zn talc	0.801
quartz	0.754	quartz	0.538	quartz	1.079	quartz	0.547
gibbsite	-3.724	gibbsite	-3.509	gibbsite	-4.034	gibbsite	-4.632
ferrihydrite	0.539	ferrihydrite	-1.534	ferrihydrite	-0.39	ferrihydrite	-0.667
goethite	3.24	goethite	1.166	goethite	2.31	goethite	2.034
hematite	8.882	hematite	4.733	hematite	7.022	hematite	6.468
anglesite	-0.226	anglesite	-0.593	anglesite	-0.513	anglesite	-0.624
goslarite	-2.665	goslarite	-4.225	goslarite	-3.452	goslarite	-4.525
Orthoclase	0.423	Orthoclase	-0.677	Orthoclase	0.691	Orthoclase	-1.659
schwertmannite	6.257	schwertmannite	-11.584	schwertmannite	-1.838	schwertmannite	-3.939
H-Jarosite	-2.899	H-Jarosite	-11.615	H-Jarosite	-6.997	H-Jarosite	-7.602
Na-Jarosite	-0.328	Na-Jarosite	-8.344	Na-Jarosite	-3.985	Na-Jarosite	-4.703
Pb-Jarosite	-5.67	Pb-Jarosite	-9.314	Pb-Jarosite	-4.953	Pb-Jarosite	-5.67
K-Jarosite	2.556	K-Jarosite	-6.827	K-Jarosite	-1.939	K-Jarosite	-2.7
AlOHSO4	-5.297	AlOHSO4	-6.33	AlOHSO4	-6.262	AlOHSO4	-6.747
$Al_4(OH)_{10}SO4$	-17.525	$Al_4(OH)_{10}SO4$	-17.915	$Al_4(OH)_{10}SO4$	-19.423	$Al_4(OH)_{10}SO4$	-21.7
alunite	-41.813	alunite	-47.153	alunite	-45.592	alunite	-47.075
gypsum	0.069	gypsum	0.055	gypsum	0.084	gypsum	0.053
kaolinite	-4.793	kaolinite	-4.795	kaolinite	-4.763	kaolinite	-7.023

Table A-19 *(Continued)*

SWG T1							
1 PV (phase 1)		10 PV (phase 1)		1 PV (phase 3)		10 PV (phase 3)	
Mineral Name	SI	Mineral Name	SI	Mineral Name	SI	Mineral Name	SI
Zn talc	-4.381	Zn talc	-9.418	Zn talc	-5.855	Zn talc	-2.487
quartz	0.645	quartz	0.498	quartz	1.011	quartz	0.474
gibbsite	-0.987	gibbsite	-4.297	gibbsite	-6.96	gibbsite	-2.248
ferrihydrite	-0.195	ferrihydrite	-0.937	ferrihydrite	-1.591	ferrihydrite	-0.248
goethite	2.506	goethite	1.763	goethite	1.109	goethite	2.453
hematite	7.413	hematite	5.926	hematite	4.619	hematite	7.306
anglesite	-0.284	anglesite	-0.337	anglesite	-0.039	anglesite	-0.449
goslarite	-2.702	goslarite	-5.104	goslarite	-4.674	goslarite	-5.183
Orthoclase	1.166	Orthoclase	-2.607	Orthoclase	-3.476	Orthoclase	0.541
schwertmannite	3.522	schwertmannite	-3.346	schwertmannite	-8.646	schwertmannite	-0.249
H-Jarosite	1.179	H-Jarosite	-2.893	H-Jarosite	-4.999	H-Jarosite	-5.667
Na-Jarosite	1.289	Na-Jarosite	-2.246	Na-Jarosite	-4.317	Na-Jarosite	-3.971
Pb-Jarosite	1.44	Pb-Jarosite	-2.246	Pb-Jarosite	-4.118	Pb-Jarosite	-3.971
K-Jarosite	4.967	K-Jarosite	0.872	K-Jarosite	-0.979	K-Jarosite	-0.73
AlOHSO4	0.58	AlOHSO4	-3.653	AlOHSO4	-6.388	AlOHSO4	-4.025
$Al_4(OH)_{10}SO4$	-3.438	$Al_4(OH)_{10}SO4$	-17.601	$Al_4(OH)_{10}SO4$	-28.324	$Al_4(OH)_{10}SO4$	-11.827
alunite	-18.19	alunite	-32.807	alunite	-41.208	alunite	-38.011
gypsum	-0.267	gypsum	-0.026	gypsum	0.117	gypsum	-0.041
kaolinite	0.464	kaolinite	-6.451	kaolinite	-10.75	kaolinite	-2.401

Table A-19 *(Continued)*

SWG T2							
1 PV (phase 1)		10 PV (phase 1)		1 PV (phase 3)		10 PV (phase 3)	
Mineral Name	SI	Mineral Name	SI	Mineral Name	SI	Mineral Name	SI
Zn talc	9.062	Zn talc	10.61	Zn talc	11.1	Zn talc	11.805
quartz	0.95	quartz	0.62	quartz	0.968	quartz	0.558
gibbsite	-2.417	gibbsite	-0.289	gibbsite	-2.409	gibbsite	0.413
ferrihydrite	0.811	ferrihydrite	1.673	ferrihydrite	1.136	ferrihydrite	1.562
goethite	3.512	goethite	4.373	goethite	3.836	goethite	4.262
hematite	9.424	hematite	11.147	hematite	10.073	hematite	10.92
anglesite	-0.497	anglesite	-2.014	anglesite	-0.72	anglesite	-1.36
goslarite	-2.607	goslarite	-4.326	goslarite	-3.457	goslarite	-4.494
Orthoclase	2.631	Orthoclase	4.531	Orthoclase	3.202	Orthoclase	5.401
schwertmannite	7.59	schwertmannite	11.803	schwertmannite	8.679	schwertmannite	10.261
H-Jarosite	-3.76	H-Jarosite	-6.533	H-Jarosite	-5.801	H-Jarosite	-8.166
Na-Jarosite	-1.496	Na-Jarosite	-3.005	Na-Jarosite	-2.801	Na-Jarosite	-4.471
Pb-Jarosite	-1.616	Pb-Jarosite	-3.808	Pb-Jarosite	-3.014	Pb-Jarosite	-4.792
K-Jarosite	2.006	K-Jarosite	-0.003	K-Jarosite	0.475	K-Jarosite	-1.282
AlOHSO4	-4.828	AlOHSO4	-5.38	AlOHSO4	-6.328	AlOHSO4	-5.328
$Al_4(OH)_{10}SO4$	-13.135	$Al_4(OH)_{10}SO4$	-7.305	$Al_4(OH)_{10}SO4$	-14.613	$Al_4(OH)_{10}SO4$	-5.147
alunite	-40.877	alunite	-47.07	alunite	-48.94	alunite	-47.889
gypsum	-0.205	gypsum	0.025	gypsum	0.156	gypsum	0.007
kaolinite	-1.785	kaolinite	1.809	kaolinite	-1.735	kaolinite	3.088

Table A-19 *(Continued)*

SGW + 10 μM Oxalic Acid T1							
1 PV (phase 1)		10 PV (phase 1)		1 PV (phase 3)		10 PV (phase 3)	
Mineral Name	SI	Mineral Name	SI	Mineral Name	SI	Mineral Name	SI
Pb-oxalate	-9.414	Pb-oxalate	-7.801	Pb-oxalate	-7.76	Pb-oxalate	-4.168
Ca-oxalate3H2O	-5.861	Ca-oxalate3H2O	-4.087	Ca-oxalate3H2O	-4.091	Ca-oxalate3H2O	-0.334
Ca-oxalateH2O	-5.43	Ca-oxalateH2O	-3.657	Ca-oxalateH2O	-3.66	Ca-oxalateH2O	0.097
Mg-oxalate	-9.491	Mg-oxalate	-9.501	Mg-oxalate	-8.697	Mg-oxalate	-6.789
Zn talc	-7.055	Zn talc	-9.336	Zn talc	-5.038	Zn talc	-6.469
quartz	0.929	quartz	0.718	quartz	1.157	quartz	0.697
gibbsite	-3.277	gibbsite	-4.542	gibbsite	-7.983	gibbsite	-4.432
ferrihydrite	-0.976	ferrihydrite	-1.549	ferrihydrite	-1.723	ferrihydrite	-0.866
goethite	1.725	goethite	1.549	goethite	0.978	goethite	1.834
hematite	5.85	hematite	5.498	hematite	4.356	hematite	6.069
anglesite	-0.249	anglesite	-0.286	anglesite	-0.022	anglesite	-0.313
goslarite	-2.85	goslarite	-5.271	goslarite	-3.931	goslarite	-4.883
Orthoclase	-0.754	Orthoclase	-2.174	Orthoclase	-4.415	Orthoclase	-1.919
schwertmannite	-1.609	schwertmannite	-4.957	schwertmannite	-9.034	schwertmannite	-3.266
H-Jarosite	1.076	H-Jarosite	-3.337	H-Jarosite	-4.064	H-Jarosite	-3.664
Na-Jarosite	0.55	Na-Jarosite	-2.801	Na-Jarosite	-3.714	Na-Jarosite	-2.905
Pb-Jarosite	0.795	Pb-Jarosite	-2.666	Pb-Jarosite	-3.507	Pb-Jarosite	-2.71
K-Jarosite	4.381	K-Jarosite	0.448	K-Jarosite	-0.397	K-Jarosite	0.328
AlOHSO4	-0.59	AlOHSO4	-3.799	AlOHSO4	-6.746	AlOHSO4	-4.281
$Al_4(OH)_{10}SO4$	-11.479	$Al_4(OH)_{10}SO4$	-18.484	$Al_4(OH)_{10}SO4$	-31.751	$Al_4(OH)_{10}SO4$	-18.635
alunite	-20.002	alunite	-33.146	alunite	-42.058	alunite	-35.771
gypsum	-0.176	gypsum	-0.052	gypsum	0.167	gypsum	0.038
kaolinite	-3.549	kaolinite	-6.503	kaolinite	-12.5	kaolinite	-6.324

Table A-19 *(Continued)*

SGW + 10 μM Oxalic Acid T2							
1 PV (phase 1)		10 PV (phase 1)		1 PV (phase 3)		10 PV (phase 3)	
Mineral Name	SI	Mineral Name	SI	Mineral Name	SI	Mineral Name	SI
Pb-oxalate	-8	Pb-oxalate	-5.099	Pb-oxalate	-5.143	Pb-oxalate	-5.149
Ca-oxalate3H2O	-4.05	Ca-oxalate3H2O	-0.25	Ca-oxalate3H2O	-0.77	Ca-oxalate3H2O	-0.18
Ca-oxalateH2O	-3.618	Ca-oxalateH2O	0.181	Ca-oxalateH2O	-0.339	Ca-oxalateH2O	0.251
Mg-oxalate	-9.623	Mg-oxalate	-7.691	Mg-oxalate	-4.776	Mg-oxalate	-5.68
Zn talc	9.039	Zn talc	10.703	Zn talc	9.925	Zn talc	10.448
quartz	0.962	quartz	0.773	quartz	1.062	quartz	0.801
gibbsite	-3.204	gibbsite	0.907	gibbsite	-2.22	gibbsite	-0.329
ferrihydrite	1.363	ferrihydrite	1.284	ferrihydrite	1.049	ferrihydrite	1.475
goethite	4.063	goethite	3.984	goethite	3.749	goethite	4.176
hematite	10.528	hematite	10.369	hematite	9.898	hematite	10.752
anglesite	-0.364	anglesite	-1.363	anglesite	-0.883	anglesite	-1.471
goslarite	-2.674	goslarite	-4.308	goslarite	-3.582	goslarite	-4.401
Orthoclase	1.974	Orthoclase	6.189	Orthoclase	3.322	Orthoclase	4.997
schwertmannite	11.959	schwertmannite	8.887	schwertmannite	8.374	schwertmannite	10.45
H-Jarosite	-2.192	H-Jarosite	-7.306	H-Jarosite	-5.275	H-Jarosite	-6.67
Na-Jarosite	0.036	Na-Jarosite	-3.982	Na-Jarosite	-2.509	Na-Jarosite	-3.342
Pb-Jarosite	0.04	Pb-Jarosite	-4.355	Pb-Jarosite	-2.767	Pb-Jarosite	-3.788
K-Jarosite	3.668	K-Jarosite	-0.773	K-Jarosite	0.649	K-Jarosite	-0.177
AlOHSO4	-5.659	AlOHSO4	-3.987	AlOHSO4	-5.746	AlOHSO4	-5.193
$Al_4(OH)_{10}SO4$	-16.33	$Al_4(OH)_{10}SO4$	-2.323	$Al_4(OH)_{10}SO4$	-13.464	$Al_4(OH)_{10}SO4$	-7.238
alunite	-44.374	alunite	-42.664	alunite	-46.077	alunite	-46.471
gypsum	0.107	gypsum	0.002	gypsum	0.01	gypsum	0.015
kaolinite	-3.337	kaolinite	4.507	kaolinite	-1.168	kaolinite	2.09

Table A-19 *(Continued)*

SGW + 100 μM Oxalic Acid T1							
1 PV (phase 1)		10 PV (phase 1)		1 PV (phase 3)		10 PV (phase 3)	
Mineral Name	SI	Mineral Name	SI	Mineral Name	SI	Mineral Name	SI
Pb-oxalate	-8.542	Pb-oxalate	-3.068	Pb-oxalate	-3.489	Pb-oxalate	-2.89
Ca-oxalate3H2O	-4.853	Ca-oxalate3H2O	0.861	Ca-oxalate3H2O	0.2	Ca-oxalate3H2O	0.983
Ca-oxalateH2O	-4.422	Ca-oxalateH2O	1.292	Ca-oxalateH2O	0.631	Ca-oxalateH2O	1.414
Mg-oxalate	-8.53	Mg-oxalate	-4.465	Mg-oxalate	-2.853	Mg-oxalate	-4.27
Zn talc	-5.966	Zn talc	-9.948	Zn talc	-1.571	Zn talc	-5.395
quartz	0.755	quartz	0.704	quartz	1.666	quartz	1.141
gibbsite	-3.813	gibbsite	-4.838	gibbsite	-5.123	gibbsite	-5.32
ferrihydrite	-1.132	ferrihydrite	-1.188	ferrihydrite	-1.117	ferrihydrite	-1.182
goethite	1.569	goethite	1.513	goethite	1.584	goethite	1.518
hematite	5.538	hematite	5.426	hematite	5.568	hematite	5.436
anglesite	-0.138	anglesite	-0.347	anglesite	-0.142	anglesite	-0.285
goslarite	-2.608	goslarite	-5.564	goslarite	-3.872	goslarite	-5.266
Orthoclase	-1.627	Orthoclase	-2.809	Orthoclase	0.258	Orthoclase	-1.24
schwertmannite	-3.207	schwertmannite	-5.313	schwertmannite	-4.592	schwertmannite	-5.865
H-Jarosite	-0.095	H-Jarosite	-3.578	H-Jarosite	-3.056	H-Jarosite	-4.75
Na-Jarosite	-0.409	Na-Jarosite	-3.214	Na-Jarosite	-2.563	Na-Jarosite	-3.898
Pb-Jarosite	-0.145	Pb-Jarosite	-2.904	Pb-Jarosite	-2.357	Pb-Jarosite	-3.747
K-Jarosite	3.396	K-Jarosite	-0.09	K-Jarosite	0.896	K-Jarosite	-0.524
AlOHSO4	-1.477	AlOHSO4	-4.16	AlOHSO4	-4.29	AlOHSO4	-5.236
$Al_4(OH)_{10}SO4$	-13.973	$Al_4(OH)_{10}SO4$	-19.731	$Al_4(OH)_{10}SO4$	-20.716	$Al_4(OH)_{10}SO4$	-22.254
alunite	-24.167	alunite	-34.34	alunite	-34.661	alunite	-38.817
gypsum	0.072	gypsum	0.068	gypsum	0.057	gypsum	0.048
kaolinite	-4.969	kaolinite	-7.122	kaolinite	-5.767	kaolinite	-7.21

Table A-19 *(Continued)*

SGW + 100 Oxalic Acid T2							
1 PV (phase 1)		10 PV (phase 1)		1 PV (phase 3)		10 PV (phase 3)	
Mineral Name	SI	Mineral Name	SI	Mineral Name	SI	Mineral Name	SI
Pb-oxalate	-4.701	Pb-oxalate	-4.232	Pb-oxalate	-3.956	Pb-oxalate	-4.372
Ca-oxalate3H2O	-0.859	Ca-oxalate3H2O	0.857	Ca-oxalate3H2O	0.3	Ca-oxalate3H2O	0.888
Ca-oxalateH2O	-0.427	Ca-oxalateH2O	1.288	Ca-oxalateH2O	0.73	Ca-oxalateH2O	1.318
Mg-oxalate	-3.473	Mg-oxalate	-4.021	Mg-oxalate	-3.766	Mg-oxalate	-4.397
Zn talc	4.893	Zn talc	11.073	Zn talc	13.682	Zn talc	13.786
quartz	0.957	quartz	0.81	quartz	1.49	quartz	1.157
gibbsite	-4.548	gibbsite	0.934	gibbsite	-1.212	gibbsite	0.044
ferrihydrite	0.03	ferrihydrite	1.565	ferrihydrite	1.467	ferrihydrite	1.898
goethite	2.731	goethite	4.265	goethite	4.168	goethite	4.598
hematite	7.862	hematite	10.931	hematite	10.736	hematite	11.596
anglesite	-0.336	anglesite	-1.538	anglesite	-0.732	anglesite	-1.682
goslarite	-2.586	goslarite	-4.464	goslarite	-3.547	goslarite	-4.506
Orthoclase	-0.053	Orthoclase	6.349	Orthoclase	6.023	Orthoclase	6.804
schwertmannite	2.763	schwertmannite	10.965	schwertmannite	11.096	schwertmannite	13.146
H-Jarosite	-3.26	H-Jarosite	-6.801	H-Jarosite	-5.275	H-Jarosite	-6.767
Na-Jarosite	-1.708	Na-Jarosite	-3.393	Na-Jarosite	-2.229	Na-Jarosite	-3.108
Pb-Jarosite	-1.747	Pb-Jarosite	-3.395	Pb-Jarosite	-2.38	Pb-Jarosite	-3.651
K-Jarosite	1.934	K-Jarosite	-0.25	K-Jarosite	1.056	K-Jarosite	0.09
AlOHSO4	-5.539	AlOHSO4	-4.13	AlOHSO4	-5.366	AlOHSO4	-5.501
$Al_4(OH)_{10}SO4$	-20.244	$Al_4(OH)_{10}SO4$	-2.386	$Al_4(OH)_{10}SO4$	-10.061	$Al_4(OH)_{10}SO4$	-6.426
alunite	-41.582	alunite	-43.382	alunite	-45.762	alunite	-48.269
gypsum	0.025	gypsum	0.028	gypsum	0.03	gypsum	0.056
kaolinite	-6.037	kaolinite	4.635	kaolinite	1.703	kaolinite	3.549

REFERENCES

Arizona Department of Environmental Quality, 2000. Preliminary Assesment/Site Inspection Report Klondyke Tailings. (EPA ID#: AZ0000309294). Klondyke, Arizona: Goodwin S.D.

Baron, D., & Palmer, C. D. (1996). Solubility of jarosite at 4-35 degrees C. *Geochimica Et Cosmochimica Acta, 60*(2), 185-195.

Blake, G.R. & Hartge, K.H. (1986). "Particle density". In Methods of Soil Analysis, Pt. 1 (Ed., A. Klute). American Soc. Of Agro., Madison, WI p. 377-382.

Chu, C. X., Lin, C. X., Wu, Y. G., Lu, W. Z., & Long, J. (2006). Organic matter increases jarosite dissolution in acid sulfate soils under inundation conditions. *Australian Journal of Soil Research, 44*(1), 11-16.

Fomina, M., Alexander, I. J., Hillier, S., & Gadd, G. M. (2004). Zinc phosphate and pyromorphite solubilization by soil plant-symbiotic fungi. *Geomicrobiology Journal, 21*(5), 351-366.

Giere, R., Sidenko, N. V., & Lazareva, E. V. (2003). The role of secondary minerals in controlling the migration of arsenic and metals from high-sulfide wastes (berikul gold mine, siberia). *Applied Geochemistry, 18*(9), 1347-1359.

Gee, G.W. & Bauder, J.W. (1986). "Particle-size Analysis". In Methods of Soil Analysis, Pt. 1 (Ed., A. Klute). American Soc. Of Agro., Madison, WI p. 383-411.

Gunsinger, M. R., Ptacek, C. J., Blowes, D. W., & Jambor, J. L. (2006). Evaluation of long-term sulfide oxidation processes within pyrrhotite-rich tailings, lynn lake, manitoba. *Journal of Contaminant Hydrology, 83*(3-4), 149-170.

Hammarstrom, J. M., Seal, R. R., Meier, A. L., & Kornfeld, J. M. (2005). Secondary sulfate minerals associated with acid drainage in the eastern US: Recycling of metals and acidity in surficial environments. *Chemical Geology, 215*(1-4), 407-431.

Allada, R. M., Peltier, E., Navrotsky, A., Casey, W. H., Johnson, A., Berbeco H. T., & Sparks, D. L. (2006). Calorimetric determination of the enthalpies of formation of hydrotalcite-like solids and their use in the geochemical modeling of metals in natural waters. *Clays and Clay Minerals*, *54*(4), 409-417.

Jones, D. L. (1998). Organic acids in the rhizosphere - a critical review. *Plant and Soil, 205*(1), 25-44.

Jones, D. L., Dennis, P. G., Owen, A. G., & van Hees, P. A. W. (2003). Organic acid behavior in soils – misconceptions and knowledge gaps. *Plant & Soil, 248*(1/2), 31-41.

Kashkay, Ch.M., Borovskaya, Yu. B., & Babazade, M. A. (1975). Determination of ΔG°_{f298} of synthetic jarosite and its sulfate analogues. *Geochemistry International*, 115-120.

Leyval, C. & EJ. Joner. (2001). Bioavailability of heavy metals in the mycorrhizosphere. In:Gobran GR, Wenzel WW, Lombi E, editors. Trace Elements in the Rhizosphere. Boca Raton, Fl:CRC Press, p 165- 185.

Ludwig, B., Khanna, P., Balkenhol, R., Friedrich, G., & Dohrmann, R. (1999). Pyrite oxidation in a sediment sample of an open-cut brown coal mine: Mineral formation, buffering of acidity and modeling of cations and sulfate. *Journal of Plant Nutrition and Soil Science-Zeitschrift Fur Pflanzenernahrung Und Bodenkunde, 162*(5), 499-509.

Martell, A.E. & Smith, R.M. (2003). NIST critically selected stability constants of metals complexes database, NIST Standard Database 46, Version 7.0. U.S. Department of Commerce, Gaithersburg, MD.

Miretzky, P., Munoz, C., & Carrillo-Chavez, A. (2006). Experimental zn(II) retention in a sandy loam soil by very small columns. *Chemosphere, 65*(11), 2082-2089.

Mulvaney, R.L. (1996). "Nitrogen-Inorganic Forms". In Methods of Soil Analysis, Pt. 3 (Ed., D.L. Sparks). American Soc. Of Agro., Madison, WI p. 1123-1184.

Nian, H., Yang, Z. M., Ahn, S. J., Cheng, Z. J., & Matsumoto, H. (2002). A comparative study on the aluminium- and copper-induced organic acid exudation from wheat roots. *Physiologia Plantarum, 116*(3), 328-335.

Singer P. C. & Stumm W. (1970). Acid mine drainage-rate determining step. *Science,167*, 1121-1123.

Sposito, G. (1989). "Salt-Affected Soils". In The Chemistry of Soils (Oxford University Press, Inc.). p. 280-300.

Sposito, G. (1989). "The chemical composition of soils". In The Chemistry of Soils (Oxford University Press, Inc.). p. 3-21.

Ostergren, J. D., Brown, G. E., Parks, G. A., & Tingle, T. N. (1999). Quantitative speciation of lead in selected mine tailings from leadville, CO. *Environmental Science & Technology, 33*(10), 1627-1636.

Ousmanova, D., & Parker, W. (2007). Fungal generation of organic acids for removal of lead from contaminated soil. *Water Air and Soil Pollution, 179*(1-4), 365-380.

Ryan, P. R., Delhaize, E., & Jones, D. L. (2001). Function and mechanism of organic anion exudation from plant roots. *Annual Review of Plant Physiology and Plant Molecular Biology, 52*, 527-560.

Salmon, S. U., & Malmstrom, M. E. (2004). Geochemical processes in mill tailings deposits: Modelling of groundwater composition. *Applied Geochemistry, 19*(1), 1-17.

Salmon, S. U., & Malmstrom, M. E. (2006). Quantification of mineral dissolution rates and applicability of rate laws: Laboratory studies of mill tailings. *Applied Geochemistry, 21*(2), 269-288.

Shum, M., & Lavkulich, L. (1999). Speciation and solubility relationships of al, cu and fe in solutions associated with sulfuric acid leached mine waste rock. *Environmental Geology, 38*(1), 59-68.

Smith, A. M. L., Dubbin, W. E., Wright, K., & Hudson-Edwards, K. A. (2006). Dissolution of lead- and lead-arsenic-jarosites at pH 2 and 8 and 20 degrees C: Insights from batch experiments. *Chemical Geology, 229*(4), 344-361.

Smith, A. M. L., Hudson-Edwards, K. A., Dubbin, W. E., & Wright, K. (2006). Dissolution of jarosite [KFe3(SO4)(2)(OH)(6)] at pH 2 and 8: Insights from batch experiments and computational modelling. *Geochimica Et Cosmochimica Acta, 70*(3), 608-621.

Wu, Z. H., Gu, Z. M., Wang, X. R., Evans, L., & Guo, H. Y. (2003). Effects of organic acids on adsorption of lead onto montmorillonite, goethite and humic acid. *Environmental Pollution, 121*(3), 469-475.

Yang, J. Y., Yang, X. E., He, Z. L., Li, T. Q., Shentu, J. L., & Stoffella, P. J. (2006). Effects of pH, organic acids, and inorganic ions on lead desorption from soils. *Environmental Pollution, 143*(1), 9-15.